The Global Wind Atlas

An EUDP project carried out by DTU Wind Energy

Final Report

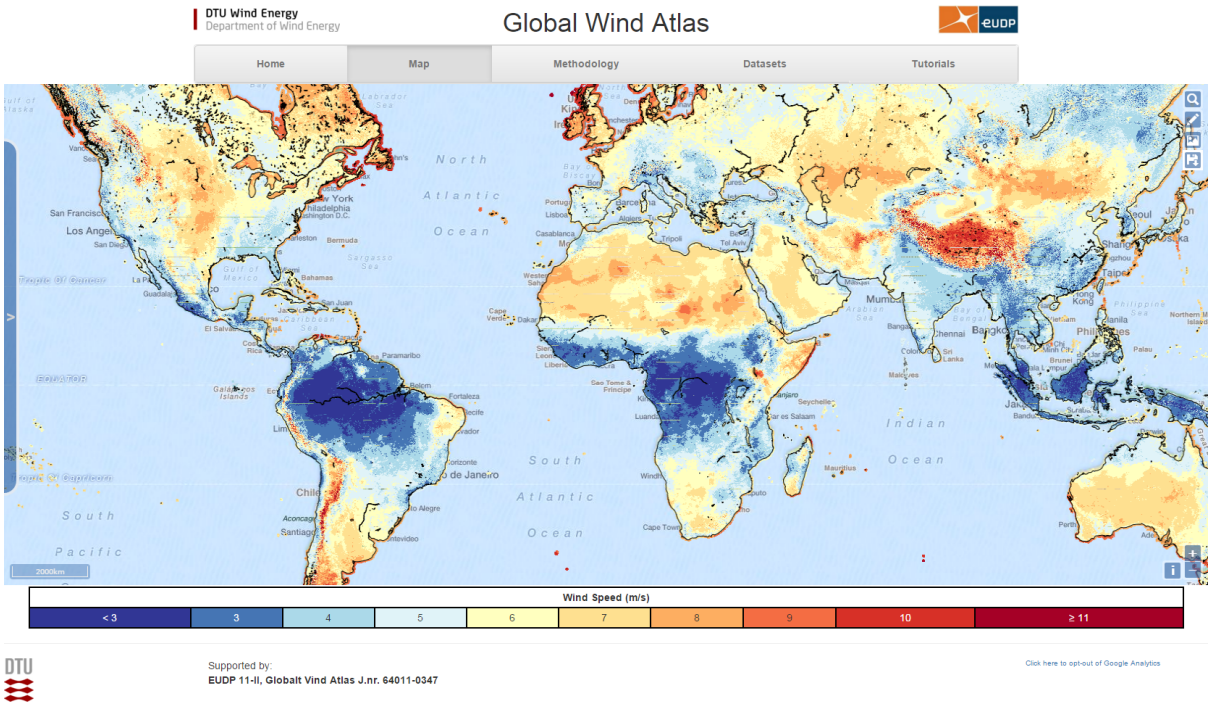

Project team:

Jake Badger, Neil Davis, Andrea Hahmann, Xiaoli Guo Larsen, Merete Badger, Mark Kelly, Bjarke T. Olsen, Niels G. Mortensen, Hans E. Jœrgensen, Ib Troen, Erik Lundtang Petersen, Patrick Volker, Julia Lange

Contributing authors to report:

Jake Badger, Andrea Hahmann, Xiaoli Guo Larsen, Merete Badger, Mark Kelly, Neil Davis, Bjarke T. Olsen, Niels G. Mortensen

Grant EUDP 11-II, Globalt Vind Atlas, 64011-0347

Contents

Part I

Project Details

Project title	Globalt Vind Atlas
Project identification	EUDP 11-II 64011-0347
Name of the programme which has funded the project	EUDP International Collaboration
Project managing company/institution	DTU Wind Energy DTU Risø Campus Frederiksborgvej 399 DK-4000 Roskilde
Project partners	no partners, DTU Wind Energy sole institution
CVR	30 06 09 46
Date of submission	30th October 2015

Part II

Short description of project objectives and results

English:

The Global Wind Atlas provides a unified, high resolution and public domain dataset of wind climate statistics for wind energy resources for the world. A wind climate is calculated every 250 m on land surfaces and coastal waters. Access on http://globalwindatlas.com/ and http://irena.masdar.ac.ae/ makes it a readily available and free wind resource dataset for wind energy sector and energy planners internationally. The method and validation are transparent and disseminated on the websites. By accounting for high resolution terrain effects, a truer, and in many places larger, estimate of global wind resource is available for the benefit of society. Website tools allow the users to analyse, plot and download the aggregated spatial and temporal wind characteristics. The application of the Global Wind Atlas datasets can enhance and clarify the role of wind energy in the future global energy mix.

Danish:

Det globale vindatlas tilbyder et samlet, højt opløseligt, offentligt datasæt over det statistiske vindklima som beskriver vindenergi-ressourcer i hele verden. Vindklimaet bliver beregnet hvert 250 m over alle landflader og kystområder. Adgangen gennem http://globalwindatlas.com/ og http://irena.masdar.ac.ae/ giver en let og gratis adgang til datasættet, til gavn for hele vindenergi sektoren og for energiplanlæggere over alt i verden. Metoden og validering af datasættet bliver formidlet på hjemmesiden. Ved at taget højde for terræneffekter i høj opløsning, kan et mere korrekt, og i mange tilfælde højere, estimat af de globale vindressourcer findes, til gavn for samfundet. Værktøjer på hjemmesiden tillader brugerne at analyser, plotte og downloade aggregerede rumlige og tidslige vind-karakteristika. Anvendelse af det globale vindatlas datasæt kan forbedre og skabe klarhed om den rolle vindenergi kan spille i fremtidens sammensætning af energikilder.

Part III

Executive summary

Up until now, policy makers and energy planners tackling the challenges of climate change, and seeking approaches for climate change mitigation, have had no global wind resource dataset appropriate for their pressing needs. Use of coarse resolution reanalysis datasets has had the serious shortcoming that the wind energy resource is underestimated, as small scale variability of winds is missing. This missing variability means a large part of the wind resource is not captured. Crucially it is the windiest sites that suffer the largest wind resource errors at coarse resolution; in simple terrain one fifth of the wind resource may be missed, for complex terrain more than half of the wind resource may be missed.

This project is built on a global methodology. It is the new and improved meteorological datasets and topographical datasets, in the public domain, that have made this project a possibility. The method employs large-scale global meteorological datasets (reanalysis), which are downscaled to high-resolution wind resource datasets via a so-called generalization step together with microscale modelling using the WAsP software developed at DTU Wind Energy. A new application of flow models in WAsP software allows calculation of high-resolution resource maps covering extensive areas. For the purpose of downscaling high-resolution datasets, appropriate surface elevation and roughness lengths have been derived from global surface elevation and land cover datasets.

The application of geospatial information systems (GIS) and web-based tools help significantly to bring the Global Wind Atlas datasets alive to end-users; the end-users can analyse spatial and temporal distributions of wind resources in areas of interest determined by the end-user. Either by specifying ad-hoc areas or by selection of areas following administrative boundaries. Furthermore, through the IRENA Global Atlas the end-user is able to relate the wind resources to other factors, such as population centres, electrical transmission grids, terrain types, and protected land areas.

The Global Wind Atlas does not provide a substitute for individual country-based wind atlases or wind resource assessment conducted commercially for wind farm developers. Those kinds of assessments require a higher precision, specific configuration for the region in question, and a more stringent validation phase. Importantly, the Global Wind Atlas data is the most appropriate wind resource dataset available for the needs of policy makers, energy planners, the Integrated Assessment Modelling (IAM) community and for Strategic Environmental Assessment (SEA).

DTU Wind Energy has developed the methodology and carried out the work in the framework of the Clean Energy Ministerial Multilateral Working Group on Solar and Wind Technologies supported by the Danish Energy Agency. The DTU Wind Energy contribution has been made stronger by this international collaboration, because leading international institutions have shared valuable knowledge and liaised on the data specifications, applications, and dissemination of the data to a large and broad range of end-users.

Part IV

Project objectives

In this part the project context, purpose and objectives are set out. The project evolved in alignment with the project proposal, in so far as the work packages' scope of tasks and outputs were satisfactorily carried out. Where the project departed from the original proposal, after approval from EUDP, was in the extension by 6 months, on top of the scheduled 36 months, and a rebudgeting of some funds to an external software development company.

In June 2014, the Global Wind Atlas project had reached a critical phase. The project required 3 main components to be in place: the topographical data sets, describing the global terrain at high resolution, the generalized wind climate datasets, describing the wind conditions at medium scale (every 50 km or so), and the calculation platform that allows the extremely extensive calculation of wind atlases to be managed.

While the setting-up of the required first component (topographical datasets) and the third component (development of the software to allow the calculation of wind atlases on a global scale) was complete, the production of the second component (generalized wind climate datasets) was challenging and delayed. This had already been alluded to in earlier status reports to the EUDP.

At that stage, although it probably would have been practically possible to create a global wind atlas by January 2015, it was seen that the quality of the final products would be very much improved if the project was allowed an extension of 6 month. The extension had no implications on the total budget of the project only on the delivery date.

The problem was not one of allocation of man power, but technical problems in the calculation of the generalized wind climates from the reanalysis datasets. Several new methods to generate the generalized wind climates had been developed, and these needed validation and to be run through the global calculation system, which takes significant amount of time to calculate. Without an extension this testing would not have been to the extent desired, and there would have given less opportunity to revise the method.

Concerning the development of the software to allow the calculation of wind atlases on a global scale, there was a need to engage the external software development company named World in a Box. The following itemized list of the tasks carried out by the company in 2014 is given below:

- System development (terrain server, calculation engine, data flows) to handle grid map results
- Work to support multi-threaded operations in the WAsP worker
- Optimisation of the task allocation service to deal with super-heavy work load
- Customisation of the spatial proximity calculations for climate locations to support very large data sets
- Extension of the results handling system to deliver and store flow corrections
- Design and development of 'Super Job Manager' to set up and control the more than 1000 jobs for Global Wind Atlas
- Experiments with separate cloud based clusters of Frogfoot systems for partitioning the Global Wind Atlas work

Project funds from the DTU labour costs were allocated, with EUDP's approval, to pay for this software development work. This software development could not have been done at DTU Wind Energy.

Chapter 1

Introduction

The Global Wind Atlas comes in a period of increasing wide spread use of a fast and accessible internet, massive open global datasets describing the earth's atmosphere and the surface conditions, powerful computer resources, and stronger international collaboration globally. That together with an urgent need to mitigate climate change by sensible renewable energy decisions has set the scene for the Global Wind Atlas.

1.1 Objectives

The objective of the Global Wind Atlas are to

- provide wind resource data accounting for high resolution effects
- use microscale modelling to capture small scale wind speed variability (crucial for better estimates of total wind resource)
- use a unified methodology
- ensure transparency about the methodology used
- verify the results in representative selected areas

The correct usage of the Global Wind Atlas dataset and tools is for aggregation, upscaling analysis and energy integration modelling for energy planners and policy makers. It is not correct to use the data and tools for wind farm siting.

1.2 Motivation

Figure 1.1 shows the wind power density at 50 m for a 50 km x 50 km area modelled at two different resolutions, namely 2.5 km and 100 m. As the resolution increases features in the terrain become better resolved. Resolved hills and ridges give rise to increased wind speeds. As wind power density is a function of wind speed cubed, the impact of the resolved terrain features is significant.

For the 50 km x 50 km area the area mean wind power density is estimated to be around 320 $\mathrm{W\,m^{-2}}$ by the modelling at a resolution of 2.5 km. For the 100 m resolution modelling

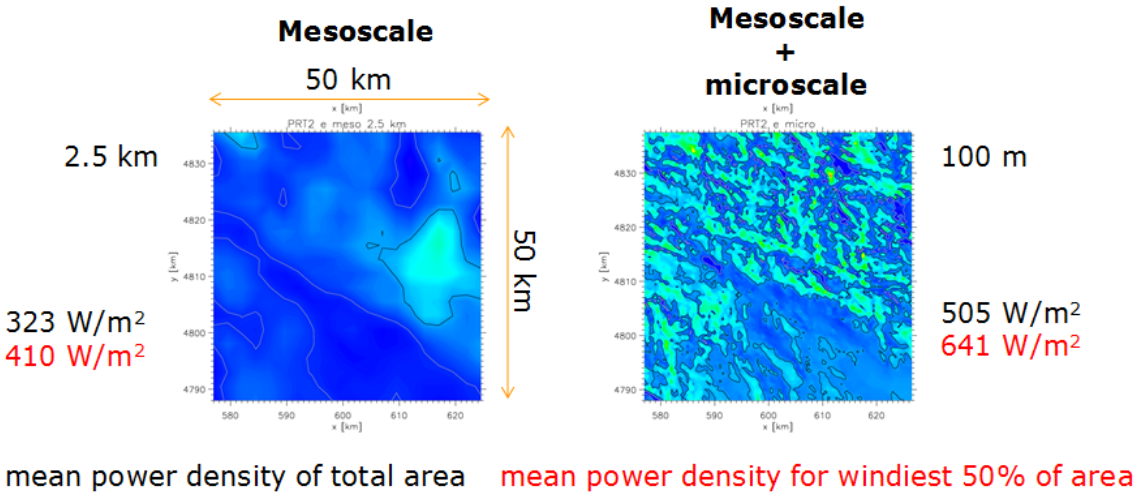

Figure 1.1 – Wind power density calculated at 50 m above the surface for a 50 km x 50 km area at two different resolutions, (left) 2.5 km and (right) 100 m. The colour scale used in each map is the same. Dark blue is low values and bright green and yellow are high values. The mean power density for the area is given in black. The mean power density for the windiest 50% area is given in red.

the mean power density is around 505 $\mathrm{W\,m^{-2}}$, i.e. an increase of 50% compared to the lower resolution estimates.

The comparison becomes more striking when the distribution of the wind power density is considered. Consider this: we split the 50 km x 50 km into two areas; the first area where the wind power density is below the median value and the second area where the wind power density is above the median value. Next we calculate the mean wind power density in the second higher wind area; the 2.5 km resolution modelling gives 380 $\mathrm{W\,m^{-2}}$, whereas the 100 m resolution modelling gives 640 $\mathrm{W\,m^{-2}}$, an increase of nearly 70%.

The impact gets stronger as we look at the even windier areas. As wind turbines will be deployed at the favourable sites, it is important to be able to capture the distribution of wind power density due to terrain features, and this is only possible by consideration of high resolution effects. As one concentrates on the most favourable areas, the wind power density goes up.

Figure 1.2 shows the calculated mean power density for the 50 x 50 km area when averaging over different amounts of the windiest areas for different modelling resolutions. It goes up most for the high resolution modelling. Even for rather simple terrain, such as in Denmark, the effect of resolution is important. A similar 50 km x 50 km area showed an increase of wind power density of around 25% for the windiest 5% of the area (i.e. the windiest 1/20th of the area).

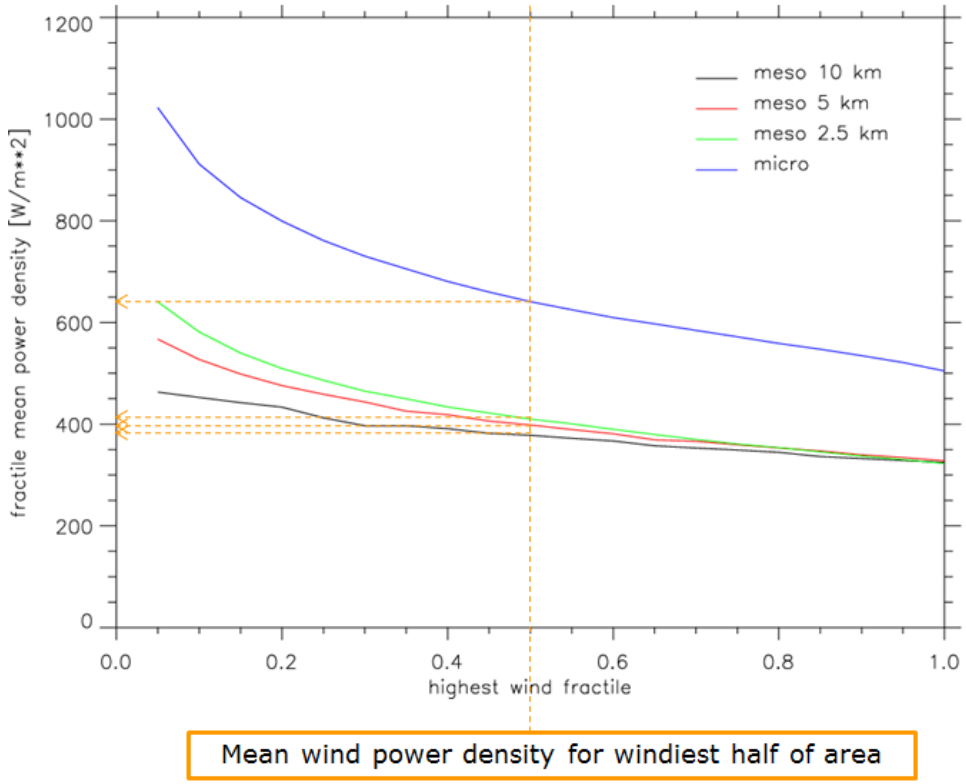

Figure 1.2 – Graph showing the mean wind power density (y-axis) for the windiest fractile area (x-axis) of the 50 km x 50 km area in Fig. 1.1, calculated from modelling using different resolutions, namely, 10, 5, 2.5, and 0.1 km. A guiding line is drawn at fractile 0.5, which gives power density values corresponding to those in Fig. 1.1. Note that when modelled at high resolution we see that the windiest areas are significantly windier than the average for the whole area.

1.3 Background

The Global Wind Atlas is part of an international collaboration. It has come about in the framework of the Clean Energy Ministerial (CEM) (http://www.cleanenergyministerial.org/) and in particular the CEM Working Group on Solar and Wind technologies, lead by Germany, Spain and Denmark. The Danish Energy Agency Energy's Technology Development and Demostration Programme (EUDP) funded the Global Wind Atlas project as Denmark's contribution to the working group's objectives. Figure 1.3 shows the relationship between DTU Wind Energy and the CEM initiatives and IRENA's Global Atlas for Renewable Energy.

Some of the working group partners we have worked with before for many years, on projects such as the MED2010 project, mapping wind and solar resources in North Africa, or in the UNEP GEF SWERA project, mapping wind and solar resources in around 15 countries over the world.

For other partners this is the first time we have worked together, such as IRENA and MASDAR institute. These partners can made possible a much greater impact of the atlas and bring members of different energy sector communities together in dialogue about what is needed. The IRENA Global Atlas of Renewable Energy has a dedicated set of tools to serve the Global Wind Atlas data to a worldwide audience.

Collaboration with the software development company World In A Box (http://www.worldinabox.eu/), based in Finland, has been an essential part of the project, in order to make the global calculation system, Frogfoot, a reality.

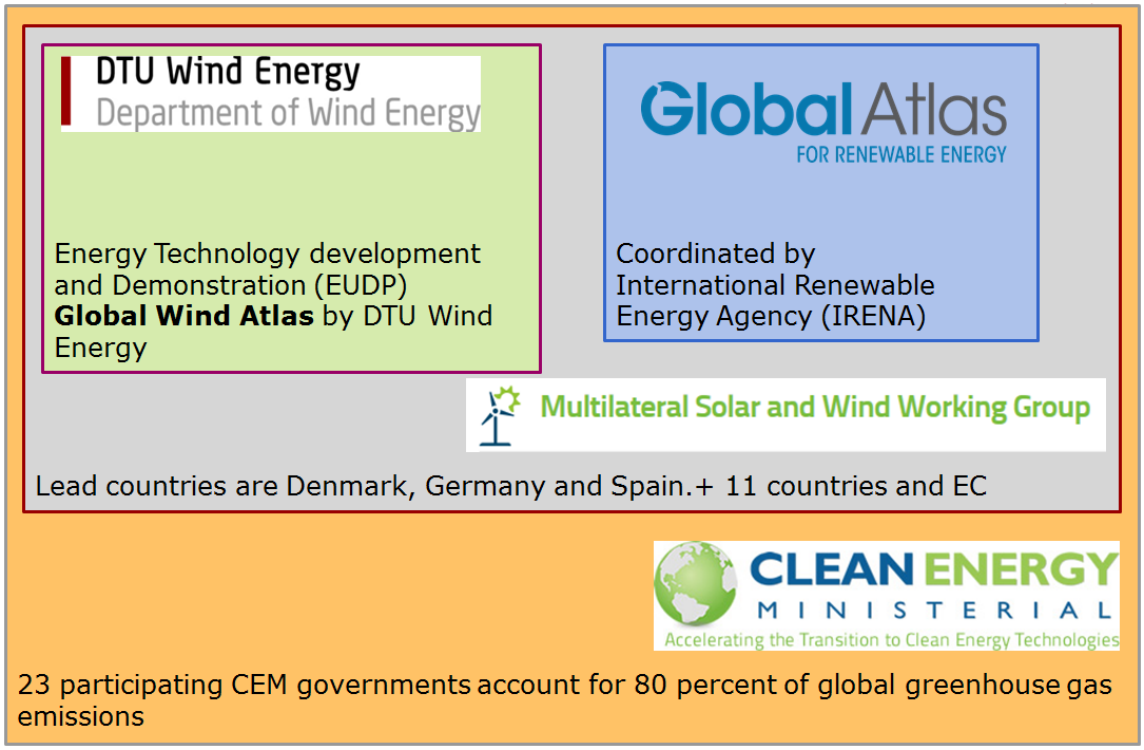

Figure 1.3 – Schematic diagram showing the relational context of the EUDP Global Wind Atlas project.

1.4 Overview of methodology

The Global Wind Atlas uses a downscaling process. A schematic of the methodology and verification methods is shown in Fig. 1.4

We start with large scale wind climate data and end with micro scale wind climate data. The large scale wind climate data is provided by atmospheric reanalysis data, from meteorological centres around the world. These data are on a grid with spacing of about 50 km depending on the dataset. We perform a generalization process on this data. The result is a set of generalized wind climates which have the same spacing as the reanalysis data that was used to create them.

Next we take this set of generalized wind climates and apply them in microscale modelling system over the globe (apart from poles and far offshore oceans areas). The modelling process is made up of a calculation for the local wind climates every 250 m at three heights, 50, 100 and 200 m. So on a 250 m grid, there is a local wind climate estimation. Local wind climate characteristics are aggregated up to a 1 km grid. Datasets and tools for analysing statistics based on the 250 m grid values are available on the Global Wind Atlas website.

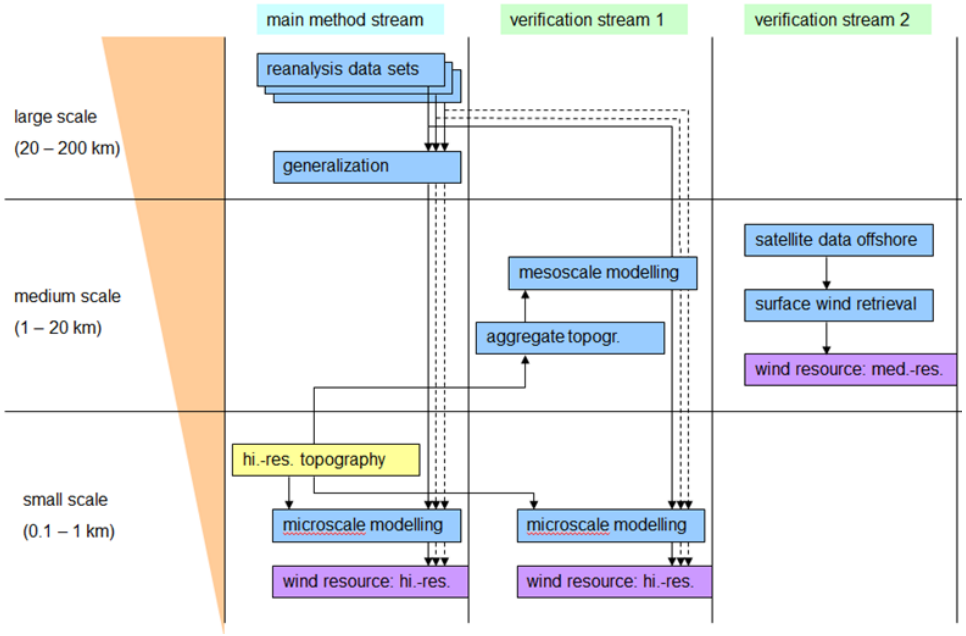

Figure 1.4 – Schematic diagram showing the downscaling process, which is key to the Global Wind Atlas methodology. The verification methods are also shown in the same diagram.

1.5 Limitation of the Global Wind Atlas

The global wind atlas covers the world providing wind climate statistics. However below we list reasons why a national wind atlas study is still required.

- Mesoscale modelling component (no mesocale modelling in Global Wind Atlas)
- Mesoscale modelling captures variance both in space and time, missing from the reanalyses
- Mesoscale modelling will increase accuracy of the atlas, by capturing features such as gap flow, barrier jets, low level jets, and sea breezes better
- Mesoscale modelling set-up can be tailored to the country meteorological and geographical settings
- Microscale modelling component enhanced
- Inputs for national microscale modelling can draw on country specific datasets and knowledge, an improvement on terrain global datasets
- Verification of numerical wind atlas outputs
- National wind atlas projects include a measurement program for verification
- High quality measurement data itself adds confidence to wind sector in country
- Local partner involvement

- Involvement in country adds not just to a better quality atlas but also increases the impact factor of the atlas
- Country partners know best how to engage the right organizations and stake holders in the energy sector

1.6 Limitation of flow modelling

The Global Wind Atlas uses the orographic flow model within WAsP, the BZ-model (Troen, 1990). This model performs well when the surrounding terrain is sufficiently gentle and smooth to ensure mostly attached flows. With the global coverage of the Global Wind Atlas, we are certainly going to be using the BZ-model in areas beyond its recommended operational envelope.

The Global Wind Atlas website allows the user to see where the flow modelling is likely to be increasingly uncertain, by adding a so called RIX layer to their map. RIX stands for ruggedness idex and is an objective measure of the steepness or ruggedness of the terrain. Large RIX values will lead to large errors in the flow modelling Bowen and Mortensen (1996). Most likely leading to an overestimate of mean wind speeds on ridge and hill tops. We therefore recommend users to inspect the RIX of their region of interest.

1.7 Disclaimer

Neither DTU however, nor any of its partners and affiliates hold the responsibility for accuracy and/or completeness of the data and shall not be liable for any errors, or omissions. It is strongly advised that the data be limited to use in informing policy discussions on the subject, and/or in creating services that better educate relevant persons on the viability of wind development in areas of interest. As such, neither DTU nor any of its partners and sponsors on the Global Wind Atlas project will be liable for any damages relating to the use of the maps for financial commitments or any similar use cases.

Chapter 2

Acknowledgements

The Global Wind Atlas project acknowledges the EUDP - Energiteknologisk udvikling og demonstration - for the financial support through grant EUDP 11-II, Globalt Vind Atlas, 64011-0347. The EUDP supported covered 85% of project costs, the rest was supported by DTU Wind Energy.

The following reanalysis dataset were used in the project. The project team wishes to thank the following institutions that created the datasets:

- National Aeronautics and Space Administration (NASA, USA) for the Modern Era-Retrospective Analysis for Research and Applications (MERRA)
  http://gmao.gsfc.nasa.gov/research/merra/
- National Center for Atmospheric Research (NCAR, USA) for the Climate Four Dimensional Data Assimilation (CFDDA)
  http://dx.doi.org/10.5065/D6M32STK
- National Oceanography National Oceanography (NOAA, USA) and National Centers for Environmental Prediction (NCEP, USA) for the Climate Forecasting System Reanalysis (CFSR)
  http://cfs.ncep.noaa.gov/cfsr/
- European Center for Medium Range Weather Forecast (ECMWF, EU) for the ERA-Interim Reanalysis (ERA-I)
  http://www.ecmwf.int/en/research/climate-reanalysis/era-interim

The project used surface elevation data from the following sources. The project thanks the following institutions and persons that created the datasets:

- National Aeronautics and Space Administration (NASA, USA) for Shuttle Radar Topography Mission (SRTM) data
  http://www2.jpl.nasa.gov/srtm/
- Jonathan de Ferranti for Viewfinder data
  http://www.viewfinderpanoramas.org/dem3.html

The project used land use classification from the following sources. The project thanks the following institutions that created the datasets:

- European Space Agency for use of GlobCover
  http://due.esrin.esa.int/page_globcover.php

- National Aeronautics and Space Administration (NASA, USA) for use of the Moderate Resolution Imaging Spectroradiometer (MODIS) data
  http://modis.gsfc.nasa.gov/about/

The company World in a Box (http://www.worldinabox.eu/) is acknowledged and thanked for their key part in the development of the global local climate calculation system employed in this project.

The following institutional collaborators are also acknowledged:

- International Renewable Energy Agency (IRENA, UAE)
  http://www.irena.org/

- National Aeronautics and Space Research Centre of the Federal Republic of Germany (DLR, Germany)
  http://www.dlr.de/

- National Renewable Energy Centre (CENER, Spain)
  http://www.cener.es/

- National Renewable Energy Laboratory (NREL, USA)
  http://www.nrel.gov/

- National Center for Atmospheric Research (NCAR, USA)
  http://ncar.ucar.edu/

Part V

Project results and dissemination of results

In this part the main activities and technical results are set out in some detail. The activities and technical results are given according to workpage in the each chapter. And in turn, one of the chapters describes the dissemination.

The project has succeeded in providing datasets and tools that are already integrated into the external renewable energy data portal provided by IRENA's Global Atlas of Renewable Energies. This was one of the main objectives of the Clean Energy Ministerial Multilaterial Work Group on Solar and Wind Technologies. The partnership with IRENA has been very fruitful, in terms of giving the Global Wind Atlas datasets and tools a very prominent place in their Global Altas. Furthermore IRENA have developed an engaging and ambitious launch programme, including coordination of press releases between IRENA, Danish Energy Agency and DTU, and two webinars, the first an official and high level launch and the second a more technical series of talks and demonstrations.

Concerning the discussion on increased exports and employment, although it is difficult to quantify, we expect that the better knowledge globally of wind climate for wind resource estimation will have a positive effect on the wind industry. The scalability of the positive effect could be vast, given the Atlas's global coverage. It is of paramount importance to follow through this work with projects to bring forward and promote the implications of the new Global Wind Atlas datasets.

Chapter 3

Reanalysis Data

Reanalysis data has been used in the wind energy sector, particularly wind resource assessment, for some years. The increasing resolution of these datasets has made the Global Wind Atlas methodology a possibility. Here details of the reanalysis data used in the Global Wind Atlas are given and the ways we reformat the reanalysis data for the purposes of Atlas are described.

3.1 Reanalysis data description

A reanalysis is a scientific method for developing a comprehensive record of how weather and climate are changing over time. In a reanalysis observations around the globe and a numerical weather prediction model, which simulates one or more aspects of Earth system, are combined objectively to generate a synthesized estimate of the state of the system. In the 2010s four large atmospheric reanalysis projects took place. These are listed in Table 3.1. All provide output at a horizontal resolution below $1^{\circ} \times 1^{\circ}$. Three of these reanalysis (i.e., CFDDA, CFSR and MERRA) were generalized and later used in the global wind atlas.

Many of the models described in Table 3.1 were run at a high spatial resolution but the data was truncated (e.g. CFSR, ERA-Interim) or interpolated (e.g. CFDDA) to a lower resolution when made available to the users. This means that the data is not available in the native model grid (e.g. there is no information on the real surface elevation and land use) and has implication for the generalization procedure carried out. We will return to this point later in Chapter 5.

Table 3.1 – Description and grid characteristics of the various modern reanalysis used to generate the Global Wind Atlas. TXXX represents the spectral truncation of the model and LXX the number of vertical levels.

Global reanalysis	model type and reference	native resolution	available resolution
Climate Forecasting System Reanalysis (CFSR)	USA NOAA spectral model Saha et al. (2010)	T382 L64	$0.5° \times 0.5°$ 6 hours
Climate Four Dimensional Data Assimilation (CFDDA)	NCAR grid point model (MM5) Hahmann et al. (2010); Rife et al. (2010)	Twin polar grids, 40 km, 28 levels	$0.4° \times 0.4°$ 6 hourly
Modern Era-Retrospective Analysis for Research and Applications (MERRA)	NASA GEOS-5 data assimilation system; grid point model Rienecker et al. (2011)	$1/2° \times 2/3°$ 72 levels	$1/2° \times 2/3°$ 6 hours
European Center for Medium Range Weather Forecast (ECMWF) Reanalysis (ERA-Interim)	ECMWF IFS Cy31r2; spectral model Dee et al. (2011)	T255 L60	$0.71° \times 0.71°$ 6 hours

3.2 Analysis and formatting

3.2.1 Climalogical statistics

The reanalysis datasets come in varying meteorological data formats. Therefore it is important to harmonize the file formating for later processing of the reanalysis datasets. For the Global Wind Atlas it is the climatological properties of the datasets that are of primary interest, rather than the datasets as a time series. Therefore the reanalysis data is compiled into a tabular form. The table content is similar to the WAsP observed wind climate file format and contains the following information. This table data stored in a single large netcdf file for each reanalysis dateset.

- Latitudes [°], Longitudes [°] and heights 50 m, 100 m, 200 m
- Sector-wise frequencies of occurrence [%] for 12 direction sectors
- Upper limit for speed class 1 (1 ms^{-1}), sector-wise frequencies in class 1
- Upper limit for speed class 2 (2 ms^{-1}), sector-wise frequencies in class 2
- .. .. ..
- Upper limit for speed class 40 (40 ms^{-1}), sector-wise frequencies in class 40

This file is called the reanalysis TAB netcdf file and contains the statistical information required for further downscaling.

Figures 3.1, 3.2, 3.3, 3.4 show the mean wind speed at 100 m above the surface for the MERRA, CFDDA, CFSR and ERA-Interim reanalyses. The general patterns of the winds are similar. Over the oceans the strong westerly in the mid-latitudes, and the trade wind belts in the subtropics are shown. However there are differences in exact placement of these features and magnitudes. For example winds over land masses appear to be lower for the ERA-Interim and CFSR reanalyses, and higher for CFDDA reanalysis. Part of the explanation for this is the difference in boundary layer parameteriz'ation schemes and surface descriptions in the reanalysis models. This is discussed in more detail in Chapter 5.

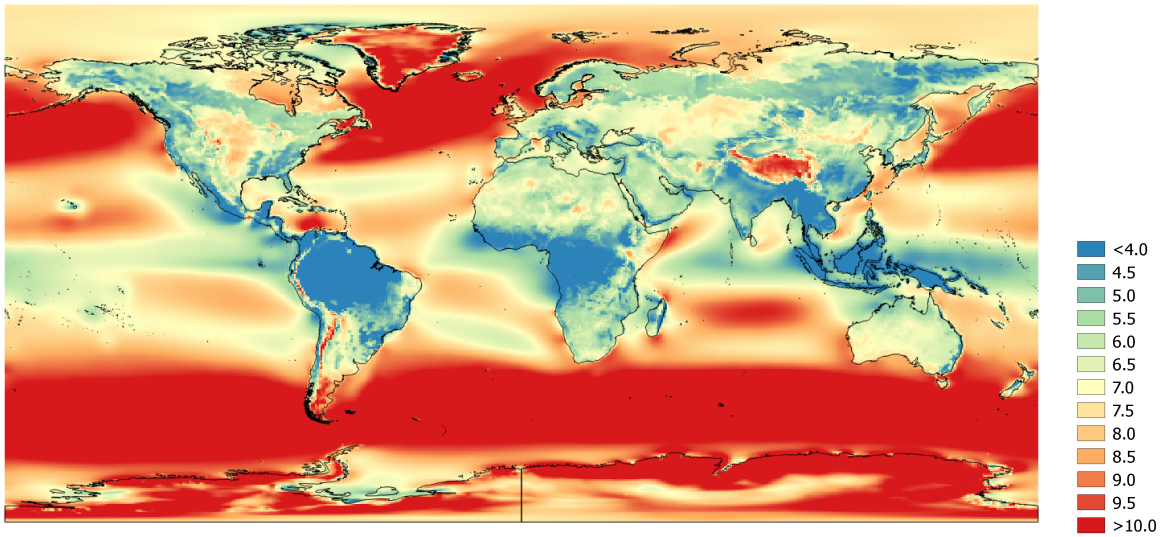

Figure 3.1 – Mean wind speed at 100m from MERRA reanalysis. Period 1979-2013.

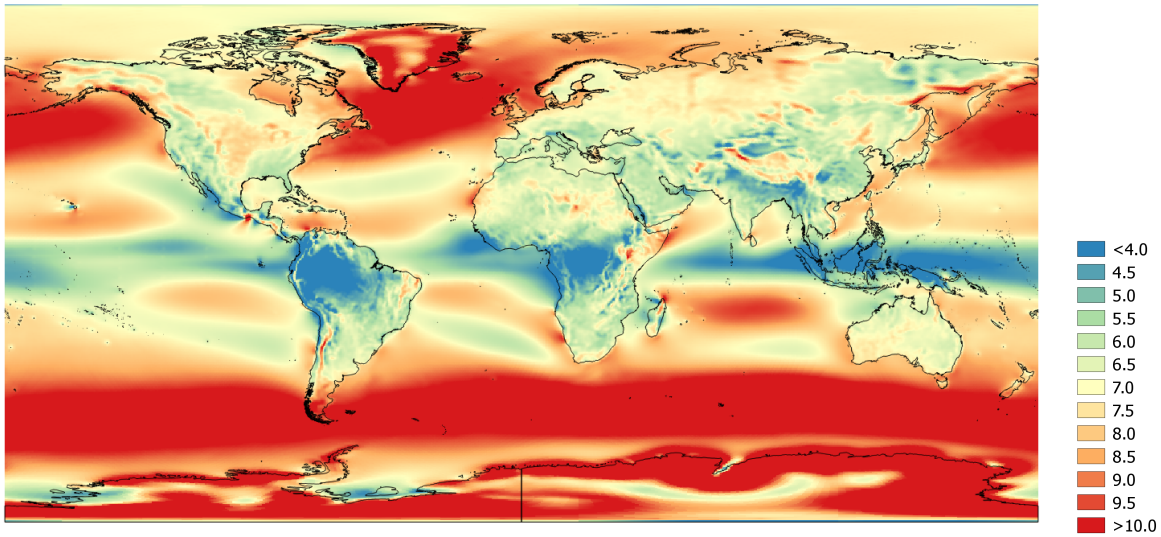

Figure 3.2 – Mean wind speed at 100m from CFDDA reanalysis. Period 1985-2005.

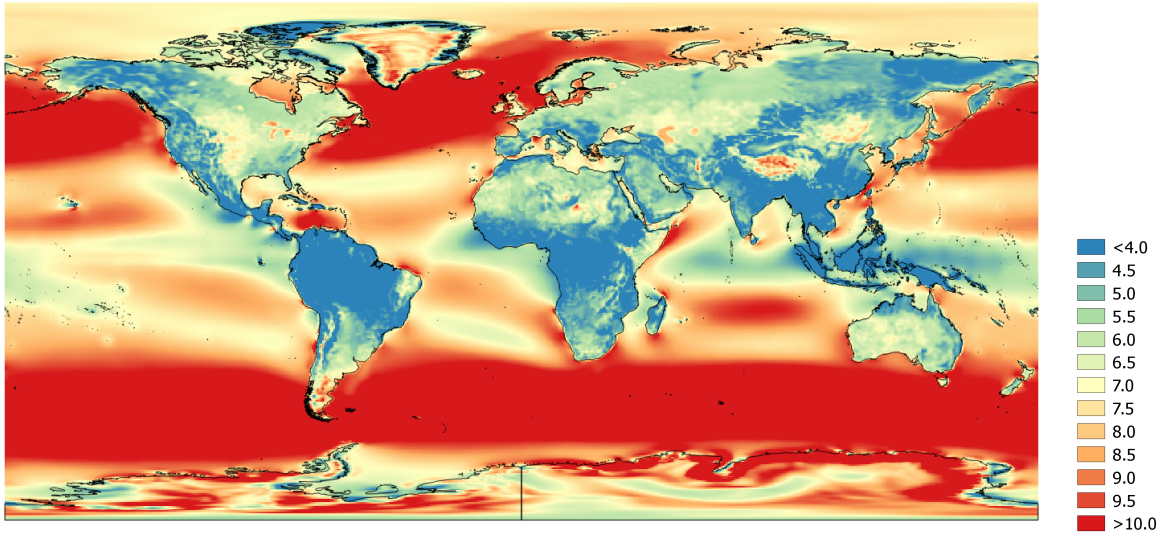

Figure 3.3 – Mean wind speed at 100m from CFSR reanalysis. Period 1979-2010.

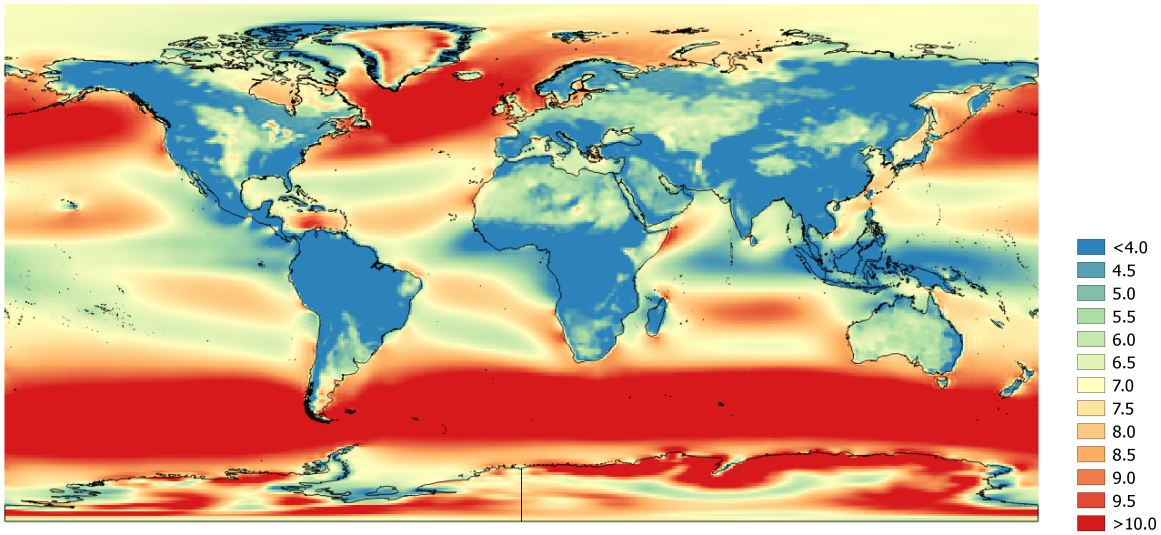

Figure 3.4 – Mean wind speed at 100m from ERA-Interim reanalysis. Period 1979-2012.

3.2.2 Daily and annual cycles

Although climatological properties are the primary interest, the Global Wind Atlas also serves information about how a location's large scale forcing varies on average throughout the day, and throughout the year. This is useful information in order to approximately gauge how wind resources are distributed temporally. For this purpose the reanalysis data is averaged according to month of year and hour of day. A tabular form is used with the following content:

- Latitudes [°], Longitudes [°] and heights 50 m, 100 m, 200 m
- Months of year
- Hours of day
- mean wind speed for month 1

- standard deviation of wind speed for month 1
- mean wind speed for month 2
- standard deviation of wind speed for month 2
- .. .. ..
- mean wind speed for hour 1
- standard deviation of wind speed for hour 1
- mean wind speed for hour 2
- standard deviation of wind speed for hour 2
- .. .. ..

This file is called the reanalysis CYCLE netcdf file. An example of the average daily and annual cycle from the CFDDA reanalysis is shown in Fig. 3.5. The wind speed values are normalized by dividing by the annual mean wind speed. This is done to make sure that the wind speed value is not misunderstood as an expected wind speed for the location. It can be seen for this location there is a strong daily cycle, with maximum wind speeds at around 12 UTC. There is also a moderate annual cycle, with maximum winds around July.

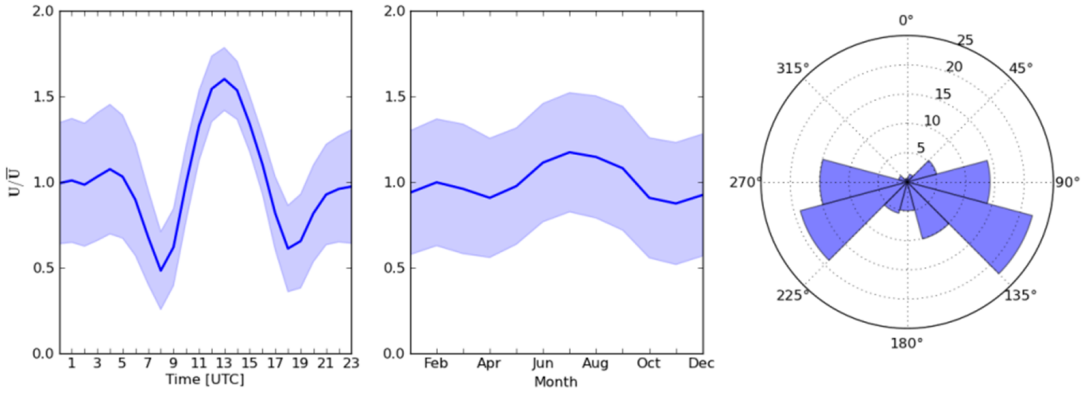

Figure 3.5 – Average daily and annual wind speed cycle, and wind direction frequency rose at 50 m from CFDDA reanalysis for a location around Northeastern Lake Victoria (0.4 °S, 34.0 °E). The shading on the cycle plots shows the standard deviation of monthly and hourly means. Period 1985-2005.

3.3 Summary

The reanalysis datasets have been described. The way they are formatted into netcdf files containing the required information for the Global Wind Atlas downscaling and annual and daily cycle charactistics has been outlined. How the reanalysis TAB file is used is described in Chapters 5 and 9. How the reanalysis data is used can be read in Chapter 9.

Contributing authors Jake Badger, Andrea N. Hahmann, Bjarke T. Olsen

Chapter 4

Topography

Public datasets describing the earth's topography have become available at increased resolution in recent years. These impressive datasets make the Global Wind Atlas feasible. For the purpose of the Global Wind Atlas, the topography description can be split into two parts:

- the description of the surface elevation; refered to here as orography, as in the WAsP terminalogy.
- the description of the surface land use or class

Orography has an important and direct influence on wind resources, because hills and ridges cause the surface winds to speed up. Land use or class has an impact on wind resource because different land uses or classes are associated with different aerodynamic surface roughnesses; rougher surfaces tend to decrease surface winds. More about the influence of the orography and surface roughness on the modelled winds are given in Chapter 6. In this chapter the sources of the data used to determine the orography and roughness in the Global Wind Atlas are described.

4.1 Orography

The Global Wind Atlas used digital elevation models from Viewfinder Paroramas (http://www.viewfinderpanoramas.org). This data was developed in support of their downloadable software that draws panoramas from viewpoints. The data has a 3 arc-second (90 m) resolution and is mainly based on data collected by the Shuttle Radar Topography Mission (SRTM). SRTM data is availible for use in WAsP through the WAsP map editor, however, it does not have any coverage north of 60 °. This would have prevented the modeling of large parts of Scandinavia, Russia and Canada. Additionally, it is known that the raw SRTM data has no-data (void) areas in mountainous and desert areas and has some other errors. These have been corrected in other datasets, but the 60° N restriction still applies in those datasets. The viewfinder DEM has voidfilled those areas using the best availible alternative sources, which depended greatly on the region being voidfilled. Detailed information about the datasets used for voidfilling can be found at http://www.viewfinderpanoramas.org/dem3.html.

The viewfinder DEM was provided in the WGS 1984 coordinate system (EPSG: 4326), as a global raster that was chopped into 1 ° by 1° tiles. Therefore the data had to be reprojected to UTM rasters to match the Global Wind Atlas tile format. This interpolation was done

using the Geospatial Data Abstraction Library (GDAL) (http://gdal.org/). In addition to reprojecting the data, the data was warped to a 150m resolution, which cooresponds to the effective resolution of the SRTM data. This conversion used the nearest neighbor resampling algorithm from the *gdalwarp* tool.

4.2 Land use to roughness length

Roughness length in the Global Wind Atlas was derived from the GlobCover 2009 land cover map. The GlobCover dataset was created by the European Space Agency (ESA) and the Universitie catholique de Louvain (UCL) to convert MERIS FR (Medium Resolution Imaging Spectrometer Instrument Fine Resolution) surface reflectance mosaics into 22 land cover classes as defined by the United Nations Land Cover Classifcation System (LCCS). The GlobCover dataset was selected as it is a relatively recent land-cover map, with a consistent approach applied to all parts of the globe. It has a 10 arc-second (300 m) resolution and was provided in the WGS 1984 coordinate system (EPSG: 4326). The data was converted to the GWA tiles using *gdalwarp* as described in Section 4.1, but the spatial resolution of 300m was retained.

While GlobCover is a full global raster, one of the classification types is no-data. This datatype was mostly in areas North of 60 °. To voidfill these regions we used the 0.5 km MODIS-based Global Land Cover Climatology (http://landcover.usgs.gov/global_climatology.php). This dataset was based on 10 years of data 2001-2010, and had 17 land cover classes. These classes were mapped to the GlobCover classes and then used to fill any no-data points.

Once the data was reprojected and the no-data points were filled, the data was converted to roughness length by defining a specific roughness length for each of the land use classes. A reproduction of this mapping is provided in Table 4.1. The mapping was created based on the class name as well as looking at a global map of the classes and using expert input from DTU Wind Energy modelers.

Table 4.1 – Land use classes and assigned surface roughness lengths.

Class Name	GlobCover Number	Modis Number	Roughness Length
Water Bodies	210	0	0.0
Permanant Snow and ice	220	15	0.004
Bare areas	200	16	0.005
Grassland, savannas or lichens/mosses	140	10	0.03
Sparse vegetation	150	None	0.05
Croplands	11, 14	12	0.1
Shrubland	130	6, 7	0.1
Wetlands	180	0.2	11
Mosaic natural vegetation / cropland	20, 30	14	0.3
Flooded forest	160	None	0.5
Mosaic grassland / forest	120	9	0.5
Flooded forest or shrubland	170	None	0.6
Urban Areas	190	13	1.0
Forests	40, 50, 60, 70, 90, 100, 110	1, 2, 3, 4, 5, 8	1.5

4.3 Discussion on limitations

Use of these global datasets for orography and land use will not give as accurate a description of topography as dedicated land surveys, such as those from large scale mapping from national cartography institutions. Although 150 m and 300 m resolution for orography and roughness length gives an impression of high resolution when related to global coverage, an actual wind turbine site will not be well represented at this resolution. Therefore the Global Wind Atlas is not appropriate for specific site assessment.

Another limitation is due to the conversion of land use or class to a single surface roughness length. This discretization of land use type is somewhat unrealistic. Furthermore, that a single land use can be assigned a single surface roughness is unlikely to be correct because a single land use may actually represent a range of vegitation covers.

For these reasons we expect uncertainty to be introduced to the wind climate calculations. However, this uncertainty needs to be balanced against the uncertainty that is inherent in not considering the high resolution topography at all. Therefore we advise that the appropriate use of the Global Wind Atlas is for initial aggregated area studies and not for site specific assessments.

4.4 Summary

The relevance of the surface description has been outlined, and broken into orography and land use or class. The sources of the topography data have been described. The limitations

of the topography data and method have been discussed. The topography will be used for the calculation of local wind climates descibed in Chapter 6. The topography data is also shown in the Atlas as outlined in Chapter 9.

Contributing authors Neil Davis, Jake Badger

Chapter 5

Generalization

The concept of a generalized wind climate is a key element of the wind atlas methodology developed at DTU Wind Energy. The European Wind Atlas (Troen and Petersen, 1989b) sets out the method fully. Since then, the generalization has been used in numerical wind atlas methodologies, where mesoscale modelling output is generalized before application in microscale modelling with WAsP. In this chapter we describe the generalization fundamentals and how the method used in the mesoscale modelling has been adapted to the reanalysis data.

5.1 The concept of generalization

The description of the topography and the land surface in the global models and in nature is very distinct. The two panels in Fig. 5.1 illustrate some of these differences. The left figure illustrates the differences in topography between reality (photo) and the reanalysis model (yellow line). The topography induced speed-up in reality and in the microscale model are thus quite different from that in the reanalysis model.

The details of the position of the coastline are misrepresented by the coarse reanalysis grid. The right figure illustrates the differences in the location of the coastline in reality (Google Earth map) and that in the reanalysis model (green and blue squares).

To avoid double counting these effects when coupling the mesoscale or global model results to the microscale model, effects in a similar scale to that simulated in the microscale model must be removed. We call this process "generalization" within the WAsP-thinking and wind atlas method developed at DTU Wind Energy.

The wind atlas method is based on the generalization of the wind climatologies derived from mesoscale or reanalysis global modeling. This generalization post-processing method has been used extensively in a number of wind resource assessment studies, particularly within the KAMM-WAsP method (Badger et al., 2014a). The method was used for the first time with WRF model simulations in the Wind Atlas for South Africa (WASA) project (Hahmann et al., 2014).

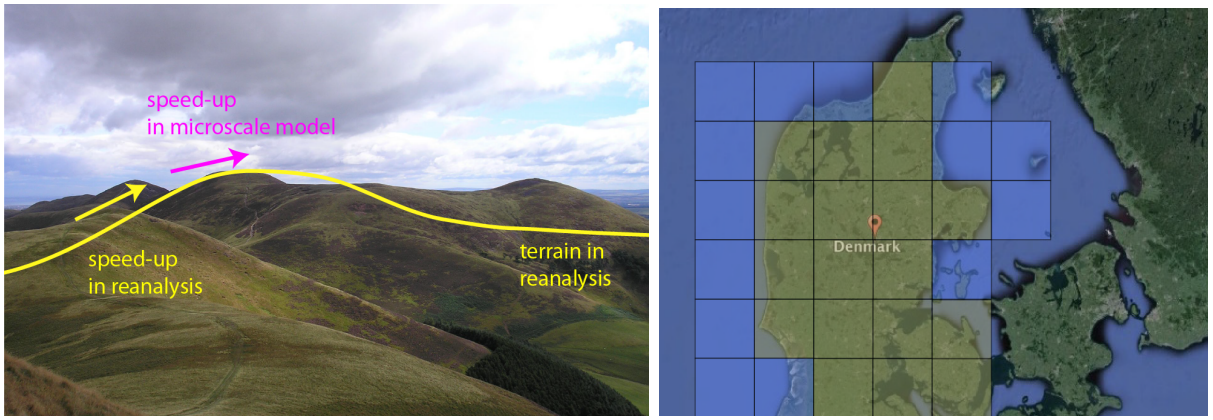

Figure 5.1 – Illustration of the conflict between representation of terrain (left) and land/ocean mask (right) in a global reanalysis and in nature.

5.2 Data processing

The starting place for applying the generalization procedure to the reanalysis data is the reanalysis TAB netcdf files described in 3. These are identical file type for each reanalyses but with different horizontal grid dimensions. These files contains the statistical information required for further downscaling.

5.3 Generalization factors

Four main parameters can be derived from the surface characteristics of the reanalysis model grid (e.g., the terrain and surface roughness length) as described in Badger et al. (2014a):

- a factor that accounts for how the model description of topography impacts the local flow (δA_o),
- a parameter that takes into account how the topography alters the wind direction ($\delta\phi_o$),
- a parameter that accounts for the local flow perturbation on wind speed due to roughness length variations (δA_r), and finally a
- grid point dependent upstream roughness length ($\hat{z}_0$).

These four parameters are computed from the reanalysis grid description (Table 3.1), that includes the topographic height and a time averaged surface roughness length. These parameters are stored in a NetCDF file and used in the generalization of the reanalysis TAB netcdf file (see Eqs. 5.1, 5.2, 5.3, and 5.4).

A similar code to that used with the KAMM/WAsP and WRF mesoscale models is used to derive the generalization parameters. A few modifications were introduced to account for the specifics of the reanalysis grids:

1. The LINCOM flow model (Dunkerley et al., 2001) used in the calculation of the local flow perturbation assumes that the horizontal grid is equally spaced in distance in the

$x \times y$ directions. The reanalysis grid is equally spaced in latitude $\times$ longitude, and in the MERRA data contains different spacing in latitude and longitude. To overcome this issue, the globe was divided into smaller patches that overlap each other and where a constant $\Delta x or \Delta y$ assumption is not too far off. The size of the patches in terms of degrees latitude $\times$ longitude was 6° $\times$ 18° in the CFDDA, 8° $\times$ 18° in the CFSR, and 8° $\times$ 18° in the MERRA. On each of these patches we assumed $dx = dy = 2\pi R(\text{dlon}/360)cos(\text{clat})$, where R is the radius of the Earth, dlon is the longitude spacing, and clat is the latitude of the center of the patch. No significant differences are found in these parameters along the edge of each patch.

2. In the direction-dependent calculation of the upstream roughness, a correction is made according to the actual distance (in km) between neighboring grid points which varies with latitude according to the angle, i.e. $ds = dx|cos\phi| + (1 - |cos\phi|)dy$, where ϕ is the direction of the sector, and dx and dy are the actual dimensions of the grid in kilometers.

Figure 5.2 displays the geographic distribution of two of these generalization parameters for the MERRA reanalysis for a patch centered over Denmark. Along the southern coast of Norway and Sweden, large changes in surface roughness length (Fig. 5.2a) are visible (from water to forest landcover). δA_r values are as large as 1.2. In opposition, the smooth topography in the MERRA reanalysis (Fig. 5.2b) results in quite small values of the topographic correction factor, e.g. $|\delta A_o| < 1.0065$ (Fig. 5.2d).

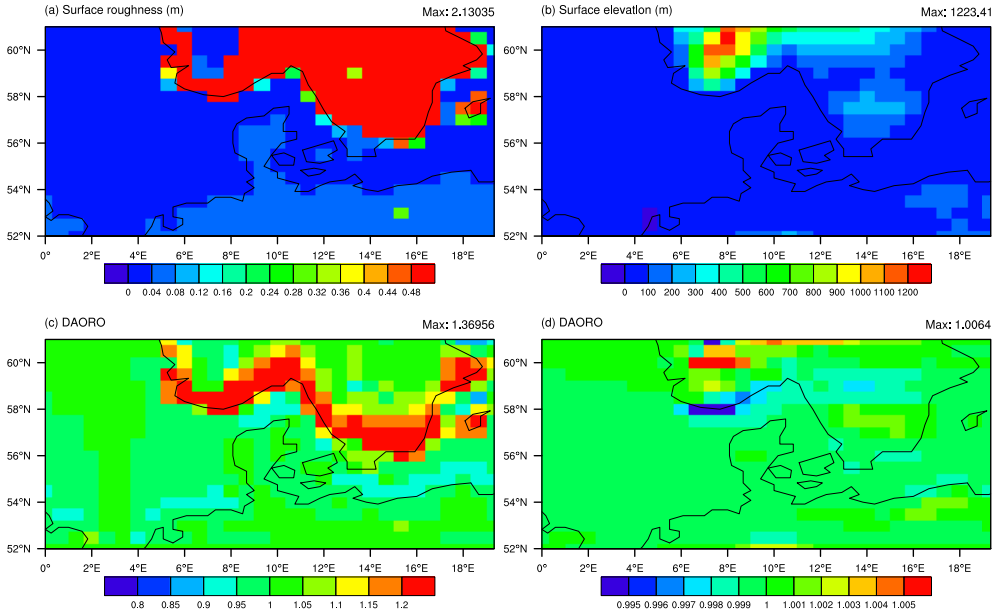

Figure 5.2 – Surface fields: (top-left) Surface roughness length (m), (top-right) surface elevation (m), and generalization parameters: (bottom-left) DAROU (δA_r) and (bottom-right) DAORO (δA_o), for the 180° sector and 100 m height for the MERRA reanalysis.

5.4 Basic generalization equations

We describe here the generalization procedure. In the first step, each center value of wind speed, $u = u(z, \phi)$, and wind direction ,ϕ, is corrected for orography and roughness change, which are a function of wind direction and height. The intermediate values, $\hat{u}$ and $\hat{\phi}$, are given by

$$\hat{u} = \frac{u}{(1 + \delta A_o)(1 + \delta A_r)} \tag{5.1}$$

$$\hat{\phi} = \phi - \delta\phi_o, \tag{5.2}$$

where δA_o, $\delta\phi_o$ and δA_r and are generalization factors for orography in wind speed and direction and roughness change, respectively, described in section 5.3 above.

From the corrected wind speed value we obtain an intermediary friction velocity, $\hat{u}_*$

$$\hat{u}_* = \frac{\kappa\hat{u}}{\ln(z/\hat{z}_0)} \tag{5.3}$$

where z is the height, $\hat{z}_0$ is the downstream surface roughness length for that sector and κ is the von Kármán constant. The stability of the surface layer is not taken into account in these calculations because it is not easily available from the reanalysis data and at the dimensions

of a global model square does not have the same sense as for a local measurement. In the next step, we use the geostrophic drag law, which is used for neutral conditions, to determine nominal geostrophic wind speeds, $\hat{G}$, and wind directions, $\delta\phi_G$, using the intermediate friction velocity and wind direction:

$$\hat{G} = \frac{\hat{u}_*}{\kappa}\sqrt{\left(\ln\frac{\hat{u}_*}{|f|\,\hat{z}_0} - A\right)^2 + B^2}, \tag{5.4}$$

$$\delta\hat{\phi}_G = -sin^{-1}\left(\frac{B\,\hat{u}_*}{\kappa\hat{G}}\right), \tag{5.5}$$

where $A = 1.8$ and $B = 5.4$ are two empirical parameters and f is the Coriolis parameter, and $\hat{\phi}_G$ is the angle between the near-surface winds and the geostrophic wind.

To obtain a new generalized friction velocity, $\hat{u}_{*G}$, for a standard roughness length $z_{0,std}$, Eq. 5.4 is reversed by an iterative method,

$$\hat{G} = \frac{\hat{u}_{*G}}{\kappa}\sqrt{\left(\ln\frac{\hat{u}_{*G}}{f\,z_{0,std}} - A\right)^2 + B^2}, \tag{5.6}$$

Finally, the generalized wind speed, u_G, is obtained by using the logarithmic wind profile law

$$u_G = \frac{\hat{u}_{*G}}{\kappa}\,ln\left(\frac{z}{z_{0,std}}\right). \tag{5.7}$$

It is assumed that the initial sector of the direction bin remains unchanged, because each sector is 30° wide and in only very rare instances $\delta\phi_G$ is larger than $\pm 15°$. This might not the case if more direction sectors are considered and the topography has larger horizontal gradients.

Once a generalized wind speed, u_G, has been found for each direction sector and standard roughness and wind speed bin a Weibull fit is done for each sector and standard roughness.

5.5 Weibull distribution fit

In this section the way the generalized wind speed data is converted into a compact file containing the generalized wind climatology is described. The resulting file is called a WAsP lib-file.

The frequency distribution of the horizontal wind speed can often be reasonably well described by the Weibull distribution function (Tuller and Brett, 1984):

$$F(u) = \frac{k_w}{A_w}\left(\frac{u}{A_w}\right)^{k_w-1}\exp\left[-\left(\frac{u}{A_w}\right)^k\right], \tag{5.8}$$

where $F(u)$ is the frequency of occurrence of the wind speed u. In the Weibull distribution the scale parameter A_w has wind speed units and is proportional to the average wind speed calculated from the entire distribution. The shape parameter $k_w(\geq 1)$ describes the skewness of the distribution function. For typical wind speed distributions, the k_w-parameter has values in the range of 2 to 3.

From the values of A_w and k_w, the mean wind speed $\overline{U}$ ($\mathrm{m\,s^{-1}}$) and mean power density $\overline{E}$ ($\mathrm{W\,m^{-2}}$) in the wind can be calculated from:

$$\overline{U} = A_w \Gamma \left(1 + \frac{1}{k_w}\right) \tag{5.9}$$

$$\overline{E} = \frac{1}{2}\rho A_w^3 \cdot \Gamma \left(1 + \frac{3}{k_w}\right) \tag{5.10}$$

where ρ is the mean density of the air and Γ is the gamma function. We use the moment fitting method as used in the Wind Atlas Analysis and Application Program (WAsP) for estimating the Weibull parameters. The method is described in detail in Troen and Petersen (1989b). Basically this method estimates A_w and k_w to fit the power density in the time series instead of the mean wind speed.

The Weibull fit is done for the ensemble of generalized wind speeds in each wind direction bin (usually 12 direction sectors), each height (50, 100 and 200 m) and each standard roughness lengths (usually 5 roughness: 0.0002 (water), 0.03, 0.1, 0.4, 1.5 m).

This sector-wise transformation of Weibull wind statistics—i.e. transforming the Weibull A_w and k_w parameters to a number of reference heights over flat land having given reference roughnesses—uses not only the geostrophic drag law, but also a perturbation of the drag law, with the latter part including a climatological stability treatment. The transformation and stability calculation is consistent with that implemented in WAsP and outlined in Troen and Petersen (1989b), with further details given in Kelly et al. (2014). The transformation is accomplished via perturbation of both the mean wind and expected long-term variance of wind speed, such that both Weibull-A_w and k_w are affected. When purely neutral conditions (zero stability effects) are presumed for the wind statistics to be transformed, there is still a perturbation introduced, associated with the generalized (reference) conditions in the wind atlas. This perturbation uses the default stability parameter values found in WAsP; it is negated upon subsequent application of the generalized wind from a given reference height and roughness to a site with identical height and surface roughness, using WAsP with its default settings. The climatological stability treatment in the generalization depends on the unperturbed Weibull parameters and effective surface roughness (Troen and Petersen, 1989b), as well as the mesoscale output heights and wind atlas reference heights (though the latter disappears upon application of wind atlas data via WAsP).

In practice, a choice has to be made when regarding whether a correction for the stability has been done or not in the calculation of A_w and k_w for each sector. We set ain_neut = True in the generalization options (i.e. the data has been transformed to neutral stratification) and no correction owing to a mean heat flux is done. The remaining stability-induced correction are done using heat fluxes of -40 $\mathrm{W\,m^{-2}}$ over land and 15 $\mathrm{W\,m^{-2}}$ over water.

5.6 Summary

In this chapter the generalization proceedure has been described. In particular the way the method has been adapted for the generalization of reanalysis data is highlighted. Also outlined is the way the generalized wind climatology is processed and formatted to be made ready for application in the microscale modelling.

Contributing authors Andrea N. Hahmann, Jake Badger

Chapter 6

Local wind climates

In this chapter the microscale modelling is described. It is here that the downscaling from the generalized wind climates to the local climates is performed every 250 m. This very large area calculation is run by a system of software and servers called Global Wind Atlas Frogfoot. The method is very similar to that used in the WAsP software. For example, the flow modelling for orography, roughness and roughness change is the same as in the WAsP software. However, the Global Wind Atlas calculation differs in a number of ways in order to allow a very large area to be covered. For example, local wind climate calculations are based on more than a single generalized wind climate, and terrain data is input as raster maps rather than vector maps.

6.1 WAsP microscale effects

6.1.1 Orography

The WAsP software contains flow models for orography, roughness and roughness change effects, and obstacles. In the Global Wind Atlas obstacles are not included.

Schematic diagrams Fig. 6.1 illustrate the change of wind flow caused by a hill. The maximum speed-up is at the top of the hill, the magnitude of the speed-up and the height above surface of the maximum speed-up is related to the geometry of the hill. WAsP uses the BZ-model (Troen, 1990) to calculate the orographic speed up. The flow model uses a high-resolution, zooming, polar grid, centered on the calculation node. More details can be found in Troen and Petersen (1989b).

6.1.2 Roughness

Surface roughness length, z_0, is a property of the surface which can be used to determine the way the horizontal wind speed varies with height, assuming a homogeous surface and neutral stability, according to

$$u(z) = \frac{u_*}{\kappa} \ln(z/z_0)$$

where z is the height above surface and κ is the von Kármán constant. Figure 6.2a shows the influence roughness has on the vertical profile of wind speed assuming the same large-scale

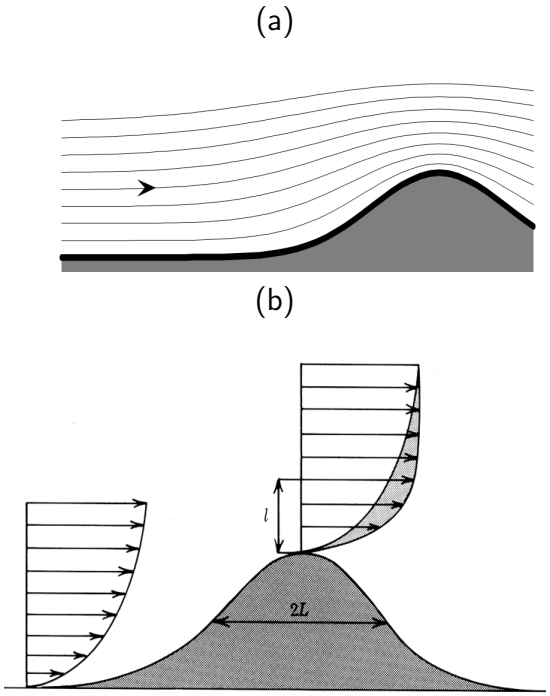

Figure 6.1 – (a) Streamlines of winds flowing over a hill. The more closely spaced streamlines at the top of the hill are associated with a speed up of the winds. (b) The vertical profile of wind speed upwind and on top of a hill, from Troen and Petersen (1989b). The speed-up is a function of height above the surface. The height of maximum speed up (l) is related to the geometry of the hill.

wind forcing. The wind speed at a given height decreases with increasing surface roughness. The equation above and the figure assume a homogeneous surface over several kilometers. However it is very common to have a heterogeneous surface and this complicates the vertical profile somewhat. Internal boundary layers develop and the profile of wind speed departs from the logarithmic wind profile.

Figure 6.2b shows an example of the vertical profile of wind speed 4 km downwind of a surface roughness change from 0.02 cm to 20 cm. The wind speed profile does not change at all heights immediately downwind of the roughness change. At first, only the lowest parts of the profile change, with the change progressively reaching higher and higher with increasing downwind distance from the roughness change. The impact of a roughness change can be felt many kilometers downwind. As a rule of thumb, at 100 m above the terrain a surface roughness change 10 km upwind may still have an influence on wind speed.

The WAsP roughness change model can account for these internal boundary layer effects due to inhomogeneous surface roughness. More details can be found in Troen and Petersen (1989b).

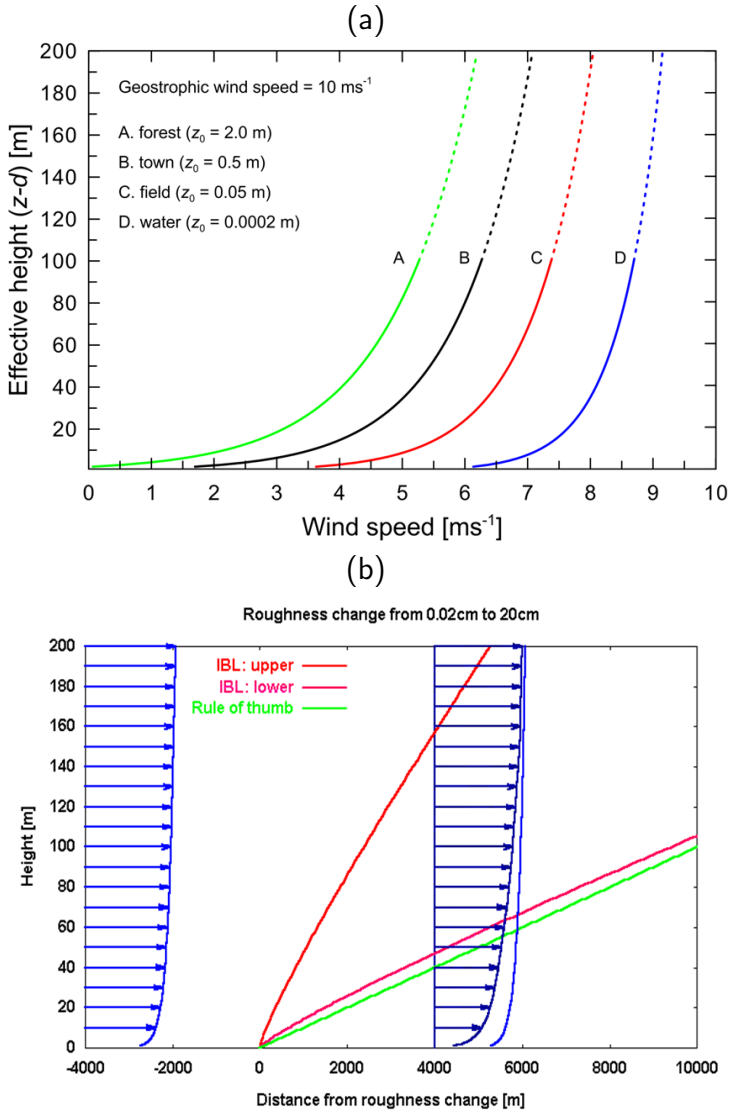

Figure 6.2 – (a) Different surface roughness lengths result in different vertical profiles of wind speed. The y-axis is height above surface and the x-axis is wind speed. For a range of surface roughness lengths, the curves show the wind speed profile for neutral conditions and a geostrophic wind of 10 m s^{-1}. (b) This graph illustrates how a roughness length change (at $x = 0$) impacts the downwind profile of wind speed. For $x < 0$ the roughness length is 0.02 cm, for $x > 0$ the roughness length is 20 cm. The two red lines show the heights of the internal boundary layers. The upper red line shows the height below which the wind profile departs from the 0.02 cm roughness profile. The lower red line shows the height where the profile is adjusted to the 20 cm roughness profile.

6.2 The calculation system

The calculation system used for the Global Wind Atlas is called Frogfoot. It has been developed in association with the software development company World In A Box http://www.worldinabox.eu/index.html . The motivation for the development of Frogfoot was to allow high resolution WAsP-like calculations of predicted wind climates to be made over large areas, using a large number of generalized wind climates. This need came about because of numerical wind atlases being carried out on nation-wide scale which generated generalized wind climates on a grid with a spacing of, typically, 5 km.

As stated before, the Frogfoot system employes the same flow modelling as WAsP. Unlike the present WAsP, the terrain description can be input using raster maps, rather than vector maps. This is convenient for the Global Wind Atlas calculation because typically the global topographical data is in raster formats. Unlike the present WAsP, the starting point for describing the large scale wind forcing is any number of geographically distributed generalized wind climate files (lib-files), whereas WAsP can only use one.

6.2.1 Frogfoot

Frogfoot is a system of programs and interlinked servers developed and set up to allow for very large geographical coverage of high-resolution wind resource maps, with inclusion of changing large-scale wind forcing and microscale flow effects.

The core components of the Frogfoot system are:

- Terrain Service
- Climate Service
- Job Service
- Results Service
- WAsP Worker

Ancillary components are:

- Job Management Console
- Climate Data Manager
- Results Exporter

The core components are essential to carry out a Frogfoot calculation. The ancillary components are needed to set-up the configuration of a Frogfoot job, as well as import and export data into or out of the system.

The framework of Frogfoot can be understood by considering the elements required to carry out a WAsP calculation of a predicted wind climate at a single location. These elements are generalized wind climate data, roughness and orography data (in the form of maps) for the area around the location of interest, and flow models inside the WAsP software. The roughness and orography data is used by the flow models to determine flow effects at the location, and these flow effects are used to modify the generalized wind climate. These elements are also

represented in the Frogfoot core components, see Fig. 6.3. For Frogfoot though, instead of considering a single point, the Job service dispatches a very large number of points within an area of interest to be calculated.

For any particular application of Frogfoot, the Job Service is set up by the Job Management Console. Here the user specifies the map data to be used, selected from map data inside the Terrain Service. Here the user also specifies the generalized wind climate data to be used, selected from generalized wind climate data inside the Climate service. The generalized wind climate data consists of a number of geo-referenced WAsP generalized wind climate files.

Within the Job Management Console the definition of the area to be calculated is specified, by a map containing a single closed contour outlining the boundary of the calculation area. The user also needs to set the grid spacing and origin of the calculation nodes. The Job Management Console will then split the job into a number of tiles which are 10 x 10 calculation nodes in size (i.e. 100 calculation nodes in all). A tile makes up a set of calculations that will be dealt with separately by distribution of the tile to a WAsP Worker. The WAsP Worker is a standalone installation of the WAsP flow models, without the user interface.

In order for the WAsP Worker to calculate the predicted wind climate at the 100 nodes, tile maps of roughness and orography are prepared by the Terrain Service. The maps are given an extent sufficient for the tile by extending the map boundary with a 25 km buffer around the extent of the tile.

The calculation also needs generalized wind climate data. This is provided by the Climate Service in the form of 100 lib-files (one for each calculation node). For each calculation node a libfile is calculated by the Climate Service based on an interpolation of the 3 nearest libfiles from the selected generalized wind climate dataset. The interpolation weighting of the libfiles is inversely proportional to distance. For each direction sector the wind speed distribution is calculated, based on the weighted combination of the Weibull distributions for the 3 nearest libfiles, then with this a new Weibull fit is performed to provide the Weibull parameters for the interpolated libfile.

Figure 6.3 shows how the different components are related to each other and the flow of data from one component to the next. Screen shots of the components are shown in Fig. 6.4. The Job Service feeds tile data to the WAsP workers. The WAsP workers are installed on computers within the same local area network as the Frogfoot servers. Once the WAsP worker has finished the calculations for one tile, the tile results are sent to the Results Service. The Job Management Console allows users to get an overview of the current jobs running on the system, as well as jobs that have been completed or paused. Once the Frogfoot job has completed, the Result Exporter is used by the user to export output in the desired format for subsequent analysis or plotting.

6.2.2 Setting up the global calculation

In order to carry out the Global Wind Atlas calculaton a convenient way of breaking the globe into managable size blocks was required. The Military Grid Reference System (MGRS) provided the basis of the job structure, see Fig. 6.5.

Still the MGRS zones were too big, so these were divided into 4 pieces, to make what is called a job tile. The result is a total of 4903 job tiles. However, in order to cover land and 30 km offshore, 2439 job tile are needed. In Fig. 6.6 the Global Wind Atlas Frogfoot job tile layout is show in Google Earth.

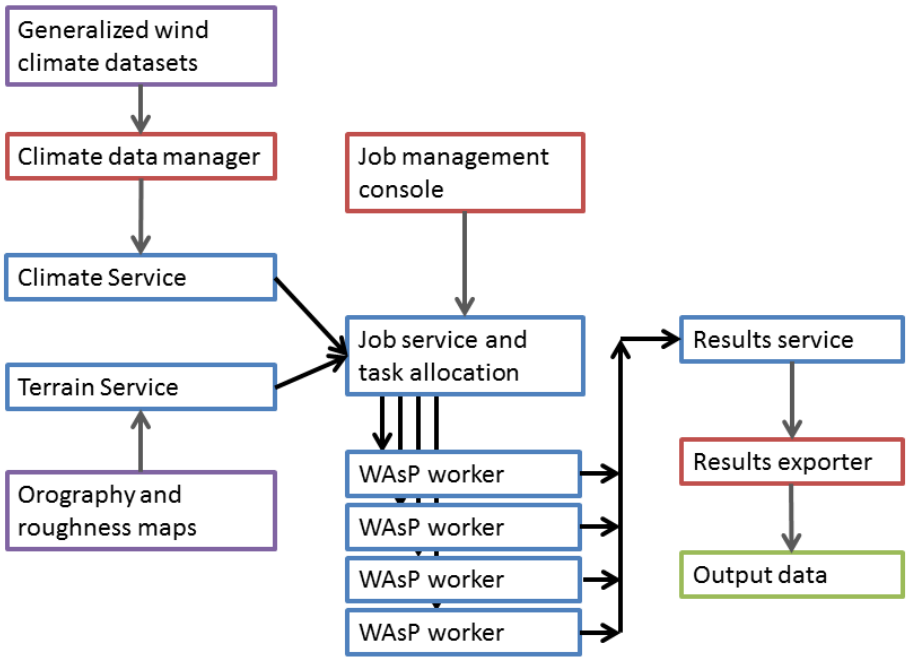

Figure 6.3 – Schematic diagram showing the relationship and flow of data between the components of the Frogfoot system. Blue boxes represent core components of Frogfoot, red boxes represent ancillary components, purple boxes represent data that is input into the system, and the green box represents the result outputs.

For the 2439 job tiles the necessary Frogfoot input data are prepared. This entails preparation of 2439 orography and surface roughness maps on the calculation projection system (Universal Tranverse Mercator), and preparation of calculation inclusion maps, in order to limit the calculation to land and 30 km offshore.

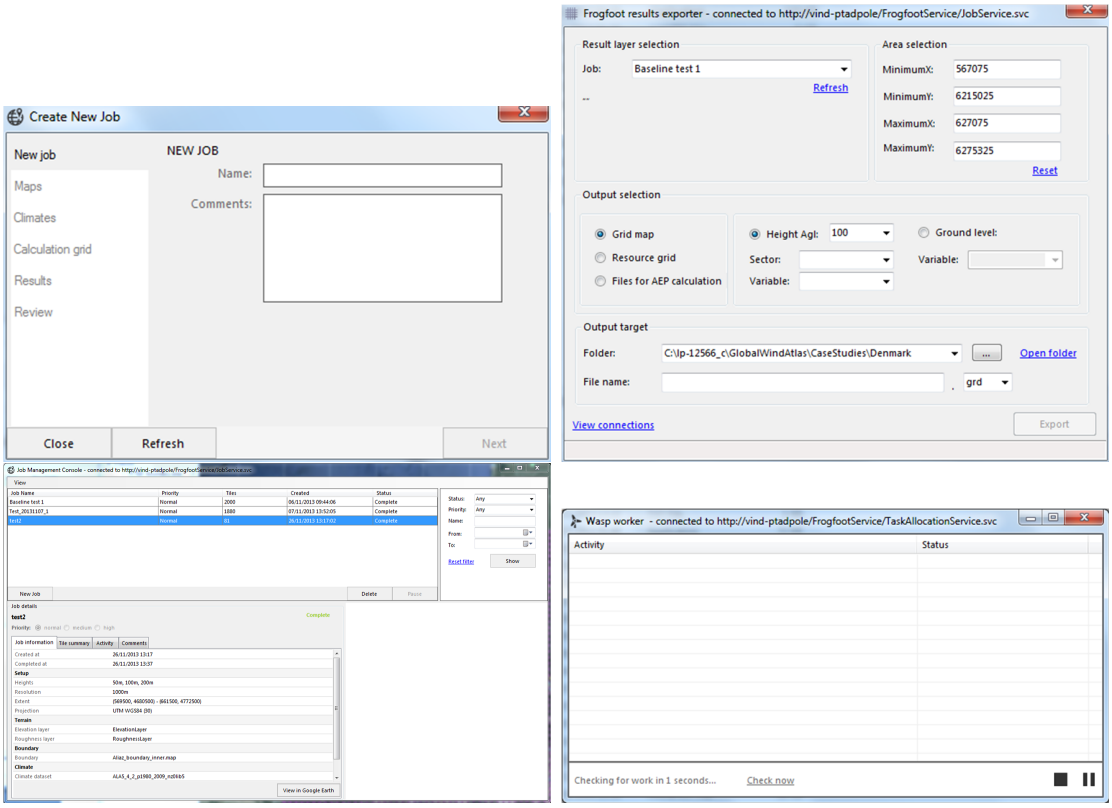

Figure 6.4 – Examples of components of the Frogfoot system. Starting at the top left and going clockwise, are shown, the Job Set-up, Results Exporter, WAsP Worker, Job Management Console.

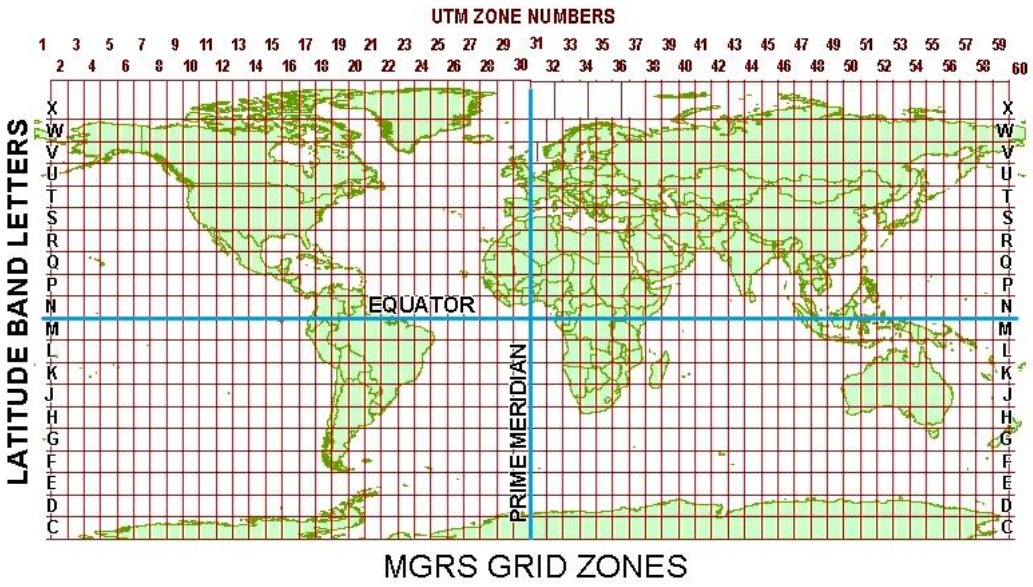

Figure 6.5 – Layout of the Military Grid Reference System (MGRS) zones over the globe. From http://earth-info.nga.mil/

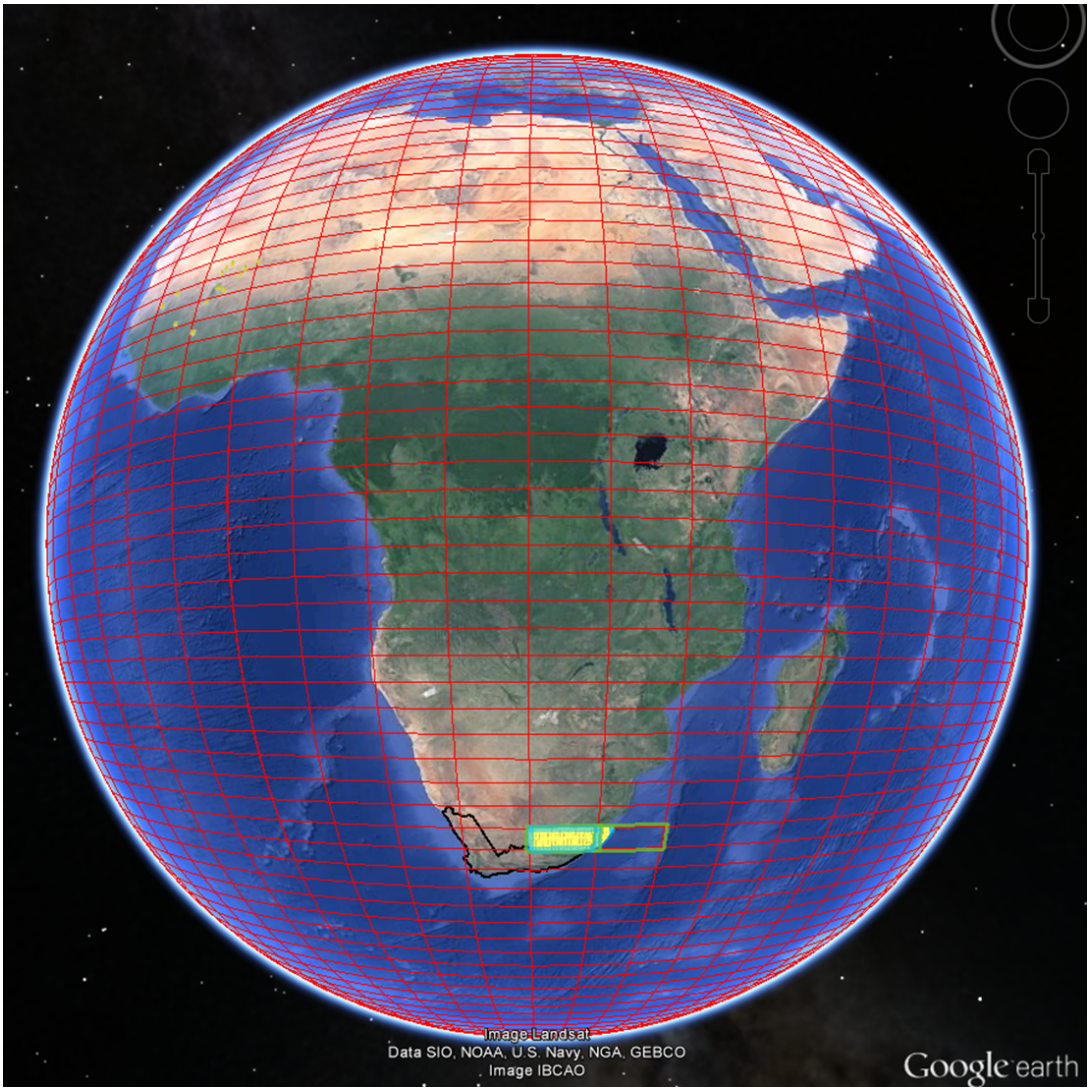

Figure 6.6 – Google Earth image showing the breakdown of the globe into Global Wind Atlas job tiles (red rectangles). Two job tiles are highlighted in South Africa, with the smaller WAsP Worker calculation tiles shown in yellow. Calculations are performed on or within 30 km of land.

6.3 Summary

In this chapter the microscale modelling system has been described. Its similarities to the WAsP software in terms of the flow modelling are highlighed. Its differences to the WAsP software, in terms of ability to cover large areas, use multiple lib-files, use raster topography maps, are outlined. The Frogfoot calculation system and the job tile configuration for the Global Wind Atlas are described.

Contributing authors Jake Badger, Niels G. Mortensen

Chapter 7

Validation

In this chapter validation of the elements of the Global Wind Atlas are described. The large spatial coverage of the Atlas means that validation is a challenge as the number of data points in relation to the number of measurement points is very large. We address this issue by considering validation in number of ways.

We can validate Global Wind Atlas winds against remote sensing data from Synthetic Aperture Radar (SAR). This method gives maps of wind climate data over large areas, in a way an output similar to the Global Wind Atlas. The limitations of this method include that only offshore areas can be mapped, and the extrapolation of wind speeds to Global Wind Atlas heights introduces uncertainty.

We can validate Global Wind Atlas winds against numerical wind atlas results from other projects. This has the advantage that the validation can be done over land. The limitation of this method is that a comparison is being made against results of modelling, so it is not a comparison against measurements.

For locations where there are measurements, validation is possible at the location, but the challenge then is to infer what is gained from that validation to all other locations. We can also validate Global Wind Atlas winds against high resolution resource maps generated from measurement based generalized winds.

This chapter attempts to give a qualitive and quantitative assessment for the validation of the Global Wind Atlas. It is important to note that the verfication is not stating whether one reanalysis dataset is better than another. It is instead a comparative assessment of the result of the generalization of the reanalyses and the high resolution modelling. So any poorer performance must be seen in this large context. Improvement in the generalization methodology, or changes to the surface topographical description would alter the results.

7.1 Synthetic aperture radar ocean derived winds

Synthetic Aperture Radar (SAR) data were used to validate Global Wind Atlas outputs over coastal seas where DTU Wind Energy has collected SAR scenes through previous projects. Additional scenes were downloaded and processed for the seas around South Africa.

The areas used for validation of offshore winds are:

- Scandinavia (Hasager et al., 2015b)

- Iceland (Hasager et al., 2015a)
- Italy (Calaudi et al., 2013)
- Aegean Sea (Badger et al., 2015)(Bingöl et al., 2013)
- The Great Lakes (Doubrawa et al., 2015)
- Southern China (Chang et al., 2015)(Chang et al., 2014)
- South Africa

This section describes the SAR data and the applied procedure for retrieving winds and wind resource maps from SAR at the standard level of 10 m above sea level.

7.2 Satellite SAR data

SAR data were obtained from the European Space Agency (ESA). The gateway to accessing ESA data is http://earth.esa.int/. Approximately 15,000 scenes from the Envisat ASAR mission in 2002-11 were selected from DTU's archive to be used for the Global Wind Atlas validation. All the SAR scenes were acquired at C-band with either vertical or horizontal polarization in transmit and receive (i.e. VV or HH polarization).

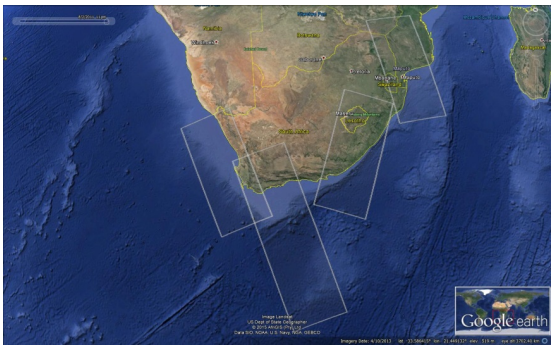

Figure 7.1 – Examples of the Envisat ASAR coverage over South Africa for four individual scenes. Image courtesy Google Earth.

Envisat was a polar-orbiting satellite scanning the Earth surface in a 400-km swath. A scene represents a fraction of the swath and can be several hundreds of km long but with a fixed width of 400 km (Fig. 7.1). The SAR principle of operation is that radar pulses are transmitted towards the Earth surface. The proportion of backscattered signal determines the image brightness and it depends on the surface properties as well as the radar viewing geometry. Over ocean surfaces, the return signal is mainly determined by Bragg scattering (Valenzuela, 1978) from capillary and short-gravity waves, which have wavelengths proportional to the radar wavelength. These waves are wind-generated and there is thus a relationship between the instant wind speed and the radar backscatter. In order to eliminate effects of longer-period waves and random noise in the SAR images, pixels are averaged to 500 m or larger cells before the wind retrieval.

7.3 SAR wind retrieval

Geophysical Model Functions (GMFs) are empirical equations for the backscatter-to-wind relationship, which are originally developed for scatterometers (Stoffelen and Anderson, 1997) , (Quilfen et al., 1998) . If the wind direction is known, these equations can be used to retrieve the wind speed from SAR observations (Monaldo et al., 2004) , (Dagestad et al., 2012) . Here we used the GMF called CMOD5.n (Hersbach, 2010) to retrieve Equivalent Neutral Winds (ENW) at 10 m. The winds represent neutral atmospheric conditions. The wind retrieval processing was performed with the APL/NOAA SAR Wind Retrieval Software (ANSWRS) with input wind directions from the US Navy Operational Global Atmospheric System (NOGAPS). The model wind directions were available at 6-hourly intervals with 1 $^\circ$ latitude and longitude resolution and they were interpolated spatially to match the SAR data. Figure 7.2 shows examples of retrieved SAR wind maps over South Africa.

For areas poleward of 50° latitude a sea ice mask was applied to filter out ice covered seas where the SAR wind retrieval could not be trusted. Ice mask data from the IMS Daily Northern Hemisphere Snow and Ice Analysis at 4 km Resolution by the US National Ice Center (http://nsidc.org/data/docs/noaa/g02156_ims_snow_ice_analysis/) were used to eliminate areas with ice cover.

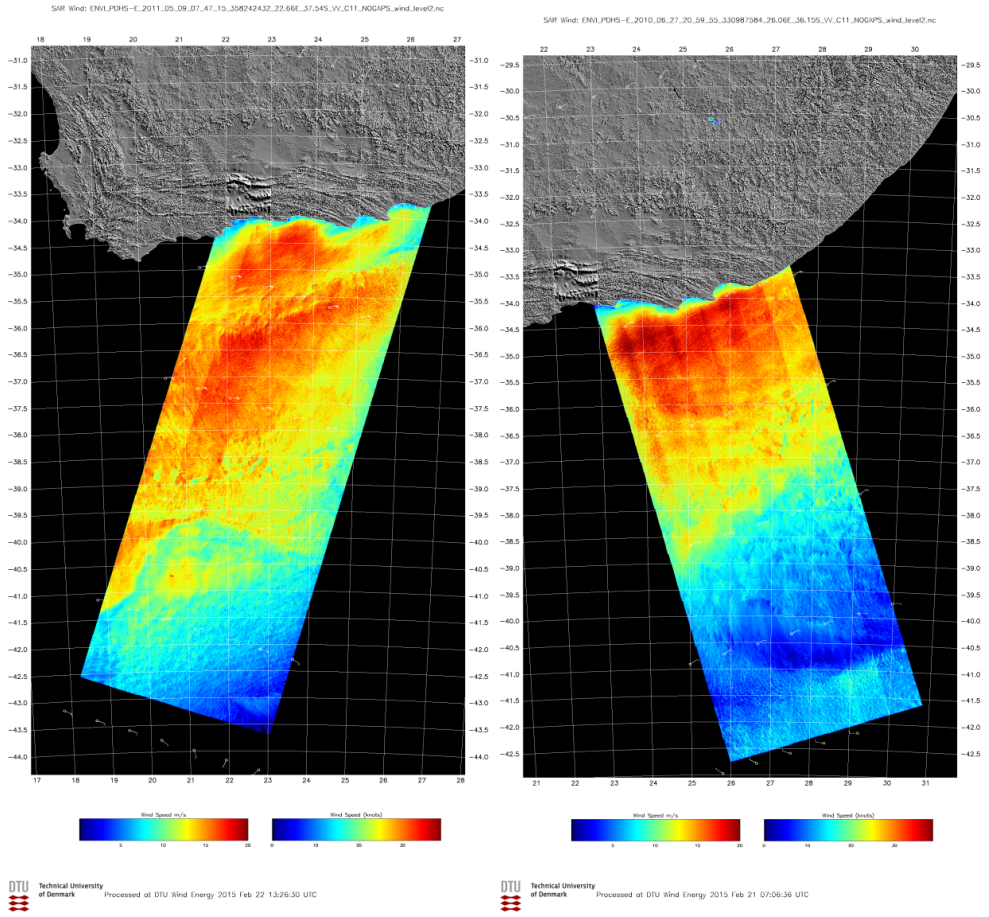

Figure 7.2 – Two examples of wind fields retrieved from Envisat ASAR over South Africa. Left: morning pass acquired May 9, 2011 at 07:47 UTC; right: evening pass acquired June 27, 2010 at 20:59 UTC. Wind barbs indicate the model wind vectors from NOGAPS.

7.4 SAR Wind resource mapping

For each validation area, all available SAR wind maps were combined in a statistical analysis in order to map the offshore wind resources. The data was first insert into a MySQL data base and organized into 1-km grid cells. Once the data is stored in the data base it can easily be retrieved based on criteria for location and time coverage. The tool S-WAsP by DTU handles the insert procedure, the data retrieval, as well as computation of wind resource statistics. The entire processing chain needed to transform raw SAR observations to wind resource maps is illustrated in Figure 3.

Over each focus area, a Weibull function was fitted to the data points available for each cell in a 0.02 degree latitude and longitude grid. This gave maps of the mean wind speed, Weibull shape and scale parameters, and wind power densities as well as uncertainty estimates for the 10-m level.

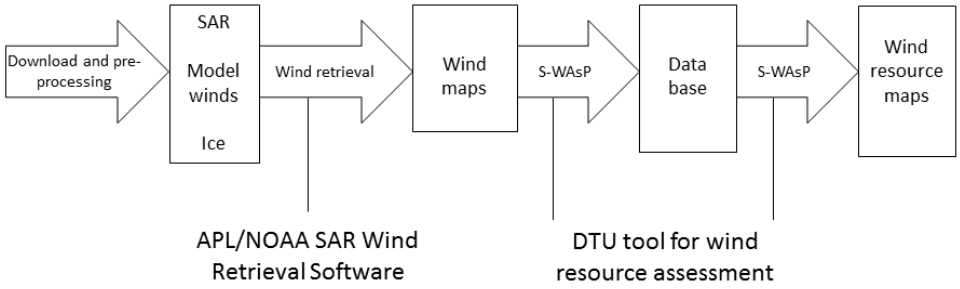

Figure 7.3 – The processing chain for SAR wind retrieval and resource mapping.

7.5 SAR case study results

The SAR winds are given at 10 m above the sea surface. The winds are extrapolated to 100 m above the surface by using the logarithmic law and a surface roughness of 0.2 mm. This assumes a neutral profile and a single water roughness. Both assumptions are likely to cause uncertainty in the estimation of the SAR 100 m winds. An improved method, that corrects for the effects of a distribution of boundary layer stability is the subject of ongoing research. A scientific paper which describes the method is in review.

7.5.1 Scandinavian Seas

Figure 7.4 shows the MERRA reanalysis wind interpolated to 100 m above surface, the Global Wind Atlas winds at 100 m, and the SAR winds at 100 m. The MERRA winds tend to be comparatively lower in the offshore coast regions, whereas the Global Wind Atlas winds are higher close to the coastline. The SAR results suggests slighly lower winds in the Danish inners seas, and a more gradual change in wind speeds off coastlines compared to the Global Wind Atlas.

7.5.2 Aegean Sea

Figure 7.5 shows the MERRA winds tend to be comparativily lower in the region, whereas the Global Wind Atlas winds and even more so the SAR winds are indicating higher winds. The SAR results show very noticable enhanced winds in the gaps between islands, and some headland areas on Turkey west coasts. The Global Wind Atlas is missing these features, having a more homogeneous wind speed. The reason these features are missing is that the reanalysis model is too coarse to capture the terrain of the islands and headland features that cause the enhanced wind speed. This aspect of missing mesoscale variability is something that occurs in other examples in this chapter.

7.5.3 The Great Lakes

Figure 7.6 shows the MERRA and Global Wind Atlas winds tend to be weaker than the SAR winds are indicating. Near the shoreline the disagreement between the Global Wind Atlas and SAR winds is lesser, but in the interior of the Great Lakes, the difference is large. The reason for these differences needs to be investigated further. Later in Fig. 7.20 it can be seen that

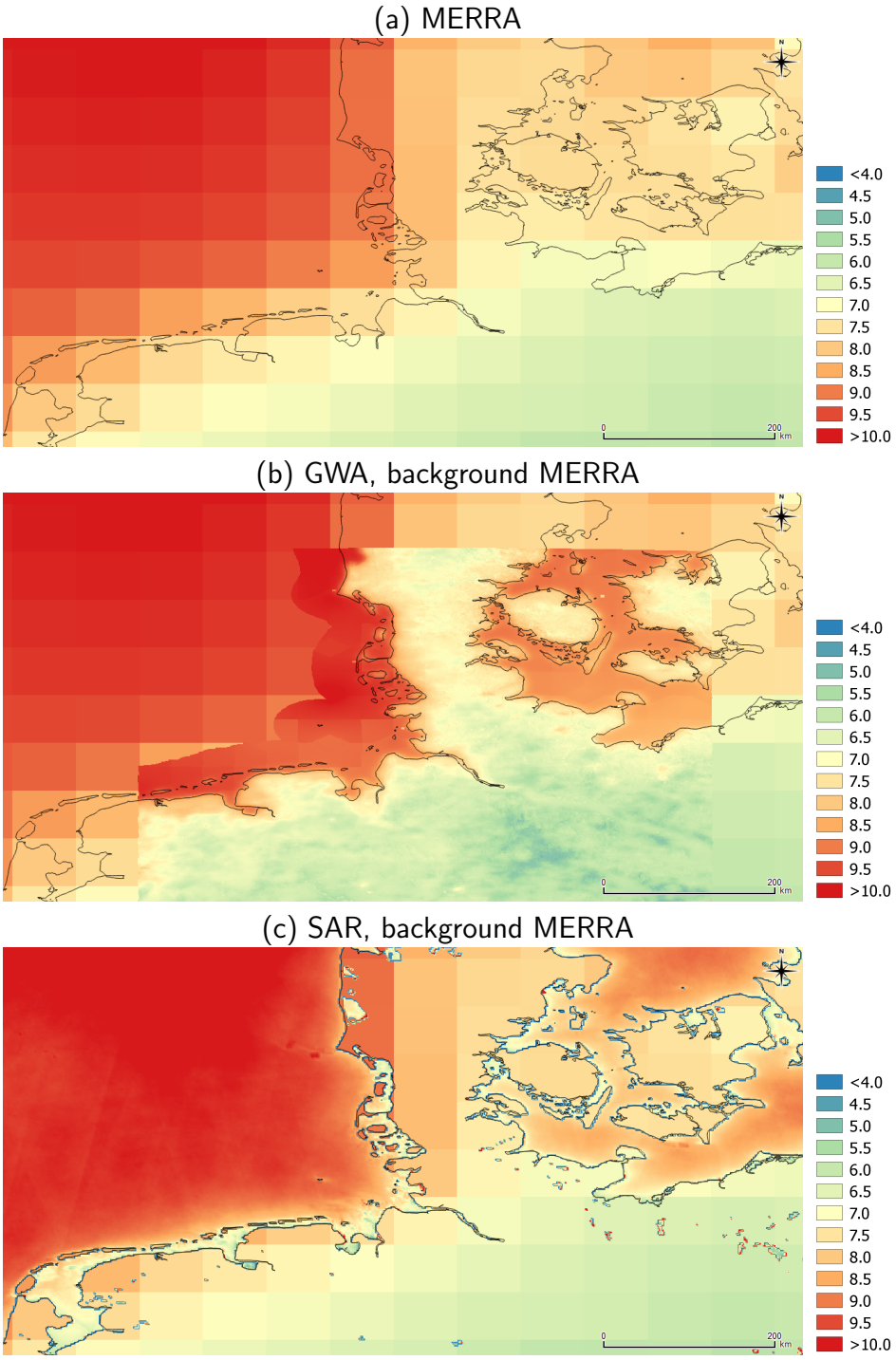

Figure 7.4 – Selected area within Scandinavian seas showing 100 m winds [$\mathrm{m\,s^{-1}}$] from MERRA, from the Global Wind Atlas and from SAR. (a) MERRA 100 m winds, (b) Global Wind Atlas 100 m winds, and (c) SAR 100 m wind. In (b) and (c) MERRA 100 m winds are given in the background to allow comparison at the edge of the Global Wind Atlas and SAR winds.

(a) MERRA

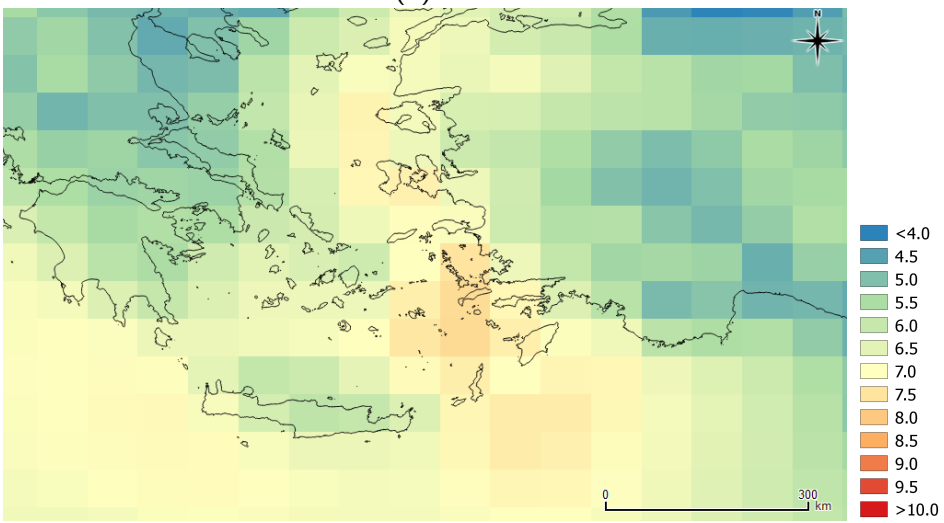

(b) GWA, background MERRA

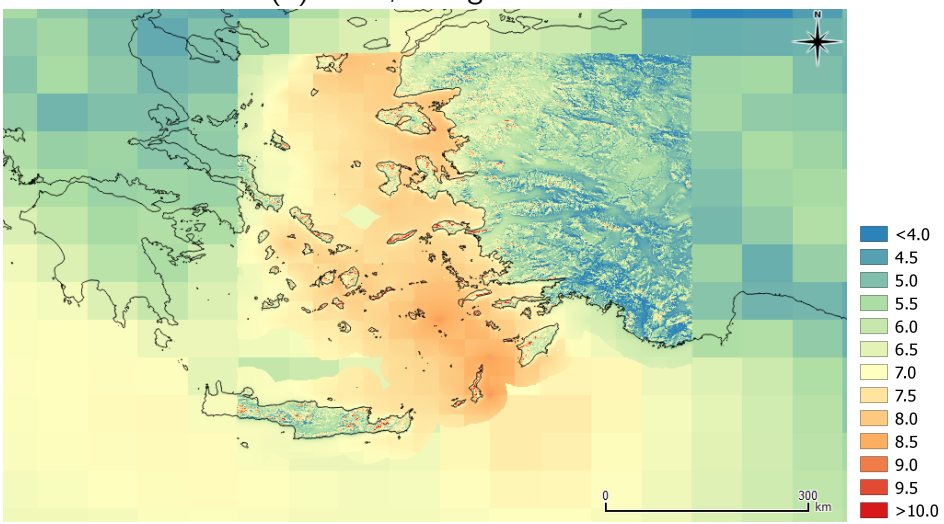

(c) SAR, background MERRA

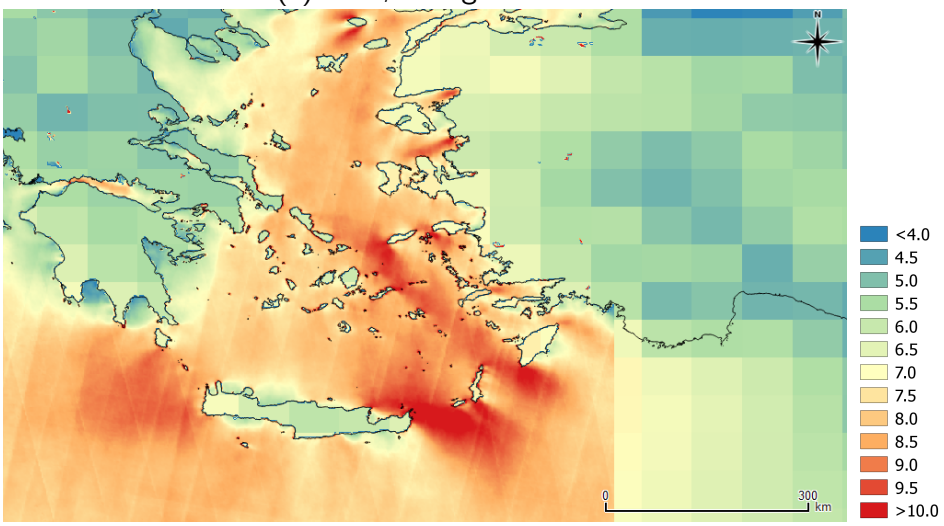

Figure 7.5 – Aegean Sea, otherwise the same as Fig. 7.4.

none of the reanalysis data suggest such high winds over the Great Lakes. This may point to the issue being how the 100 m SAR winds are extrapolated, in particular stability and surface roughness may diverge from the used assumptions. Also the sampling of the SAR scenes is the area could favour seasons with higher winds (winter). In Doubrawa et al. (2015) a method which corrects for any season bias in the same collected images, shows annual mean winds more in line with the reanalysis and Global Wind Atlas winds.

7.5.4 Southern China Sea

Figure 7.7 shows MERRA winds tend to be comparativily lower in the offshore coast regions, whereas the Global Wind Atlas winds are higher close to the coastline. The SAR results suggests slighly higher winds. The South China Sea is in the tropics and has with a high sea surface temperature. This induces unstable atmospheric conditions and deviations from the neutral wind profile assumption.

7.5.5 South Africa, Western Cape coast

Figure 7.8 shows MERRA winds tend to be comparativily lower, whereas the Global Wind Atlas winds are higher close to the coastline. The SAR results suggests much higher winds off the western most part of the Western Cape, but similar winds close to the coastline elsewhere. The high winds indicated by SAR off the western most part of the Western Cape could be due to mesoscale spatial variability and the influence of the cold Benguela Current. Another perspective is that this cold current creates a large departure from the assumption of neutral stability used for the extrapolation of SAR winds to 100m, there by adding a bias to the SAR winds estimate.

(a) MERRA

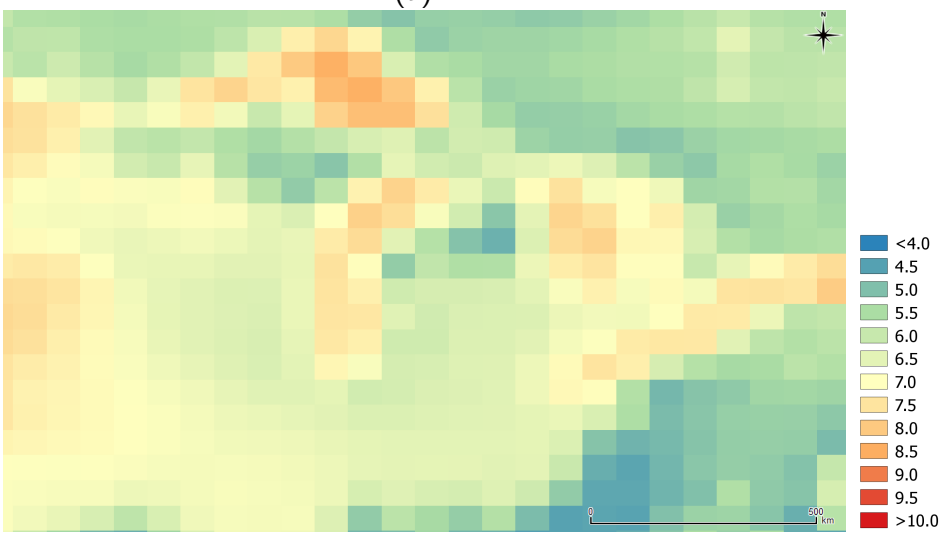

(b) GWA, background MERRA

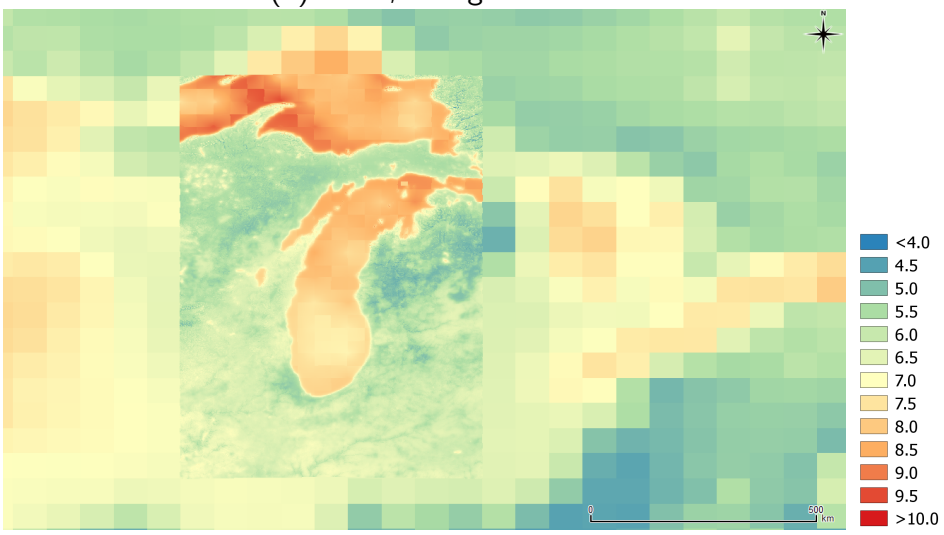

(c) SAR, background MERRA

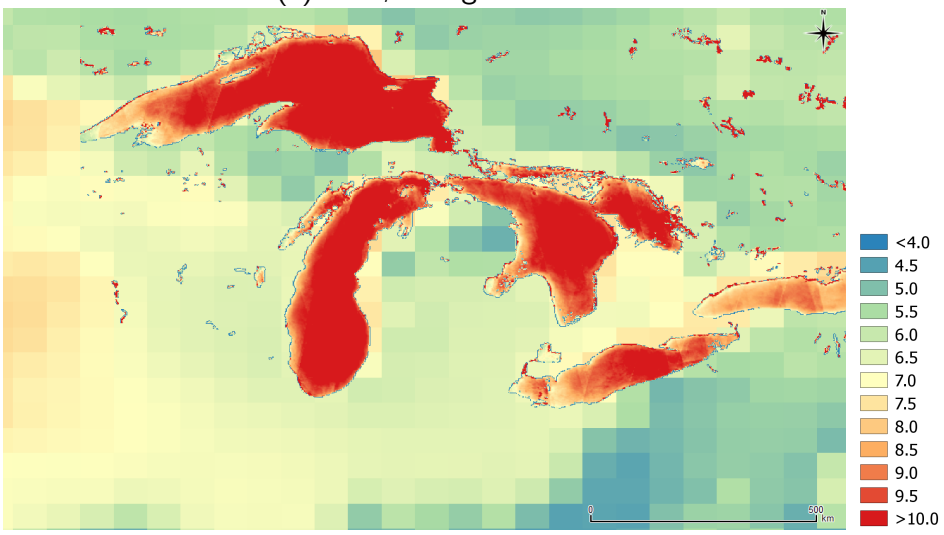

Figure 7.6 – Great Lakes, otherwise the same ass Fig 7.4.

(a) MERRA

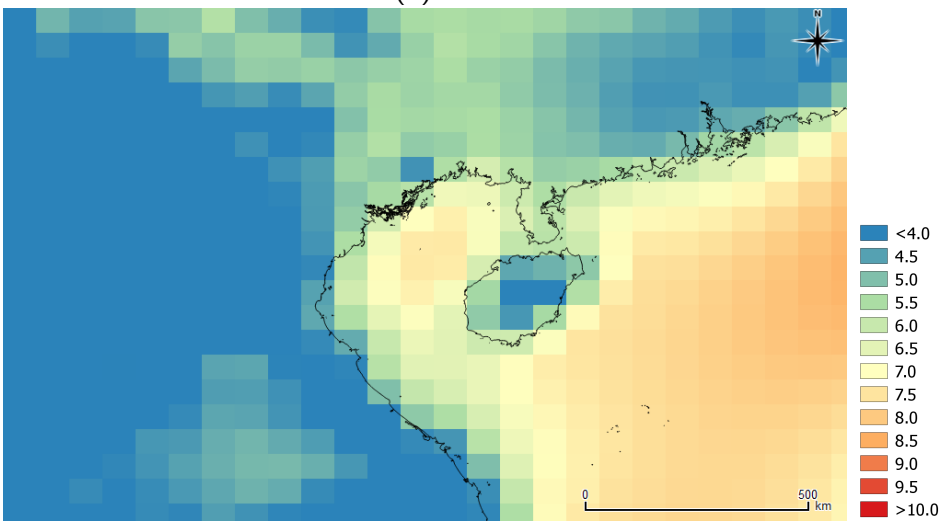

(b) GWA, background MERRA

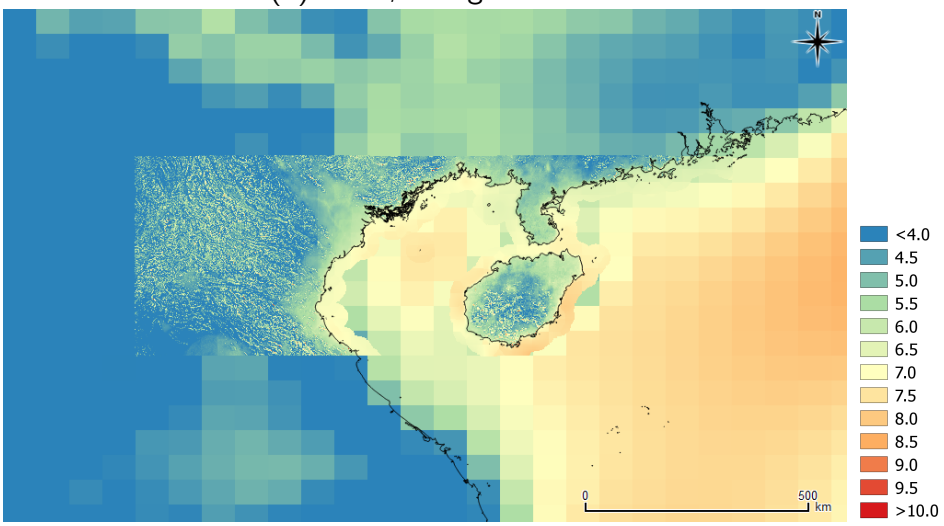

(c) SAR, background MERRA

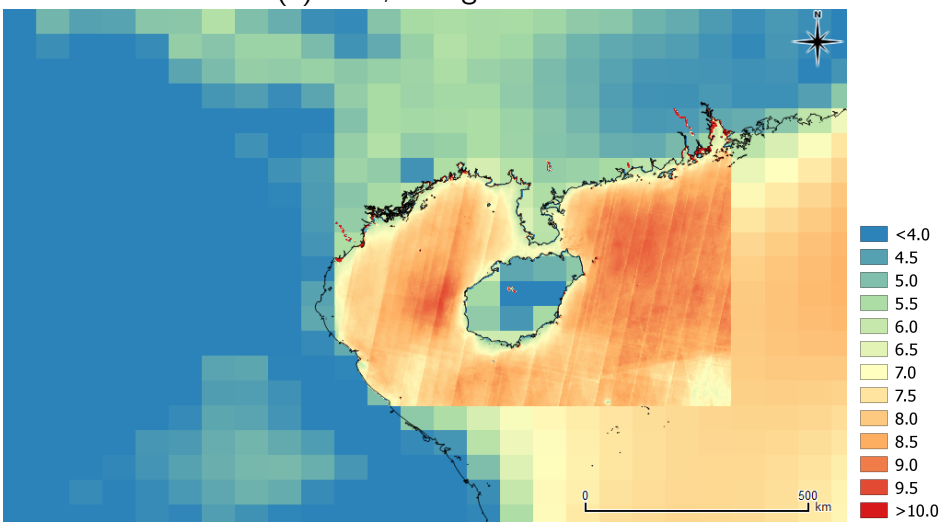

Figure 7.7 – Southern China Sea, otherwise the same ass Fig 7.4

(a) MERRA

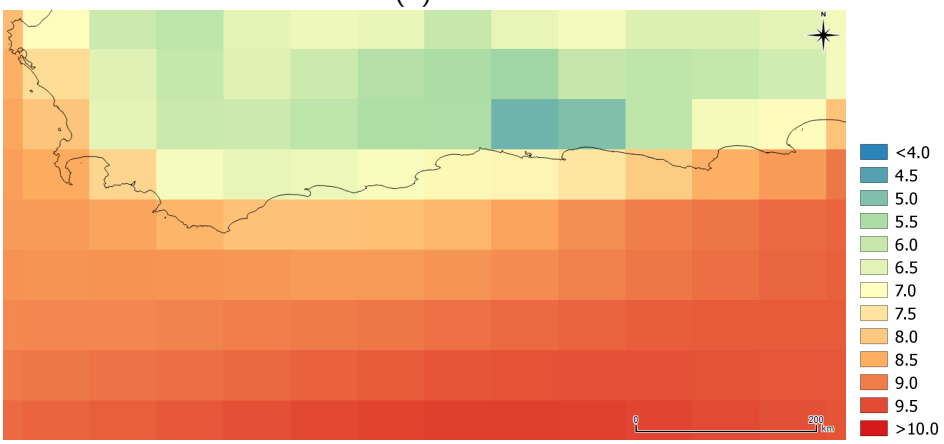

(b) GWA, background MERRA

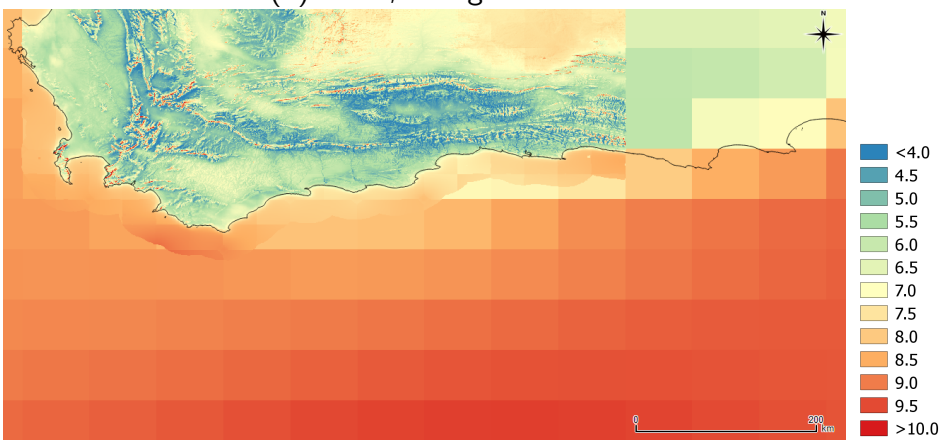

(c) SAR, background MERRA

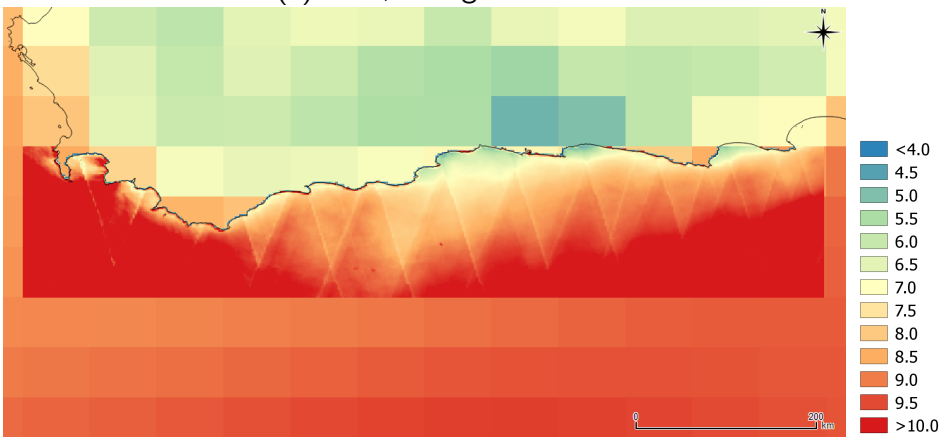

Figure 7.8 – South Africa, Western Cape coast, otherwise the same ass Fig 7.4

7.6 Reanalysis comparison

In this section, high resolution results from the Frogfoot system are compared for a number of different regions. The wind speed and power density are compared in two ways. The first is to compare exact grid point location results with each other. The second is to compare the ranked results. This method puts less emphasis on where precisely the wind resource is, but tests how the distribution of wind resource is captured in the test area.

7.6.1 Alaiz

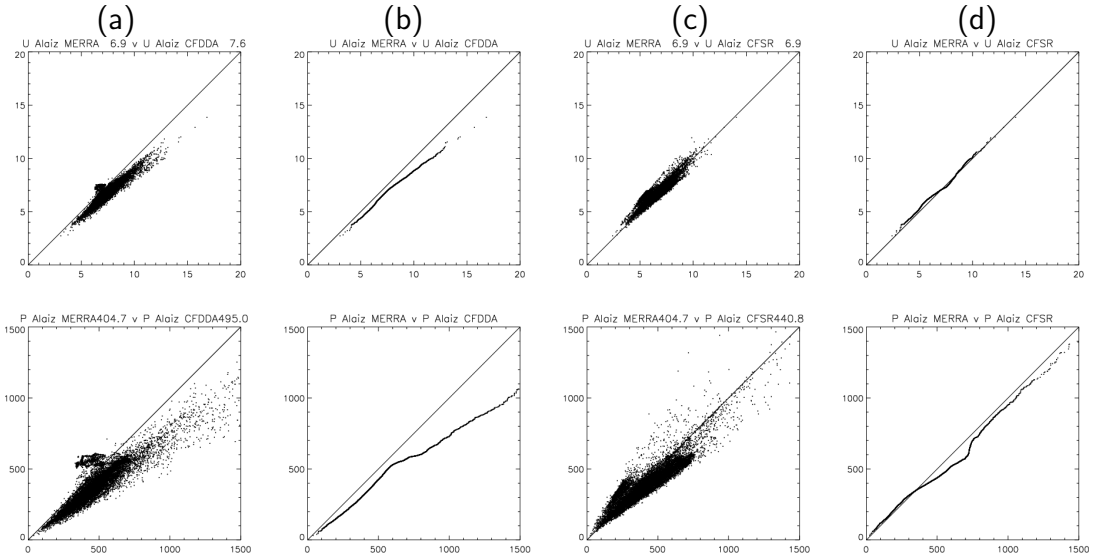

Figure 7.9 – Alaiz region case (30T-1) 100 m wind speed [$\mathrm{m\,s^{-1}}$] (upper) and wind power density [$\mathrm{W\,m^{-2}}$] (lower) scatter plots comparing Frogfoot results from different reanalyses. (a) and (b) MERRA v CFDDA, (c) and (d) MERRA v CFSR. In (a) and (c) the grid point to grid point scatter plot is given. In (b) and (d) the ranked values are plotted against each other.

The Alaiz test area is composed of Global Wind Atlas job tile 30T-1. The location is northern Spain. Figure 7.9 shows that in the lower portion of the wind power density distribution, results from the MERRA and CFDDA are not so different, however for higher power sites the generalized CFDDA gives higher powers than the generalized MERRA. The power density distributions of the MERRA and CFSR based results are rather similar, over the entire range.

7.6.2 Denmark

The Denmark test area is composed of Global Wind Atlas job tile 32U-4. Figure 7.10 shows that the results from the MERRA and CFDDA are not so different. The power density distribution of the MERRA and CFSR based results show a tendency for the CFSR based results to have higher power.

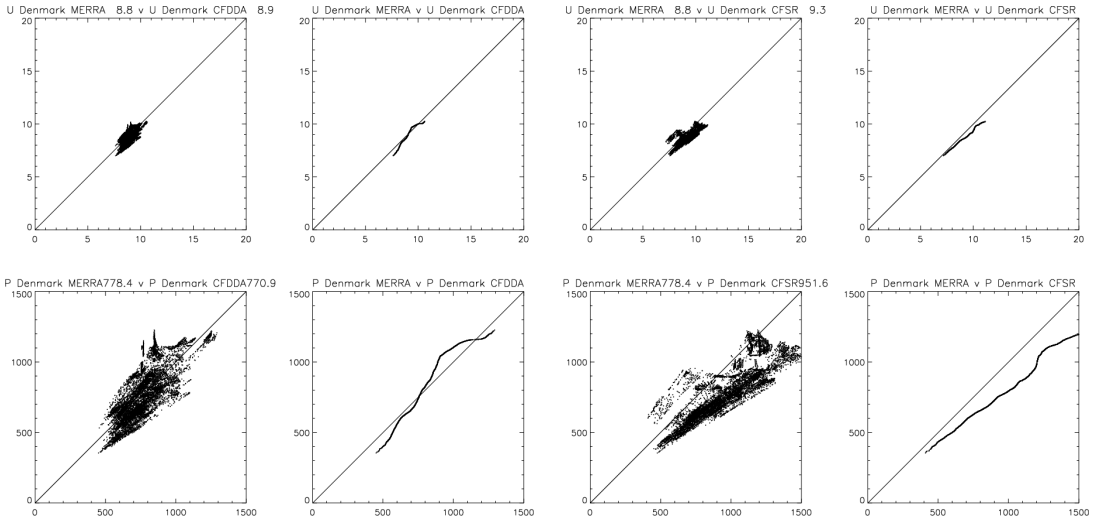

Figure 7.10 – Denmark region case (32U-4), otherwise same as 7.9

7.6.3 Egypt

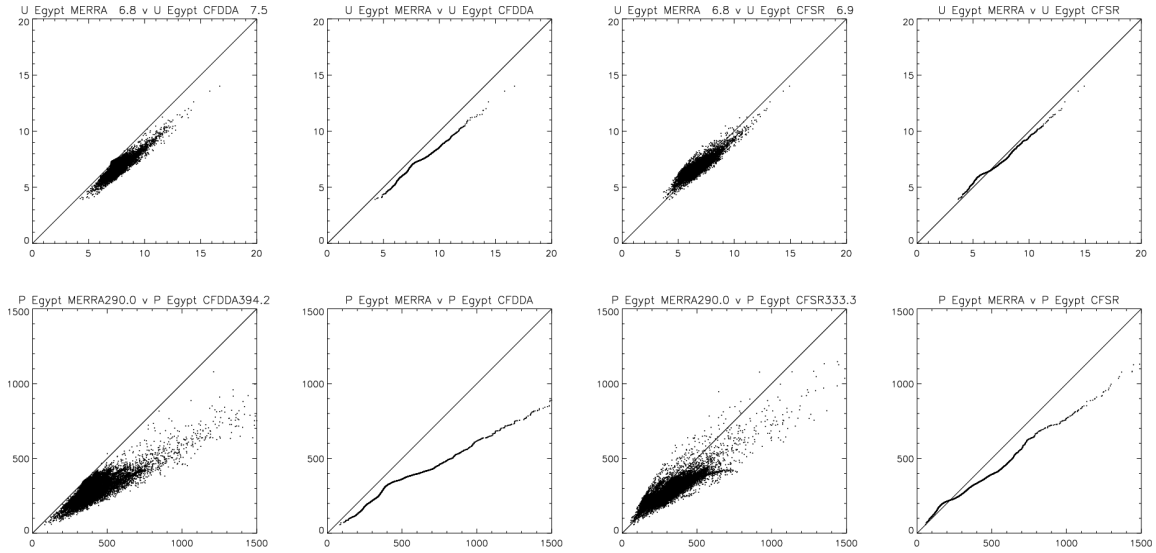

Figure 7.11 – Egypt region case (36R-3), otherwise same as 7.9

The Egypt test area is composed of Global Wind Atlas job tile 36R-3. Figure 7.11 shows tresults from the MERRA and CFDDA indicating CFDDA to give higher estimates of wind power density. The generalized MERRA and CFSR based results also sho a tendency for the CFSR based to have higher power compared to MERRA, but less so than CFDDA.

7.6.4 Columbia Gorge

The Columbia Gorge test area is composed of Global Wind Atlas job tile 10T-4. It is located in the northwest USA. Figure 7.12 shows that for the least windy portion of the wind power density distribution results from the MERRA and CFDDA are similar; in the middle portion,

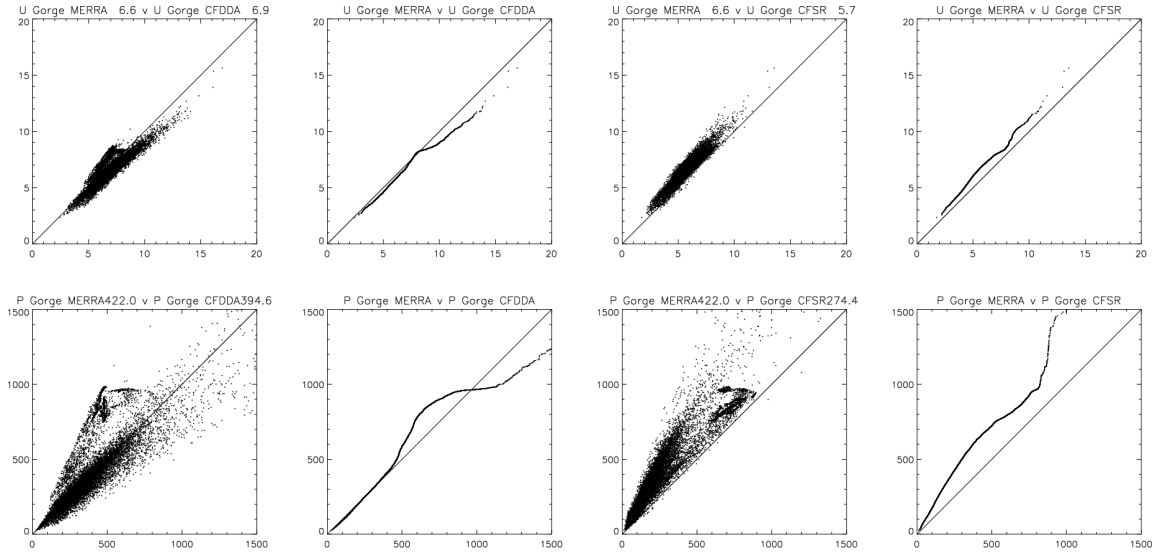

Figure 7.12 – Columbia Gorge region case (10T-4), otherwise same as 7.9

MERRA estimates higher than CFDDA, and in the higher portion CFDDA estimates higher than MERRA. The power density distribution of the MERRA and CFSR based results indicate MERRA estimating higher than CFSR throughout the distribution.

7.6.5 Mali

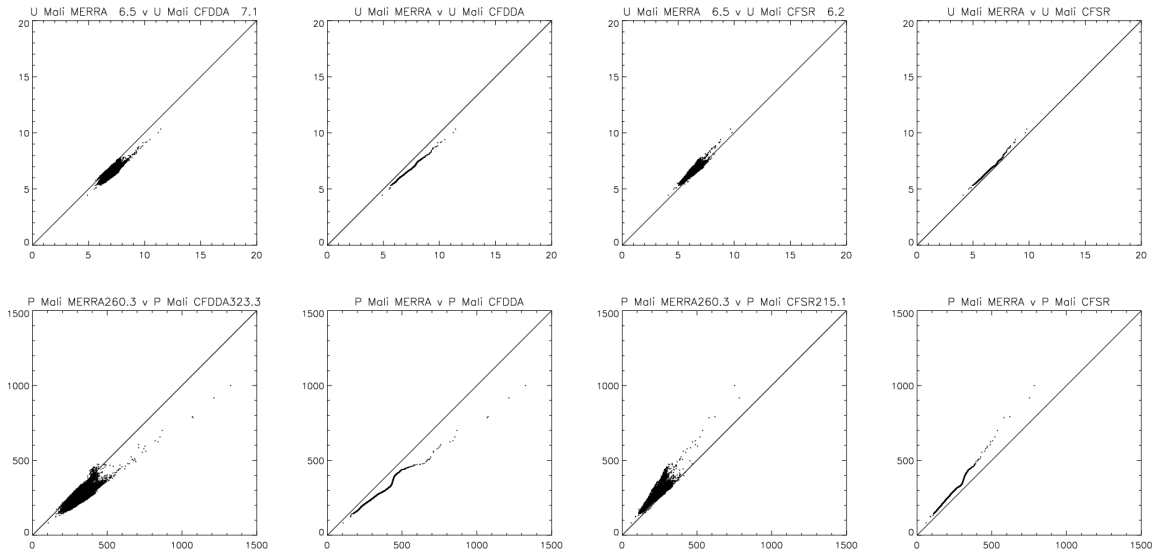

Figure 7.13 – Mali region case (30P-4), otherwise same as 7.9

The Mali test area is composed of Global Wind Atlas job tile 30P-4. It is located in central Mali. Figure 7.13 shows that the wind power density distribution results from the MERRA and CFDDA indicated CFDDA to give higher estimates of wind power density. The power density distribution of the MERRA and CFSR based results also shows a tendency for the MERRA based results to have higher power compared to CFSR.

7.6.6 South Africa

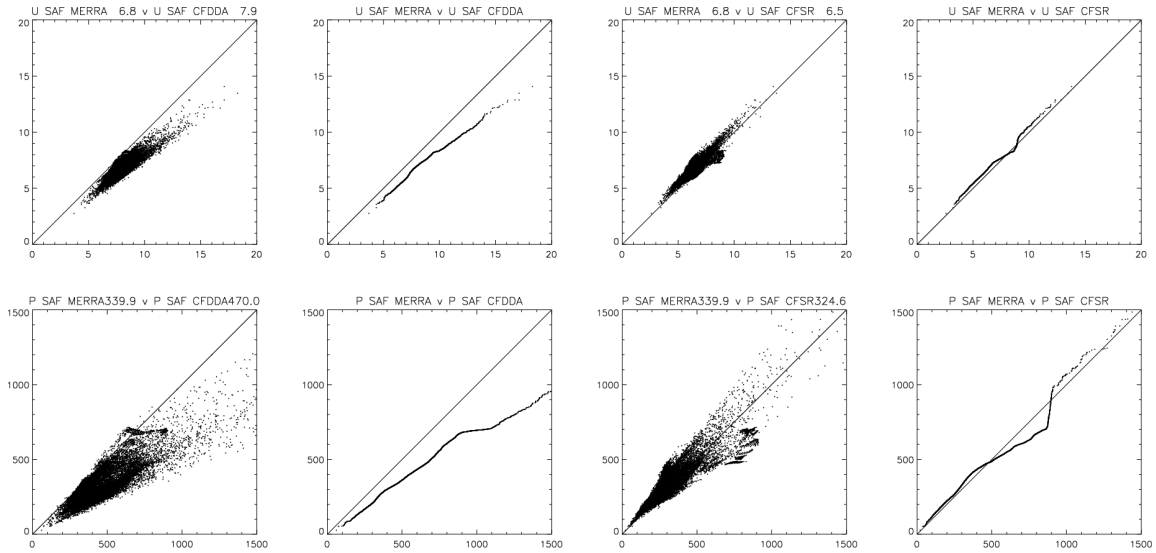

Figure 7.14 – South Africa region case (34H-4), otherwise same as 7.9

The South Africa test area is composed of Global Wind Atlas job tile 34H-4. Figure 7.14 shows that the wind power density distribution results from the MERRA and CFDDA indicate CFDDA to give higher estimates of wind power density. The power density distribution of the MERRA and CFSR based results also show good agreement.

7.6.7 Aegean Sea

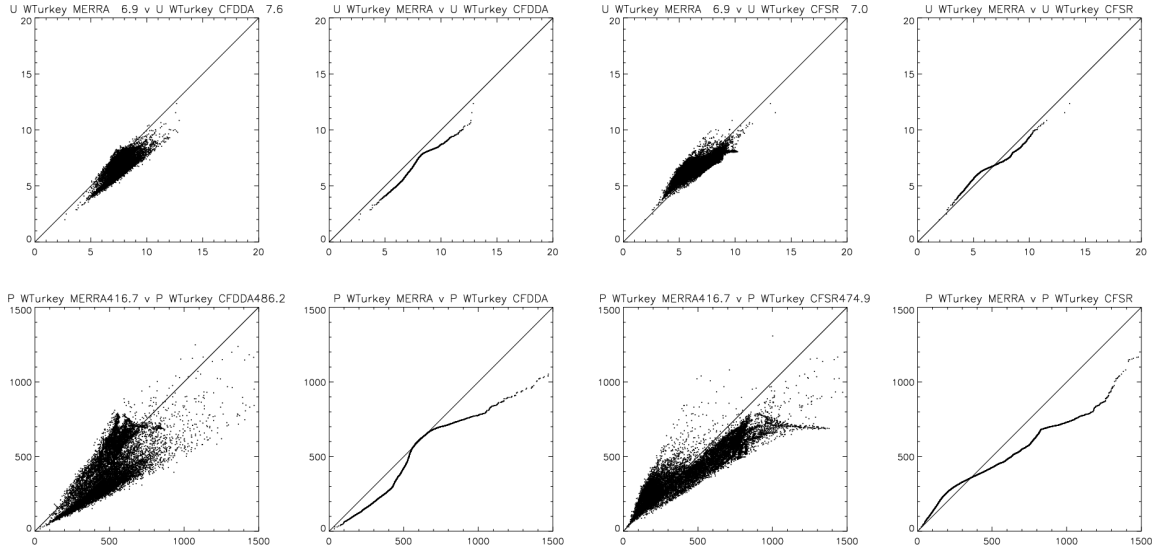

Figure 7.15 – Aegean sea region case (35S-4), otherwise same as 7.9

The Aegean Sea test area is composed of Global Wind Atlas job tile 35S-4. Figure 7.14 shows that the wind power density distribution results from the MERRA and CFDDA indicate

CFDDA to give higher estimates of wind power density, especially in the upper part of the distribution. The power density distribution of the MERRA and CFSR based results also shows CFSR to give higher estimates of power density.

7.7 Comparison other wind atlases

In this section the Global Wind Atlas results are compared with results based on different generalized wind climates. This is possible in regions of interest that have been covered by either observation wind atlas studies or numerical wind atlas studies.

7.7.1 Part of Denmark

Figure 7.16 shows three independent results for part of Denmark at high resolution (job tile 32U-4). The generalized wind climates used in the calculation are different, whereas the topographical descriptions are the same. The results appear very similiar irrespective of whether the generalized wind climates come from MERRA (as in the Global Wind Atlas), from the European Wind Atlas (Troen and Petersen, 1989a), or from mesoscale modelling using the KAMM/WAsP methodology (Badger et al., 2014a). The KAMM/WAsP study for Denmark is validated and described in Frank et al. (2001).

7.7.2 Part of Mali

Figure 7.17 shows four independent results for part of Mali at high resolution (job tile 30P-4). As in the Danish case, the generalized wind climates used in the calculation are different, whereas the topographical descriptions are the same. Result from the MERRA and CFSR generalized wind climates are similar, whereas those from generalized CFDDA show stronger winds. Compared to the validated results from the KAMM/WAsP study Nygaard et al. (2010), MERRA and CFSR give the closest results.

7.7.3 Alaiz

Alaiz is one of the test sites for the CENER, Spain. It has been the location for a number of flow studies, including a study using the KAMM/WAsP method (Badger et al., 2014a). Figure 7.18 shows four independent results for Alaiz at high resolution (job tile 30T-1). Results from the MERRA and CFSR generalized wind climates are similar, whereas those from generalized CFDDA show slightly stronger winds. Compared to the validated results based on the mesoscale KAMM/WAsP study Badger et al. (2014a), CFSR appears to give the closest results. The mesoscale based results (Fig. 7.18d) show greater spatical variability, with lower wind speed values in the low wind speed areas caused by mountain lee effects.

7.7.4 Part of Vietnam

Figure 7.19 shows four independent results for part of Vietnam; three at high resolution (job tile 48Q-2 and 48Q-3) and one result from WRF mesoscale modelling (Badger et al., 2014b), a project funded by the World Bank. Results from CFSR generalized climates give the weakest

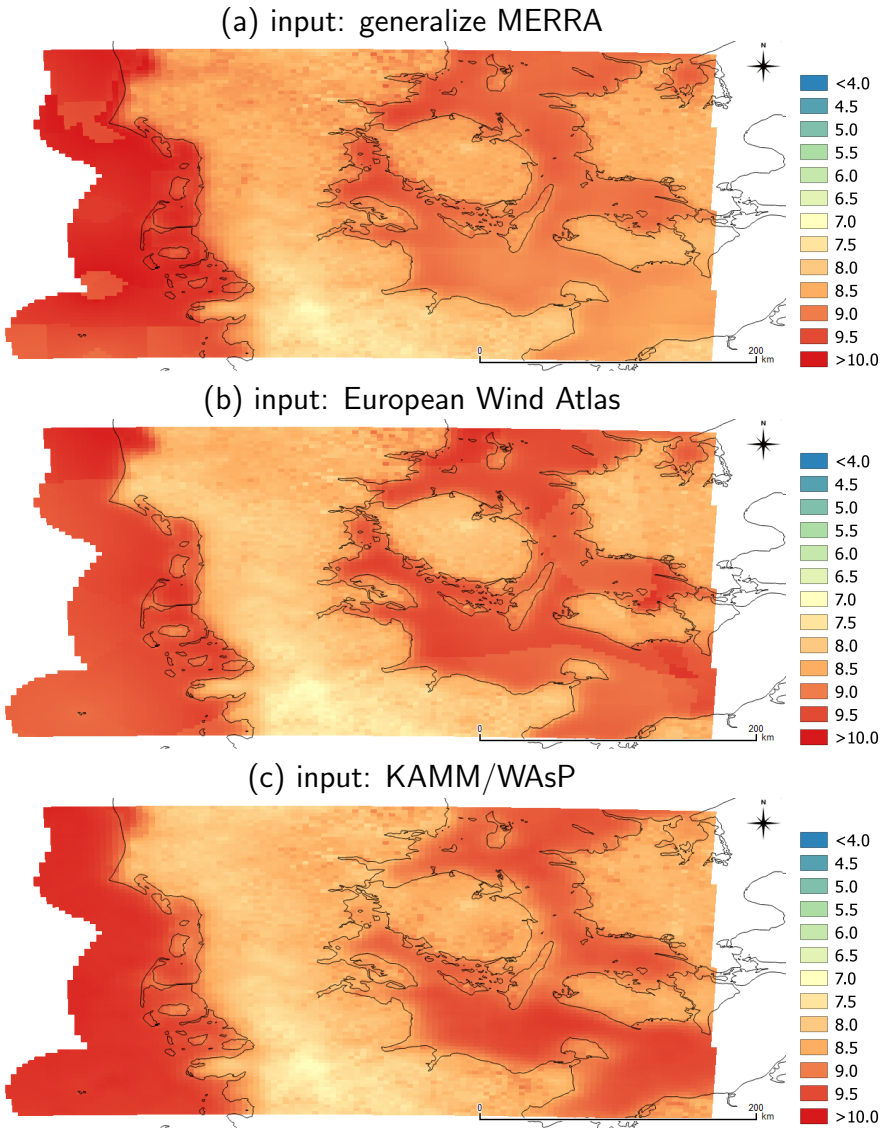

Figure 7.16 – Comparison of high resolution mean wind speed [$\mathrm{m\,s^{-1}}$] based at 100 m on different sources of generalized wind climates for part of Denmark (job tile 32U-4). Input from generalized wind climates based on (a) MERRA, (b) European Wind Atlas, and (c) KAMM/WAsP.

(a) input: generalized MERRA

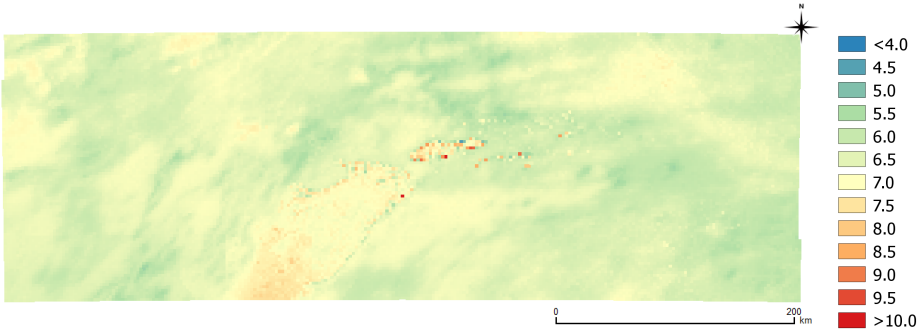

(b) input: generalized CFSR

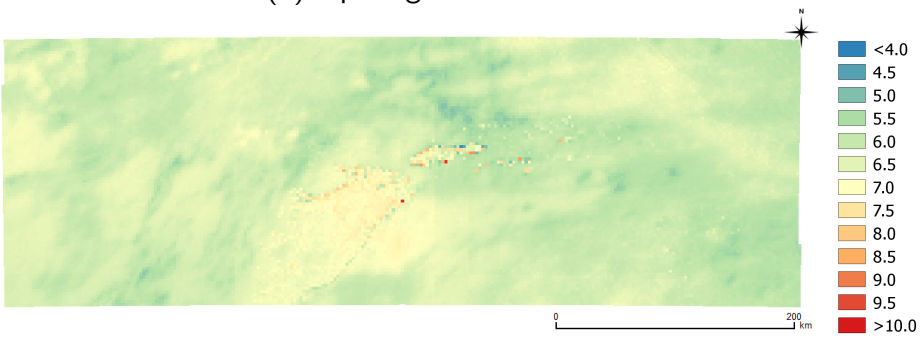

(c) input: generalized CFDDA

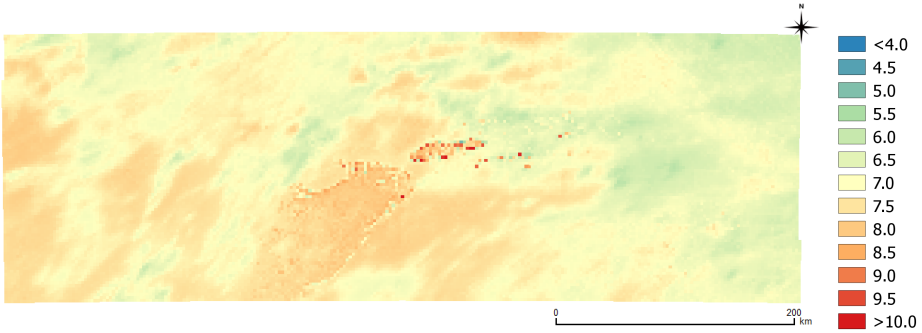

(d) input: KAMM WAsP

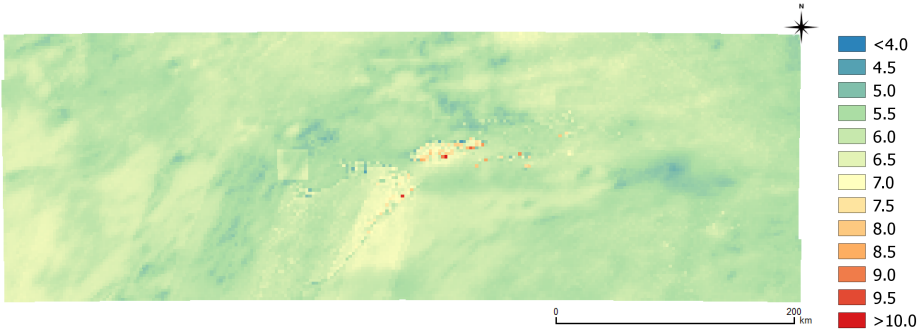

Figure 7.17 – Comparison of high resolution mean wind speed [$\mathrm{m\,s^{-1}}$] at 100 m based on different sources of generalized wind climates for part of Mali (job tile 30P-4). Input from generalized wind climates based on (a) MERRA, (b) CFSR, and (c) CFDDA.

(a) input: generalized MERRA

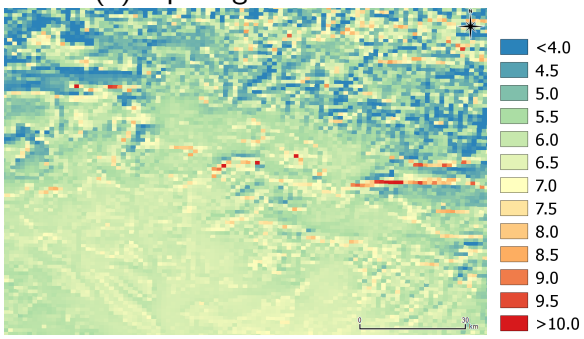

(b) input: generalized CFSR

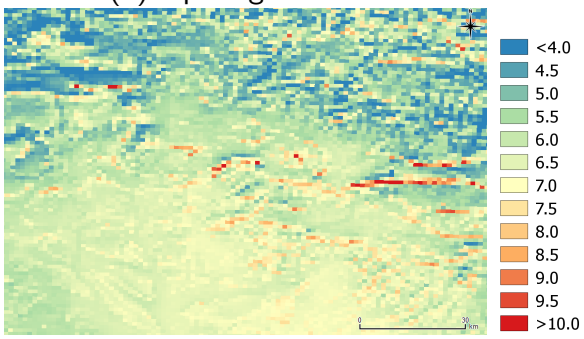

(c) input: generalized CFDDA

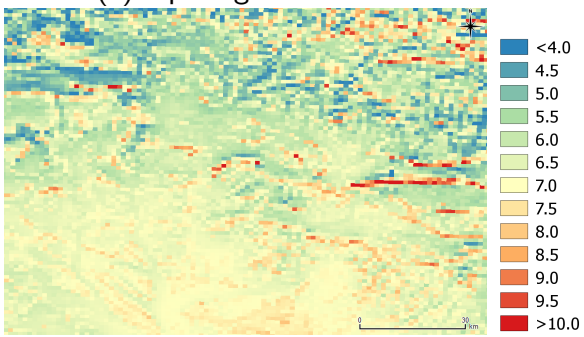

(d) inset, input: KAMM WAsP background, input: generalize MERRA

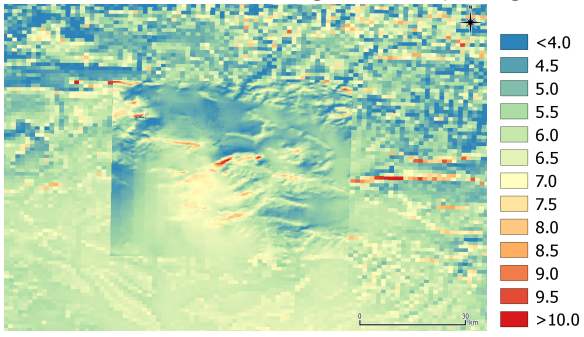

Figure 7.18 – Comparison of high resolution mean wind speed [$\mathrm{m\,s^{-1}}$] at 100 m based on different sources of generalized wind climates for Alais (job tile 30T-1). Input from generalized wind climates based on (a) MERRA, (b) CFSR, (c) CFDDA, and (d) KAMM/WAsP.

winds. Results from the MERRA generalized climates give slightly stronger winds. Results from CFDDA generalized climates give higher winds compared to the other reanalysis; over the sea there is better agreement with SAR winds. Compared to the WRF mesoscale modelling results at 5 km resolution (i.e. no micrsocale modelling performed) in the low land areas, where microscale effects are smaller, MERRA and CFDDA appear to give best agreement.

7.7.5 Part of Illinois and Great Lakes

Figure 7.20 shows four independent results for part of Illinois at high resolution (job tile 16T-1 and 16T-2). Illinois has been mapped using generalized wind climates based on observations (Munoz-Najar, 2015), shown here in Fig. 7.20d. Results from CFSR and MERRA generalized climates match quite well the observational wind atlas results. Results from CFDDA generalized climates give higher winds compared to the other reanalysis. None of the results suggest the very high winds indicated by the SAR winds shown in Fig. 7.6.

7.7.6 Part of South Africa

Figure 7.21 shows four independent results for part of South Africa at high resolution. Western Cape has been mapped in the WASA project using WRF mesoscale modelling (Hahmann et al., 2014). The WASA project results are validated against measurements. Results from CFSR and MERRA generalized climates show similar magnitude winds. Over land, results from CFDDA generalized climates give higher winds compared to the other reanalysis. The WASA generalized wind climates give results with much more spatial variability, including a region of low winds that none of the reanalyses capture.

In Fig. 7.22, the high resolution results based on the generalized reanalyses are compared in scatter plots to the high resolution results based on the WASA generalized wind climates. It appears that the CFDDA results give good agreement in the higher portion of the distribution, where it is over sea areas, and also ridge and mountain tops. But it overestimates the winds where WASA suggests low wind areas. MERRA and CFSR indicate a similar ability to capture the distribution of wind speeds, with reasonable agreement in the lower to middle part of the distribution but underestimation in the upper part of the distribution.

(a) input: generalized MERRA, background SAR

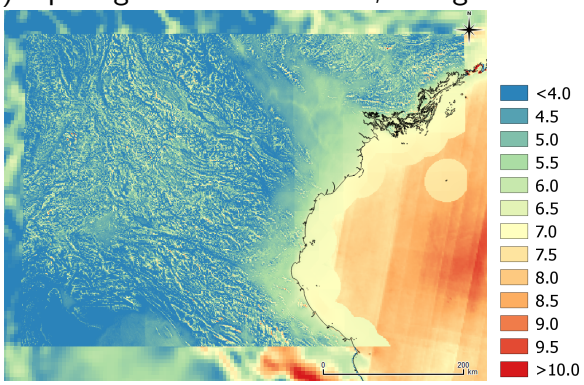

(b) input: generalized CFSR, background SAR

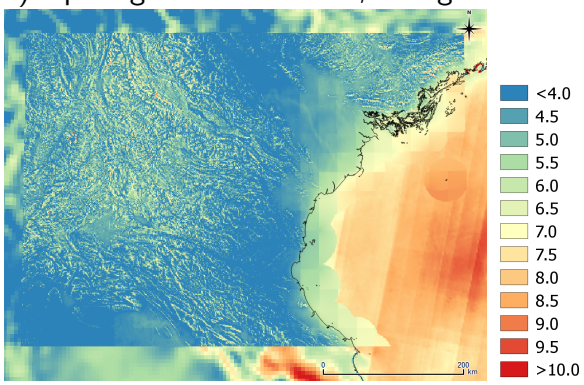

(a) input: generalized CFDDA, background SAR

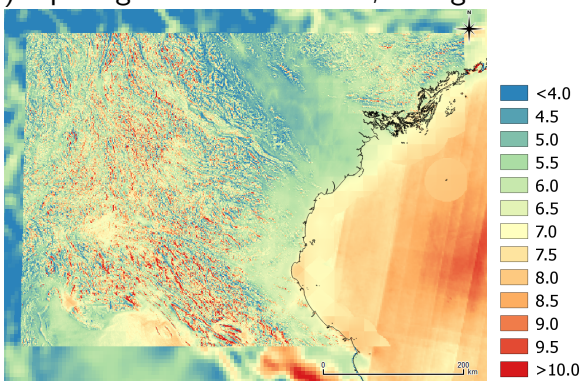

(a) input: generalized WRF mesoscale, background SAR

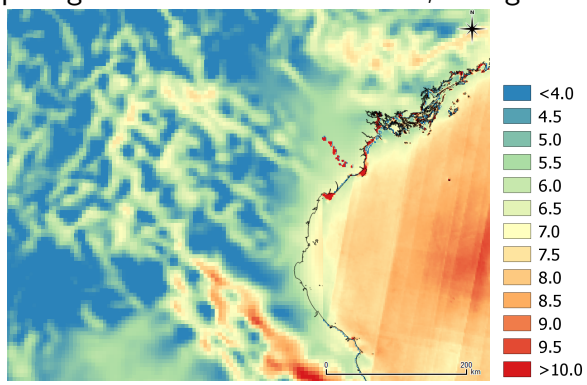

Figure 7.19 – Comparison of high resolution mean wind speed [$m\,s^{-1}$] at 100 m based on different sources of generalized wind climates for part of Vietnam (job tile 48Q-2 and 48Q-3). Input from generalized wind climates based on (a) MERRA, (b) CFSR, (c) CFDDA and (d) WRF mesoscale modelling. Mean winds at 100 m from SAR are plotted as background.

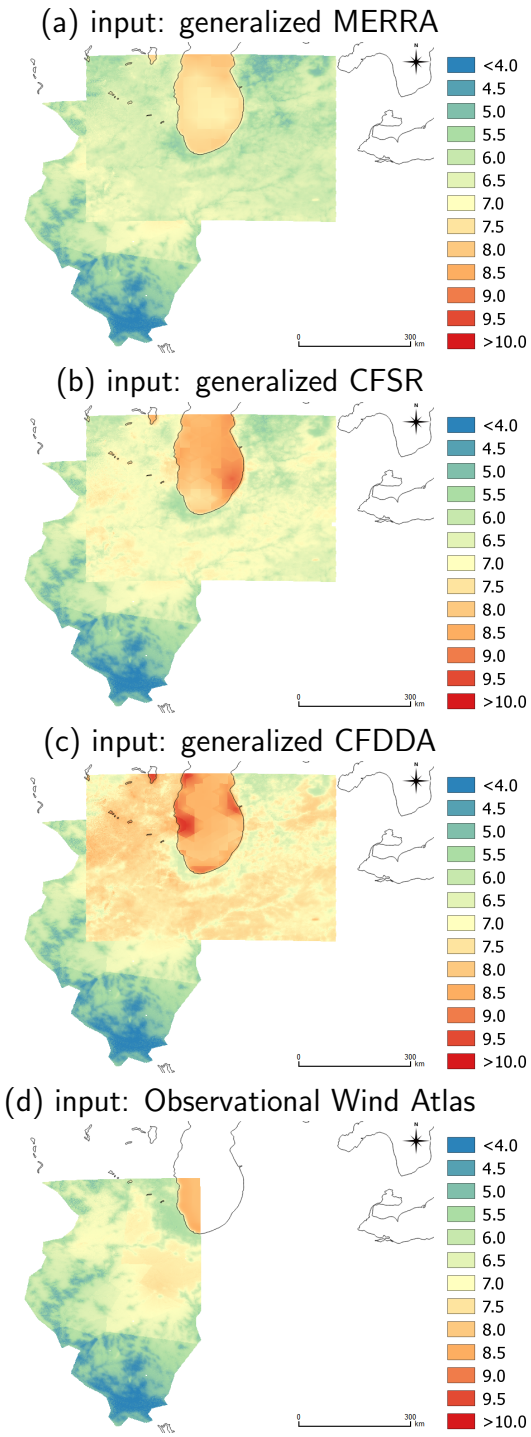

Figure 7.20 – Comparison of high resolution mean wind speed [$\mathrm{m\,s^{-1}}$] at 100 m based on different sources of generalized wind climates for part of Illinois and Great Lakes (job tiles 16T-1 and 16T-2). Input from generalized wind climates based on (a) MERRA, (b) CFSR, (c) CFDDA, and (d) an observational wind atlas.

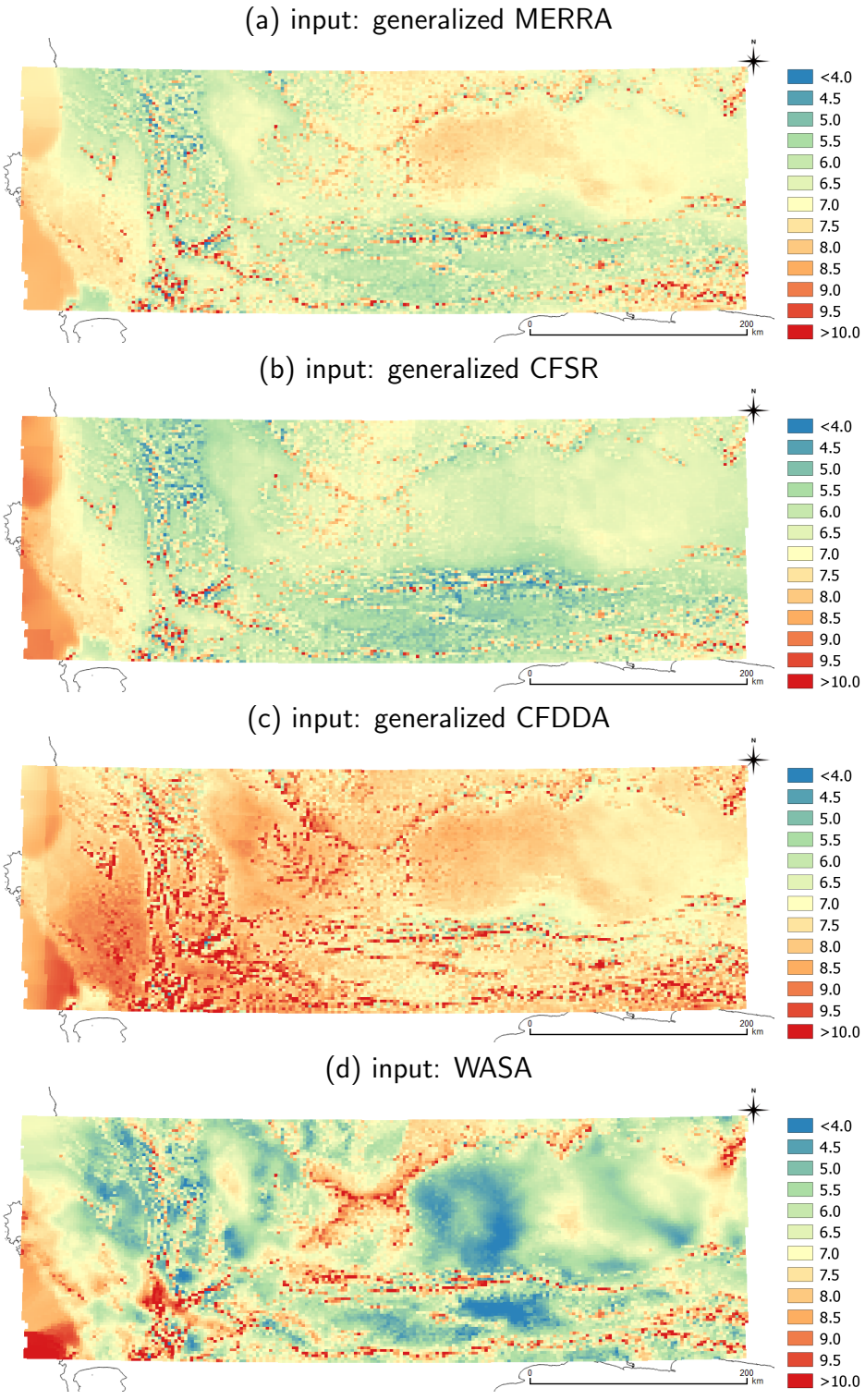

Figure 7.21 – Comparison of high resolution mean wind speed [$m\,s^{-1}$] at 100 m based on different sources of generalized wind climates for part of South Africa (job tile 34H-4). Input from generalized wind climates based on (a) MERRA, (b) CFSR, (c) CFDDA, and (d) WASA

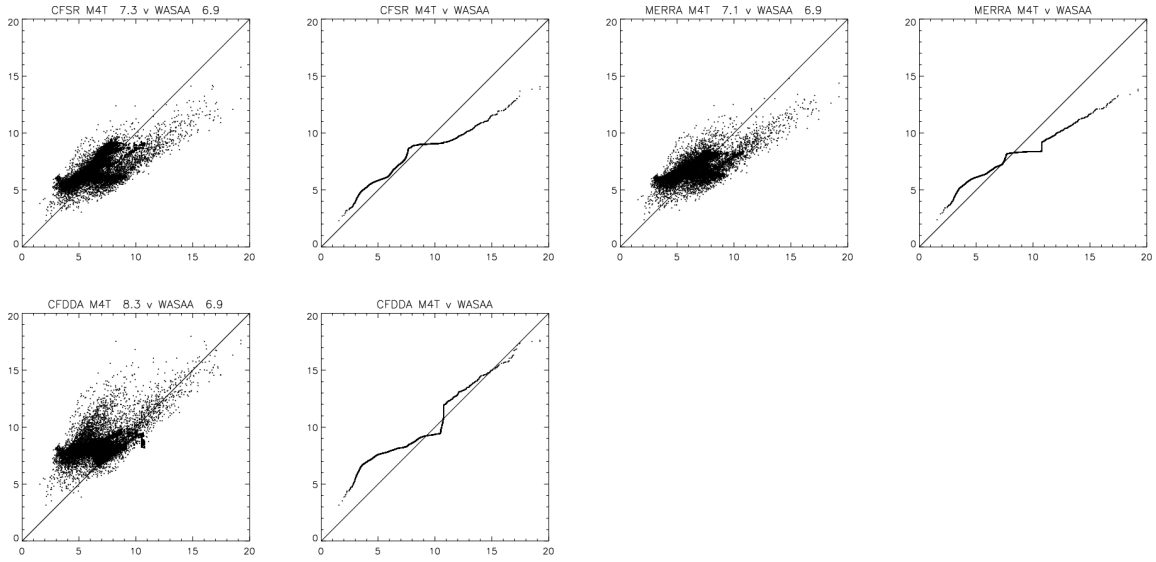

Figure 7.22 – South Africa region case (34H4) wind speed scatter plots comparing Frogfoot results using generalized wind climates from WASA project and different reanalysis, namely, CFSR, MERRA and CFDDA. The grid point to grid point scatter plot is given then the ranked values are plotted against each other.

7.8 Summary

As one can infer from the test cases shown above, there are some differences between the re-analysis datasets, and subsequently between the generalized wind-climate statistics derived from them.

The differences between re-analysis datasets extend beyond wind velocities and subsequent power densities. This includes not only spatial and temporal variability due to differing underlying model characteristics, but also surface parameters; of these, one is important in the generalization procedure: the roughness length.

The generalization of wind speeds invokes the geostrophic drag law and a (perturbed) log-law, both of which involve the roughness length. Together, these relations lead to an increase in generalized wind speed for an increase in background roughness, and vice-versa. The three reanalysis datasets each have different background roughnesses, which contribute to some of the differences in generalized winds shown. Most simply, the tendency of the CFDDA to give higher wind speeds over land, along with prescribing larger roughnesses (relative to the other datasets) over modest terrain leads to larger generalized winds. Over modest and flat terrain the CFSR roughness can be yet larger, which can lead to generalized CFSR winds larger than generalized MERRA winds, in locations where the CFSR and MERRA winds are comparable.

Further refinements of the generalization process and/or reanalysis roughnesses can lead to yet more compatible results between generalized wind data from different re-analyses; this is the subject of ongoing research.

Contributing authors Jake Badger, Merete Badger, Mark Kelly, Xiaoli Guo Larsén

Chapter 8

Dissemination

8.1 Webpages

The main means of dissemination of the Global Wind Atlas is through two websites: the Global Wind Atlas website hosted by DTU Wind Energy offering a very comprehsive set of maps and tools and as selectable layers and web tools on IRENA's Global Atlas for Renewable Energies.

8.1.1 DTU Wind Energy's dedicated Global Wind Atlas website

Figure 8.1 shows the Global Wind Atlas website created especially for the project and dedicated to serve users with the datasets and tools developed within the project. The website also provides guidance about the appropriate use of the data, documents the methodologies, and describes the data sources. The website also includes video tutorials on how to navigate around the website. More details of what is available on this website are given in Chapter 9.

The website address is http://globalwindatlas.com/.

8.1.2 IRENA Global Atlas for Renewable Energies

Figure 8.2 shows IRENA's Global Atlas that also serves the Global Wind Atlas project data. This positions the data in a central and expanding site for accessing renewable energy data and also datasets associated with societetal needs and infrasture. IRENA also accesses some of the tools developed by DTU in the project. The energy modelling community can also develop their own tools that link and analysis the Global Wind Atlas datasets in the context of geographical information, such as population density, and road and power transmission networks.

The IRENA Global Atlas website is http://irena.masdar.ac.ae/

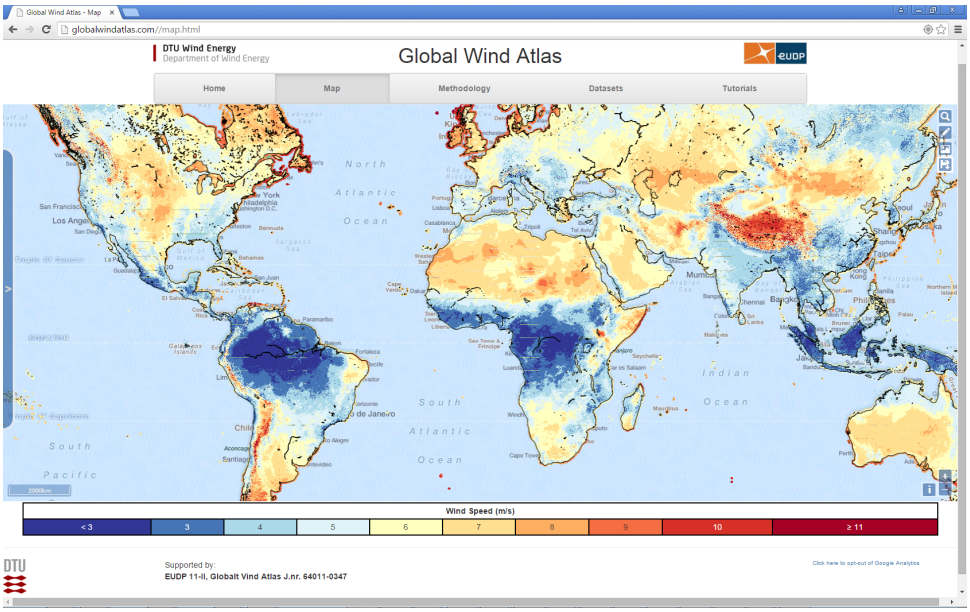

Figure 8.1 – Screenshot of the Global Wind Atlas website at DTU Wind Energy, http://globalwindatlas.com/

.

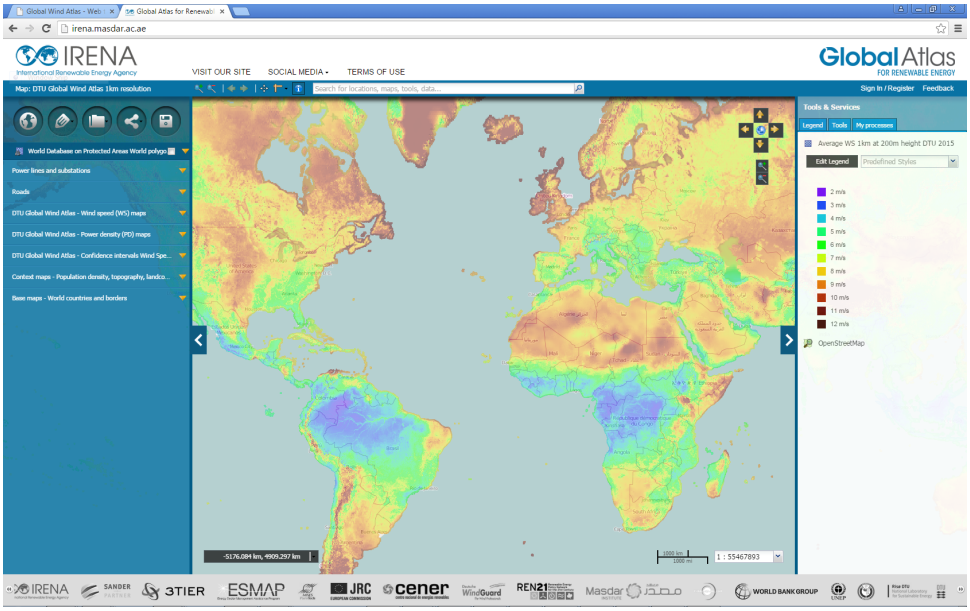

Figure 8.2 – Screenshot of the IRENA Global Altas website where the Global Wind Atlas datasets and tools can also be found, http://irena.masdar.ac.ae/

8.2 Launch

For the launch of the Global Wind Atlas, IRENA personel were of great assistence in proposing and coordinating a series of high profile events and press releases from the principle stake holders of the project. The details of the press releases and the speakers at the webinar events can be seen in this section.

8.2.1 Press releases

IRENA, the Danish Energy Agency and DTU released press releases at 11:00 CET on 21st October 2015. The texts for the press releases are given below.

Danish Energy Agency and DTU press release

In Danish:

Nyt vindatlas skal fremme bæredygtig elproduktion i hele verden

I dag lanceres et globalt vindatlas, som kan forbedre udnyttelsen af vindenergi over hele kloden. Danmark har spillet en afgørende rolle i udviklingen af vindatlasset, som er et gratis redskab for alverdens energiplanlæggere.

Det nye vindatlas er offentligt tilgængeligt og leverer et mere detaljeret globalt dataset end nogensinde før, som giver energiplanlæggere mere præcise vinddata for bestemte områder. Atlasset får stor betydning for udviklingen af fremtidige vindmodeller og kan dermed medvirke til at forbedre den globale udnyttelse af vindenergi.

" Danmark får i dag 40 procent af sin elektricitet fra vindmøller, og vindsektoren har stor betydning for både energiforsyning og jobskabelse i Danmark. Det glæder mig meget, at Danmark har bidraget til udvikling af det ny vindatlas, såandre lande ogsåfår et godt grundlag for udnyttelse af vindenergien. Danmark har tidligere i samarbejde med Sydafrika udarbejdet et sydafrikansk vindatlas, som har skabt grobund for udvikling af vindenergisektoren der," siger energi-, forsynings- og klimaminister Lars Chr. Lilleholt.

Danmarks Tekniske Universitet (DTU) er verdensførende, når det gælder udvikling af vindmodeller, og DTU har da ogsåhaft en central rolle i den tekniske udvikling af det nye vindatlas.

"En vindmølles elproduktion kan forbedres drastisk, såfremt den placeres i det optimale område. Med det ny atlas kan vi udpege de bedste områder - og det endda over hele jordkloden," siger Innovationschef Kenneth Thomsen fra DTU Vindenergi.

Efterspurgt i ulande

Ifølge International Renewable Energy Agency (IRENA) er det globale vindatalas efterspurgt af mange udviklingslande, som søger teknisk viden i forbindelse med udvikling af en grøen energipolitik. Atlasset kan ogsåbruges til at identificere lande, hvor en mere nuanceret og verificeret kortlægning af vindressourcer vil kunne føre til en øget udnyttelse af vindenergien. Hvor vindressourcerne ser lovende ud, bliver næste skridt at kontakte de store producenter af vindmøller, f.eks. danske Vestas Wind Systems.

"Det globale vindatlas en stor gevinst for alle nationer, der ønsker at udforske mulighederne for vindenergi i deres land, og Vestas er selvsagt interesseret i at hjælpe med at finde den optimale vindenergiløsning til de specifikke vindforhold," siger Vice President

for global public affairs hos Vestas, Morten Dyhrholm.

Offentliggœrelse af det ny vindatlas foregår via et webinar kl. 15:00 onsdag den 21. oktober, hvor alle er velkomne. Registrering sker påtinyurl.com/GWAWebinar

FAKTA om det globale vindatlas

Danmark er medlem af organisationen International Renewable Energy Agency (IRENA), som står bag Global Atlas for Renewable Energy. Det nye globale vindatlas bliver en del af IRENA Global Atlas sammen med data fra 1.500 databaser, som sammenholdes med det geografiske informationssystem (GIS) og softwareprogrammet Global Atlas Pocket. IRENA har involveret mere end 50 organisationer fra 67 lande, som alle har bidraget til udviklingsarbejdet de seneste fire år.

Datakilderne og metodologien er beskrevet i detaljer, såder er åbenhed om metoderne over for vindenergisektoren. Det nye vindatlas leverer vindressourcedata helt ned til en kilometers oplœsning, baseret påberegninger i endnu hœjere oplœsning. Efter offentliggœrelsen kan det nye atlas findes her: globalatlas.irena.org. Særligt interesserede i modellering og dybdegående analyser kan besœge DTU's Global Wind Atlas-server: globalwindatlas.com

IRENA's globale vindatlas er finansieret af en lang række institutioner. Det danske program for energiteknologisk udvikling og demonstration (EUDP) har bevilget 6,95 mio. kr. til projektet, mens DTU har bidraget med 1,25 mio. kr. til det ny vindatlas.

Udarbejdelse af specifikke nationale vindatlas verificeret med målinger indgår ogsåi Energi-, Forsynings- og Klimaministeriets bilaterale samarbejder med Sydafrika og Mexico. Samme metode anvendes i œvrigt nu ogsåaf Verdensbanken i deres indsats for fremme af vindenergi i andre lande, herunder Pakistan og Vietnam.

Yderligere oplysninger fås hos:

- DTU, seniorforsker Jake Badger, 4677 5094, jaba@dtu.dk
- DTU, sektionsleder Hans E. Joergensen, 4057 6034, haej@dtu.dk
- Energistyrelsen, specialkonsulent Mikkel Svane-Petersen, 3392 6643, mspe@ens.dk
- Energistyrelsen, specialkonsulent Anders Hasselager, 4172 9152, ah@ens.dk
- IRENA, communications officer Hillary McBride, +971 56 410 3572, hmcbride@irena.org

IRENA press release

IRENA and DTU Launch World's Most Detailed Wind Resource Data

Global Wind Atlas provides accurate wind resource data down to the kilometre, boosting support for global wind energy development

Abu Dhabi, U.A.E, 21 October, 2015

The most detailed data and statistics on global wind energy potential are now available online, thanks to a free resource launched today by the International Renewable Energy Agency (IRENA) and the Technical University of Denmark (DTU). The Global Wind Atlas provides wind resource data at one-kilometre resolution. Prior to this release, global wind data was only publically available at 10-kilometre resolution or poorer, which resulted in underestimations, increased risk and increased costs for wind energy planners.

"Wind energy potential across the globe is vast, but the upfront costs of measuring

potential and determining the best locations for projects is an obstacle in many countries," said IRENA Director-General Adnan Z. Amin. "The new Global Wind Atlas provides this needed data directly and for free, making it a ground-breaking tool to help jumpstart wind energy development worldwide."

The Wind Atlas is the newest addition to the datasets available through IRENA's Global Atlas, a renewable energy mapping tool. The dataset uses microscale modeling to capture wind speed variability on small scales, allowing for better estimates. When locating wind farms, developers naturally pick areas with the highest wind speeds. In datasets that provide average wind speeds over large areas, the enhancement of wind speeds due to small scale features such as hills and ridges are not captured, making the resource appear weaker than it actually is. The Wind Atlas can prevent this underestimation, provide visual maps showing wind speeds at three different heights, and also provide tools to generate and export data and statistics such as wind roses and wind speed distributions over a chosen area.

"The release of the Global Wind Atlas demonstrates the support of the international community to expand global renewable energy to address global climate change, increase electricity access and stimulate economic development," said Danish Minister for Energy, Utilities and Climate, Lars Christian Lilleholt. "Denmark, together with South Africa, has already developed the South African Wind Atlas and we have seen the value of the tool in the development of the wind energy sector."

The Wind Atlas builds on decades of expertise in wind mapping at the Technical University of Denmark. It was funded by Denmark as part of its commitment to the Clean Energy Ministerial (CEM) process, and represents the achievement of the goal set forth by the CEM's Multilateral Solar and Wind Working Group to help increase the global share of renewable energy by providing the world with detailed and validated wind potentials through an online platform.

Access the Global Wind Atlas maps here: http://bit.ly/1PDgGrt and the new toolset here: http://bit.ly/1MAJrjs

About the International Renewable Energy Agency (IRENA)

The International Renewable Energy Agency (IRENA) is mandated as the global hub for renewable energy cooperation and information exchange by 143 Members (142 States and the European Union). Roughly 29 additional countries are in the accession process and actively engaged. IRENA promotes the widespread adoption and sustainable use of all forms of renewable energy, including bioenergy, geothermal, hydropower, ocean, solar and wind energy in the pursuit of sustainable development, energy access, energy security and low-carbon economic growth and prosperity. www.irena.org

About the Global Atlas

The IRENA Global Atlas for Renewable Energy aims to close the gap between nations that have, and nations that do not have, access to the necessary datasets, expertise and financial support to evaluate their national renewable energy potentials. As of January 2015, 67 countries and more than 50 institutes and partners were contributing to the initiative. The geographic information system (GIS) and mobile app (Global Atlas Pocket) provide free access to over 1,500 datasets that contain solar, wind, geothermal, biomass, and marine energy potential for locations around the world. Online simulation tools allow to process this information and assess renewable energy potentials.

About the Technical University of Denmark (DTU)

DTU was founded in 1829, and has ever since been dedicated to developing the natural and the technical sciences with a view to creating value for society. During the past two centuries, DTU has undergone a transformation from a 19th century polytechnical institution to a present-day international, multidisciplinary institution that caters for research, teaching, and collaboration across scientific, professional, and geographical borders.

Contact information:

Hillary McBride, Communications Officer, IRENA, hmcbride@irena.org T: +971 2 417 9000; M: +971 56 410 3572

Stay in touch with IRENA

www.twitter.com/irena

www.facebook.com/irena.org

8.2.2 Launch webinar events

On the day of the launch, IRENA coordinated and hosted a launch webinar with high level speakers from the relevant stake holders, see agenda in Table 8.1. At the end of the webinar there was the possibility to ask questions. The estimated number of attendees is 150

On the 3rd November there will be a technical webinar hosted by the National Renewable Energy Laboratory (NREL), USA. The agenda is given in Table 8.2. The number of registered participants was over 110 at the time of writing, one week ahead the seminar.

8.2.3 Radio media

Following the launch Danish Radio P1 conducted an telephone interview about the Global Wind Atlas with project manager Jake Badger on the afternoon program Orientering. The interview can be found here (in Danish):

http://www.dr.dk/radio/ondemand/p1/orientering-2015-10-21#!/46:20

Kristin Deason, IRENA (5 mins)	Welcome to all participants Overview of agenda and introduction of speakers
Adnan Amin, Director General, IRENA (5 mins)	Importance of renewable resource data Accelering the transition towards a doubling of the share of renewable energy Concrete impact of the GWA to support islands Energy corridors, scenario analysis
Christian van Maarschalkerweerd, Head of Office, Danish Energy Agency (5 mins)	Danish and international cooperation to create a highly valuable public good Background of the Global Wind Atlas and origination from the Major Economies' Forum (MEF) Global Wind Atlas as commitment to the CEM's Multilateral Solar and Wind Working Group
Kenneth Thomsen, Innovation Manager, DTU Wind Energy (5 mins)	Background on GWA collaboration DTU's extensive experience in wind energy Characteristics of GWA data: accuracy, validation, quality
Steve Sawyer, Secretary General, GWEC (5 mins)	Importance of the GWA to the wind industry Raising the profile of wind in new markets Providing certainty to investors in projects and supply chain
Kristin Deason, IRENA (10 mins)	Questions and answers session Questions from webinar participants Jake Badger, DTU, and Nicholas Fichaux, IRENA, panalists available to answer questions

Table 8.1 – Agenda for the launch webinar hosted by IRENA.

Sean Esterly, NREL (5 mins)	Welcome to all participants Welcome to all participants Overview of Clean Energy Solutions Center Overview of agenda and format
Nicolas Fichaux, IRENA (15 mins)	GWA Overview Welcome to all participants Introduction, what is the Global Wind Atlas Background of the Global Wind Atlas and origination from the Major Economies' Forum (MEF) Background on GWA collaboration Importance of renewable resource data Accelerating the transition towards a doubling of the share of renewable energy Se4All and therefore SDG7 Characteristics of GWA data: accuracy, validation, quality Questions and Answers
Jake Badger, DTU Wind Energy (20 mins)	Technical Details Description of methodology used to develop the dataset Data quality and validation methods
Adulmalik Oricha Ali, IRENA (35 mins)	Demonstation Live demo of Global Wind Atlas How to access the dataset How to use the tools
Sean Esterly, NREL (10 mins)	Additional Questions and answers Questions from webinar participants

Table 8.2 – Agenda for the technical webinar hosted by NREL.

8.3 Project workshops

Just as in the project proposal, two workshop hosted by DTU Wind Energy were carried out. The first workshop, within the first year of the project, had as the target group the technical partners and end-users within the CEM Working Group on Solar and Wind Technologies. A dialogue was undertaken to find the meeting point of expectations, requirements and what is possible. The outcomes of the workshop determined some of the design specification for the final products of the project.

The second workshop in the last months of the project, had as the target group the end-users. Here the results were presented, the methodologies explained and the new website and tools demonstrated. The purpose was not only to present the project outcomes, but to gather feedback from end-uses on further application of the datasets.

8.4 Workshop I

On 12 – 13 December 2012 at DTU Wind Energy RisœCampus, the first end-user workshop was held. The agenda is given in Table 8.3. The number of attendees was 28.

During the workshop there was time allocated to group discussion on the following topics. The workshop was split into 3 groups.

- Topic 1 Global Wind Atlas Wish List

  In this discussion the groups needed to outline wished for aspects of the GWA. This was done in order to avoid the situation where a potential end-user says, 'I looked at the atlas products/datasets, why didn't you make this product/dataset?'

- Topic 2 Deployment of wind power

  In this discussion the groups needed to highlight ways to encourage the 'greatest possible deployment of wind energy globally?', from the perspective of data provision.

- Topic 3 SWOT analysis

  In this discussion the groups listed strength (S), weaknesses (W), opportunities (O) and Threats (T) associated with the Global Wind Atlas.

	Day 1, Wednesday 12th December 2012
09:30	Registration
10:00	Welcome, Introductions, Motivation and Contexts Hans Joergensen (DTU Wind Energy), Welcome and introduction Nicolas Fichaux (IRENA), The bigger scene, The Global Wind Atlas Jakob Mann (DTU Wind Energy), Context within New European Wind Atlas
11:00	Presentation covering the Global Wind Atlas project method, limitations and status Jake Badger (DTU Wind Energy)
12:00	Lunch
13:00	Presentations demonstrating a selection end-users current practices, needs and wishes Olexandr Balyk (DTU Management Engineering) - CANCELLED DUE TO ILLNESS Lars Bregnbaek (Energianalyse A/S) Soeren Krohn (SKPower) Per Nœrgaard (DTU Institut for Elektroteknologi) Discussion
15:00	Break
15:30	Group discussions: Group work 'I looked at the atlas products/datasets, why didn't you make this product/dataset?!' 'How to get greatest possible deployment of wind energy globally?' SWOT analysis
17:00	Close

	Day 2, Thursday 13th December 2012
09:00	Welcome to day 2
09:15	Presentation showing examples demonstrating web based renewable energy tools Nicolas Fichaux (IRENA) Dan Getman (NREL) Discussion on maximizing applications and relevance of such tools for wind energy
10:00	Group discussions: Open Space Uncertainty: how should this be expressed Data must match modelling development By what means will the different end-users get best use out of the Global Wind Atlas
10:30	Break
11:00	Working through together the group discussion about Uncertainty from Open Space
12:00	Lunch
13:00	Working through together the discussion from group work (day 1)
15:00	Wrap up (DTU)
15:15	Close

Table 8.3 – Agenda for the 1st Global Wind Atlas workshop hosted at DTU Wind Energy.

8.5 Workshop II

On 20 – 21 May 2015 at DTU Wind Energy RisœCampus , the second end-user workshop was held. The agenda is given in Table 8.4. The number of attendees was 24.

	Day 1, 20th May 2015
09:30	Registration
10:00	Welcome and context
	Hans Joergensen, Head of Section, DTU Wind Energy
10:30	Presentations covering the methodology
	Methodology Outline, Jake Badger, DTU Wind Energy
	Reanalysis data and generalization, Andrea Hahmann, DTU Wind Energy
	Elevation and land cover classification, Neil Davis, DTU Energy
	Microscale modelling and outputs, Jake Badger, DTU Wind Energy
12:00	Lunch
13:00	Presentation and demonstrating a selection of applications
	The user interface, Neil Davis, DTU Wind Energy
	Participants' hands-on try out, ALL
15:00	Break
15:30	Presentations of applications
	The effect of microscale spatial variability of wind on estimation of technical and economical wind potential, Olexandr Balyk, DTU Management Engineering
	Requirements for renewable energy resource data in energy modelling, Iratxe Gonzalez-Aparicio, Joint Research Centre, Petten (NL)
	Discussion, All
17:00	Close
	Day 2, 21st May 2015
09:00	Welcome to Day 2 with summary of Day 1
09:30	Working with the global wind atlas data
	The Global Wind Atlas data inventory, Jake Badger, DTU
	Participants hands-on use and designing of post-processing applications, ALL
	Feedback (All)
	(Break 10:15 - 10:40)
12:00	Lunch
13:00	Technical aspects of dissemination
	WMS & WPS / postGIS external interfaces, Neil Davis, DTU
	Participants hands-on design mock-ups (All)
	Feedback (All)
	(Break 14:00 - 14:15)
15:00	Close

Table 8.4 – Agenda for the 2nd Global Wind Atlas workshop hosted at DTU Wind Energy.

8.6 Collaboration meetings

During the project a number of collaboration meetings with partners in the CEM Multilateral Working Group on Solar and Wind Technologies was held. These are listed below.

Location: Mines Paris Tech, Paris, France
Date: 17th September 2012
DTU Wind Energy partipant: Jake Badger
Purpose: Discussions on technical specification and issues regarding IRENA's Global Atlas and integration of Globa Wind Atlas results.

Location: DLR, Stuttgart, Germany
Date : 8th April 2013
DTU Wind Energy partipants: Jake Badger and Ferhat Bingö l
Purpose: Discussions on technical specification and issues regarding IRENA's Global Atlas and integration of Globa Wind Atlas results.

Location: IRENA, Abu Dhabi, UAE
Date: 20th January 2014
DTU Wind Energy partipant: Jake Badger
Purpose: Discussions on technical specification and issues regarding IRENA's Global Atlas and integration of Globa Wind Atlas results.

Location: NOAA, USA and Johns Hopkins University, Maryland, USA
Date: 11 - 17 June 2015
DTU Wind Energy partipant: Merete Badger
Purpose: Discussions on application of Synthetic Aperture Radar scenes for Global Wind Atlas validation.

8.7 Guests

During the project we were pleased to have the visits of two members of staff from the National Center for Atmospheric Research (NCAR), Boulder, USA. In the proposal the suggestion was for one guest from NCAR to visit us for three weeks. During the project, we could see that it would be better to instead have two visitors for one week each. In this way we were able to interact with NCAR over a broader range of very relevant expertise.

Josh Hacker visited DTU Wind Energy, over the period 8 - 12 June 2015 inclusive. Josh Hacker is Program Director at the Research Applications Laboratory, Joint Numerical Testbed. He is expert in data assimilation for using measurement data in atmospheric models.

He held numerious meetings with department staff involved in the Global Wind Atlas, and he gave two seminars. The first was an educational lecture the second was a departmental seminar.

Guest 1st seminar title: Data assimilation: brief fundamentals and some things to consider
Guest 2nd seminar title: Ensemble sensitivity analysis: applications and challenges

Terri Betancourt visited DTU Wind Energy, over the period 6 - 10 July 2015 inclusive.

Terri Betancourt is Program Manager at the Research Applications Laboratory, National Security Applications Program. She is an expert in software engineering solutions for bringing meteorological model results into end-user applications. Her experience was relevant for discussion concerning how the Global Wind Atlas should be disseminated to end-users. She gave one seminar to the department.

Guest seminar title: How social media and gaming have reshaped the data space

8.8 Conferences

Below conferenced attended to disseminate the project objectives, methods, outcomes and applications are listed.

Conference: 4th World Climate Research Programme International Conference on Reanalyses
Dates and place: 7-11 May 2012, Silver Spring, Maryland, USA
Type: Poster presentation
Title: Application of reanalysis datasets for calculating a new and global wind resource atlas including high-resolution terrain effects
Authors: Jake Badger, Hans Jœrgensen, Mark Kelly, Ferhat Bingö l, Andrea Hahmann, Merete Badger, Niels Gylling Mortensen, Ivan Moya Mallafre (CENER), Shannon Cowlin(NREL), Donna Heimiller (NREL), Julie K. Lundquist (NREL and University of Colorado), Doug Arent (NREL)

Conference: Danish Wind Consortium 2013
Date and place: 27-28 May 2013, Fredericia, Denmark
Type: Oral presentation
Title: Global Wind Atlas Progress and perspectives
Authors: Jake Badger

Conference: International Conference Energy and Meteorology 2013, ICEM2013
Dates and place: 25-28 June 2013, Toulouse, France
Type: Oral presentation
Title: Analysis and Application of Reanalysis Datasets for Global Wind Resource Assessment
Authors: Jake Badger, Mark Kelly, Xiaoli Guo Larsen, Andrea Hahmann

Conference: World Future Energy Conference 2014, IRENA side-event
Dates and place: 20 January 2014, Abu Dhabi, UAE
Type: Oral presentation
Title: EUDP Global Wind Atlas: New, Unique, and Dedicated dataset for the Global Atlas
Speaker: Jake Badger

Conference: European Geophysical Union
Dates and place: 17 April 2015, Vienna, Austria

Type: Oral presentation EGU2015-9259
Title: A global wind resource atlas including high-resolution terrain effects
Authors: Andrea Hahmann, Jake Badger, Bjarke Olsen, Neil Davis, Xiaoli Larsen, and Merete Badger

http://meetingorganizer.copernicus.org/EGU2015/orals/17148

Conference: European Wind Energy Association Technical Workshop on Resources
Dates and place: 2 - 3 June 2015, Helsinki, Finland
Type: Oral presentation
Title: The new worldwide microscale wind resource assessment data on IRENA's Global Atlas
Authors: Jake Badger, Neil Davis, Andrea Hahmann, Bjarke Tobias Olsen, Xiaoli Guo Larsen, Mark C. Kelly, Patrick Volker, Merete Badger and Tobias Torben Ahsbahs Niels Gylling Mortensen, Hans Ejsing Jœrgensen, Erik Lundtang Petersen, Julia Lange, and Nicolas Fichaux.

http://www.ewea.org/events/workshops/past-workshops/resource-assessment-2015/programme/

Conference: 9th Quebec Wind Energy Conference
Dates and place: 16th June 2015, Quebec, Canada
Type: Oral presentation
Title: A Global Wind Resource Atlas including High-resolution Terrain Effects
Authors: Neil Davis, Jake Badger, Andrea Hahmann, Bjarke Tobias Olsen, Xiaoli Guo Larsen, Mark C. Kelly, Patrick Volker, Merete Badger and Tobias Torben Ahsbahs Niels Gylling Mortensen, Hans Ejsing Jœrgensen, Erik Lundtang Petersen, Julia Lange, and Nicolas Fichaux. Denmark (DTU)

Conference: International Conference Energy and Meteorology 2015, ICEM2015
Dates and place: 22-26 June 2015, Boulder, Colorado, USA
Type: Oral presentation
Title: The Global Wind Atlas: The New Worldwide Microscale Wind Resource Assessment Data and Tools
Authors: Jake Badger, Neil Davis, Andrea Hahmann, Bjarke Tobias Olsen, Xiaoli Guo LarsÃƒÂ©n, Mark C. Kelly, Patrick Volker, Merete Badger and Tobias Torben Ahsbahs Niels Gylling Mortensen, Hans Ejsing Jœrgensen, Erik Lundtang Petersen, Julia Lange, and Nicolas Fichaux.
http://icem2015.org/wp-content/uploads/2015/07/1630_JakeBadger.pdf

Type: Oral presentation
Title: The Global Wind Atlas: Comparison of Downscaling from Atmospheric Reanalysis and WRF Mesoscale Simulations
Authors: Jake Badger, Andrea N. Hahmann, Tobias T. Ahsbahs, Bjarke
T. Olsen, Merete Badger, Xiaoli Larsen, Mark C. Kelly, Patrick Volker
http://icem2015.org/wp-content/uploads/2015/07/1650_AndreaNahmann.pdf

8.9 Book chapters

The Global Wind Atlas project and its purpose were described in a book chapter by Gryning et al. (2014) in the book 'Weather Matters for Energy' edited by Alberto Troccoli, Laurent Dubus and Sue Ellen Haupt.

8.10 Seminars

The following seminars have been given.

DTU Wind Energy Department seminar
Date: 6th May 2015 Title: The Global Wind Atlas: The New Worldwide Microscale Wind Resource Assessment Data and Tool
Speaker: Jake Badger

United Nations training: Southeast Asia regional training programme on renewable energy resource assessment and mapping
Date: 28th September 2016 Title: The Global Wind Atlas: The New Worldwide Microscale Wind Resource Assessment Data and Tools Speaker: Jake Badger

8.11 Related projects

The New European Wind Atlas (NEWA) is a new ERANET+ project that started in 2015. A presentation about the Global Wind Atlas was given at the NEWA kick-off meeting.

Title: How elements of Global Wind Atlas contribute to the New European Wind Atlas
Speaker: Jake Badger

8.12 Masters student projects

The following DTU Masters students worked with the Global Wind Atlas data and methods during their dissertation projects.

Author: Andres Munoz-Najar
Dissertation title: Measurement Based Wind Atlas for Illinois And Comparison Against Re-analysis Data and Energy Production
Completed: January 2015

Author: Tobias Ahsbahs
Dissertation title: Approaches to validate wind resource grid data

Completed: March 2015

Author: Gabriel Zeitouni
Dissertation title: Site assessment of a Wind Farm in the Northeast of Brazil and Generalised Wind Climate Comparison for the Global Wind Atlas
Completed: August 2015

Part VI

Utilization of project results

The Global Wind Atlas project results comprise of all the datasets generated within the project. These are already utilized in the Global Wind Atlas disseminating websites and web tools provided by DTU Wind Energy and IRENA. These will be described in some detail in the next chapter.

These high resolution datasets are useful in a number of ways. Some of the data can be classed into three types. First, the input data to microscale modelling, such as the description of surface elevation and roughness length. Having this available for inspection on one website is in itself advantageous, for many wind resource assessment practicioners. Second, there are datasets that describe some of the flow behaviour coming from the modelling. These are disseminated on the website as we believe these to be useful for people working in the field of resource assessment and they have an educational value. Third, we disseminate the results datasets, which describe the wind speed and direction distributions and power densities. When applied in aggregated analyses these are of value for assessing the amount of resourse in an area of interest. Tools to carry out this analysis are provided by the websites at DTU Wind Energy and IRENA.

The future context is to link the online provision of these datasets to other wind resource calculation software. We are presently working on integration of these datasets to be a part of the EUDP project Online WAsP. That project can exploit a lot of the Global Wind Atlas input and results datasets.

The next step in the dissemination of the Global Wind Atlas datasets will be to make them available through web coverage services (WCS), an Open Geospatial Consortium (OGC) standard, so that these data can be applied as map data by 3rd party applications. Already OGC standard web process services (WPS) and web map services (WMS) are employed.

The next step in the application of the Global Wind Atlas datasets will be in projects aiming to calculate levelized cost of wind energy. We would also like to add the provision of some kind of time series information about the resource. This can be especially valuable for inital specification of isolated power system design in remote areas.

In addition we would like to collaborate on projects that can apply the data to instigate resource assessment projects that result in feasible and concrete wind farm projects; with the final aim being to create a pipeline of feasible projects.

Chapter 9

Atlas Design

In this chapter the elements of the Global Wind Atlas output are described. These elements are available on the Atlas webpage. They can be described as being either datasets or tools. The datasets can be divided into four types: input data, flow modelling data, full calculation output data and aggregated data.

The tools are functions that perform analysis on the Atlas data for a region of interest defined by the users. The region of interest is defined by the user either by drawing a free hand polygon, or by selecting a country or administrative region using the region selection tool.

The principle of the Global Wind Atlas is to make available the data relevant to the calculation of the wind climatologies. This is ensure transparancy of methodology. For example, the user can see what has been used for surface roughness length in their region of interest. The user can also see the flow modelling effects and the terrain ruggedness. This allows the user to see inside the methodology and assess the model behaviour. It also allows the user to assess the quality of the input data, which has direct influence on the quality of the output data.

9.1 Datasets

9.1.1 Input data

These datasets cover the input data used in the Global Wind Atlas methodology. The user is encouraged to browse these datasets for their areas of interest in order to get an impression of the representation of orography, land use and surface roughness, and spatial variation of large scale wind forcings.

- Large-scale wind forcing
  These datasets include the mean wind speed from reanalysis model output and the mean generalizaed wind speed from reanalysis models.

- Land use and roughness
  These datasets include the land use from the GlobCover and MODIS landcover datasets. The GlobCover is the primary source of land use, but in locations where there are gaps in GlobCover, the MODIS land use is used. The roughness length values are set based

on each land use class (see 4). The derived aerodynamic surface roughness length at 300 m resolution used in the microscale modelling is given here.

- Terrain Height
  The Viewfinder derived orography dataset at 150 m used in the microscale modelling is given here.

9.1.2 Flow modelling data

These datasets tell the user about the flow modelling characteristics. Details of the flow modelling can be found 6. Using these data, the user can gain an understanding of the microscale phenomena that are important in their region of interest. For example, one can see if roughness change effects have an impact, or whether there is a significant orographic speed up effect. Here also the ruggedness index (RIX) is given. This is useful for users to assess uncertainty in the modelling output.

Roughness effects

- WAsP Meso roughness per direction sector
  This dataset gives the roughness length that is used as the basis when calculating the roughness speed up effects. It is dependent on direction sector. The dataset is from the 250 m resolution dataset sampled at 1 km spacing.

- WAsP Roughness speed up per sector at 100 m
  This dataset gives the roughness speed-up as a percentage at 100 m. From these values you can see how the actual surface roughness distribution gives an increase or decreasing of the wind speed compared to a surface with constant roughness equal to the meso roughness. The dataset is from the 250 m resolution dataset sampled at 1 km spacing.

Orography effects

- WAsP Orographic speed up per sector at 100 m
  This dataset gives the speed up as the percentage speed increase due to orography as compared to a completely flat terrain. The dataset is from the 250 m resolution dataset sampled at 1 km spacing.

- WAsP Ruggedness Index
  This dataset gives the percentage of the terrain within 3.5 km which is steeper than a gradient of 0.3. The dataset is from the 250 m resolution dataset sampled at 1 km spacing. (see Bowen and Mortensen (1996) and Wood (1995))

Modelling set-up information

- MRGS Tiles
  Here the locations of the Military Grid Reference System (MGRS) zones, subdived into strips 2 $^\circ$ in latitude (typically 4 subdivisions), are displayed. This reference system gives each of the Global Wind Atlas job tile a unique identity. This is useful if a user wants to find out the particular job tile number for a particular region.

- Computation Boundaries
  Here the computation area within a Global Wind Atlas job tile is displayed. This shows explicity where calculations are performed on nodes with a 250 m spacing. It can be seen that the computation area boundary follows a 30 km buffer around coastlines and that they are divided along modified MGRS zones.

9.1.3 Full calculation output data

These data are direct values from the microscale local wind climatology caculation. Due to the size of the dataset, only a subsample set of data are served on the website. Those interested in applying the full calculation data should contact DTU Wind Energy.

High-resolution wind speed and power density

- Direct result 1000 m sampling at 50, 100, 200 m
  This dataset gives the value of the wind speed directly from the microscale modelling result, without any aggregation, sampling the 250 m spaced calculation nodes every 1 km. The locations of these sampled values correspond to the locations the modelling data is given.

9.1.4 Aggregated data

In order to give the user quick access to the richness of the Global Wind Atlas results, an aggregation method has been devised. With the dataset listed below the user can see the characteristics of the windiest sites inside a 1 x 1 km area, and can see how much variation of resource there is within that area.

High-resolution wind speed

- Aggregated mean wind speed at 50, 100, 200 m
  This dataset gives the mean wind speed for a 1 x 1 km area, composed of 16 calculation nodes with a spaced of 250 m. In proximity to a computational boundary there may be fewer than 16 calculation nodes. The resolution is 1 km.

- Aggregated Top-Quartile mean wind speed at 50, 100, 200 m
  This dataset gives the mean wind speed for the windiest 4 calculation nodes for a 1 x 1 km area, composed of 16 calculation nodes with a spacing of 250 m. This value represents the mean wind speed for the best sites in the 1 x 1 km area. In proximity to a computational boundary there may be fewer than 16 calculation nodes. The resolution is 1 km.

- Aggregated Top-Quartile Bottom-Quartile mean wind speed difference at 50, 100, 200 m
  This dataset gives the difference between the mean of the windiest 4 calculation nodes and the mean of the least windy 4 calculation nodes for a 1 x 1 km area. This indicates the variation of wind resource within the 1 x 1 km area. In locations where this difference is small, the resource is homogeneous, and wind turbine micrositing may be less important. In locations where this difference is large, the resource is heterogeneous on small scales, and micrositing of wind turbines is likely to be very important.

High-resolution power density

As in the aggregated mean wind speed datasets described above, the analogous datasets are provided for the power density.

- Aggregated mean power density speed at 50, 100, 200 m
- Aggregated Top-Quartile mean power density at 50, 100, 200 m
- Aggregated Top-Quartile Bottom-Quartile power density wind speed difference at 50, 100, 200 m

9.2 Other geographical information

In addition to the wind climatology datasets described above some geographical information is also provide to enhance the navigation experience when using the Global Wind Atlas website.

- Coastlines
  Coastlines can be added. The user can choose coastlines in black or white depending on the what gives better contrast against rendered maps.
- Base layers
  A background map or background satellite imagery can be selected.

9.3 Tools

There are a number of tools available with the Global Wind Atlas. The tools are function that perform analysis on the Atlas data for a region of interest defined by the users.

9.3.1 Applying input data

To describe the broader wind conditions four of the tools use data from reanalysis models to show the temporal variability in the data as well as the predominant wind directions. Two reanalysis data are availible for plotting. MERRA data is availible on a 1/2 degree latitude by 2/3 degree longitude grid every 6 hours from 1979 - 2013. CFDDA data is availible on a global 0.4 degree grid hourly from 1985 - 2005.

- Generalized wind climate downloader tool
  The generalized wind climate data in the form of files in the WAsP libfile format can be downloaded. The data is derived from the reanalysis data and generalization method described in Chapter 5. In Table 9.1 the description of the WAsP libfile from the Global Wind Atlas is given.

Line	content
1	Reanalysis identification string ix and iy index values for the calculation point in the GWA job tile <coordinates>lon_string,lat_string,0.0 </coordinates>
2	Number of roughness classes, heights and sectors in data set. In GWA the values are 5,3,12
3	Reference roughness lengths [m]. In GWA the values are: 0.0, 0.03, 0.10 and 0.40, 1.5 m
4	Reference heights above ground level [m]. In GWA the values are: 50, 100 and 200 m a.g.l.
5	Frequencies of occurrence for reference roughness 1 (0 m)
6	Weibull A-parameters for reference height 1 (50 m) in [ms-1]
7	Weibull k-parameters for reference height 1 (50 m)
8-9	Weibull A- and k-parameters for reference height 2 (100 m)
10-11	Weibull A- and k-parameters for reference height 3 (200 m)
12-16	As lines 5-9, but for reference roughness 2 (0.03 m)
17-21	As lines 5-9, but for reference roughness 3 (0.10 m)
22-26	As lines 5-9, but for reference roughness 4 (0.40 m)
27-31	As lines 5-9, but for reference roughness 5 (1.50 m)

Table 9.1 – Generalized wind climate data in WAsP lib-file format.

- Wind rose tool
  The wind rose shows the aggregated frequency for twelve 30-degree sectors centered on the cardinal directions. This data is taken from the reanalysis data so the frequencies are based off the period of reporting for each.

- Temporal Histogram tool
  The temporal histogram shows the aggregated frequency for 1 $\mathrm{m\,s^{-1}}$ wind speed bins over the selected area. This data is taken from the reanalysis data so the frequencies are based off the period of reporting for each. However, it should be noted that the renalysis wind speeds are instantaneous values.

- Annual and Daily cycle tools
  The annual and diurnal cycle plots show the area averaged wind speeds for each month of the year and hour of the day respectively. The y-axis shows the period wind speed divided by the mean wind speed for the entire period. The circles show the mean of the period, while the shadded region shows $+/-$ two standard deviations of the data. Due to the MERRA data only being availible every 6 hours a diurnal cycle plot is not availible for this dataset.

9.3.2 Applying full calculation output data

The tools below use the full calculation output data sampled at 1000 m spacing.

- Area wind speed and power density plot
  This chart shows the mean wind speed (y-axis) for the windiest percent area (x-axis) of

the selected area. This shows the windiest sites in many cases are significantly windier than the average for the region of interest. When showing power density this effect is stronger, and the windiest sites can lift the mean power density for the whole region of interest significantly.

- Areal Histogram tool
  This chart shows the percentage (y-axis) of the selected area which has a mean wind speed in a given interval (x-axis).

9.4 Summary

In this chapter the dataset and tools available on the Global Wind Atlas website have been described. More information about the datasets and ways to access them can be found at http://mapserver.globalwindatlas.com/ . Also video tutorial on how to use the website are provided on http://globalwindatlas.com/tutorials.html .

Contributing authors Jake Badger, Neil Davis

Part VII

Project conclusion and perspective

Chapter 10

Conclusions

The Global Wind Atlas project has produced a completely new kind of dataset. A dataset that on one hand can give an overview of global wind resource and on the other hand goes into the necessary high detail required to get the overview. The problem in the past has been that the overview was provided by coarse resolution wind data, either because this was the only data available or because the importance of the high resolution terrain effects was not fully realized. Now this problem has been fully addressed by the Global Wind Atlas.

Furthermore the data is readily available on websites using open standards. This maximizes the possibility for the data to be shared across the energy sector community and applied in energy planning.

We are actively seeking new projects that can exploit the Global Wind Atlas data further. One very promising area is the calculation of global technical potential of wind energy. This calculation has been made by various authors and the spread in the estimate is very large. Figure 10.1 shows a summary table from the IPCC Special Report on Renewable Energy Sources and Climate Change. The range in global technical potential is 19 – 125 PWh per year, including onshore and near shore areas.

We would like to use the EUDP Global Wind Atlas to determine global potential accounting for high resolution effects and get a better spatial breakdown. The challenge is to create a consistent approach, with a range of tested assumptions, available for the community to scrutinize. The Global Wind Atlas makes this easier via transparency of methodology and it can provide the data to allow annual energy production calculation for a given set of technical assumptions. The use of open standards also promotes the integration of the datasets into community models.

We have made a first approximate calculation of the global technical potential using the Global Wind Atlas results and the following assumptions:

- 5 MW per km^2 capacity density
- 100 m hub height
- no exclusion zones

These assumptions are very questionable, especially the no exclusion zones, but the idea is to get a first estimate of an upper limit of the technical potential, before accounting for other limits.

Table 7.1 | Global assessments of the technical potential for wind energy.

Study	Scope	Methods and Assumptions[1]	Results[2]
Krewitt et al. (2009)	Onshore and offshore	Updated Hoogwijk and Graus (2008), itself based on Hoogwijk et al. (2004), by revising offshore wind power plant spacing by 2050 to 16 MW/km²	*Technical (more constraints):* 121,000 TWh/yr 440 EJ/yr
Lu et al. (2009)	Onshore and offshore	>20% capacity factor (Class 1); 100 m hub height; 9 MW/km² spacing; based on coarse simulated model data set; exclusions for urban and developed areas, forests, inland water, permanent snow/ice; offshore assumes 100 m hub height, 6 MW/km², <92.6 km from shore, <200m depth, no other exclusions	*Technical (limited constraints):* 840,000 TWh/yr 3,050 EJ/yr
Hoogwijk and Graus (2008)	Onshore and offshore	Updated Hoogwijk et al. (2004) by incorporating offshore wind energy, assuming 100 m hub height for onshore, and altering cost assumptions; for offshore, study updates and adds to earlier analysis by Fellows (2000); other assumptions as listed below under Hoogwijk et al. (2004); constrained technical potential defined here in economic terms separately for onshore and offshore	*Technical/Economic (more constraints):* 110,000 TWh/yr 400 EJ/yr
Archer and Jacobson (2005)	Onshore and near-Shore	>Class 3; 80 m hub height; 9 MW/km² spacing; 48% average capacity factor; based on wind speeds from surface stations and balloon-launch monitoring stations; near-shore wind energy effectively included because resource data includes buoys (see study for details); constrained technical potential = 20% of total technical potential	*Technical (limited constraints):* 627,000 TWh/yr 2,260 EJ/yr *Technical (more constraints):* 125,000 TWh/yr 450 EJ/yr
WBGU (2004)	Onshore and offshore	Multi-MW turbines; based on interpolation of wind speeds from meteorological towers; exclusions for urban areas, forest areas, wetlands, nature reserves, glaciers, and sand dunes; local exclusions accounted for through corrections related to population density; offshore to 40 m depth, with sea ice and minimum distance to shore considered regionally; constrained technical potential (authors define as 'sustainable' potential) = 14% of total technical potential	*Technical (limited constraints):* 278,000 TWh/yr 1,000 EJ/yr *Technical (more constraints):* 39,000 TWh/yr 140 EJ/yr

Figure 10.1 – IPCC Special Report on Renewable Energy Sources and Climate Change estimates of global wind resources.

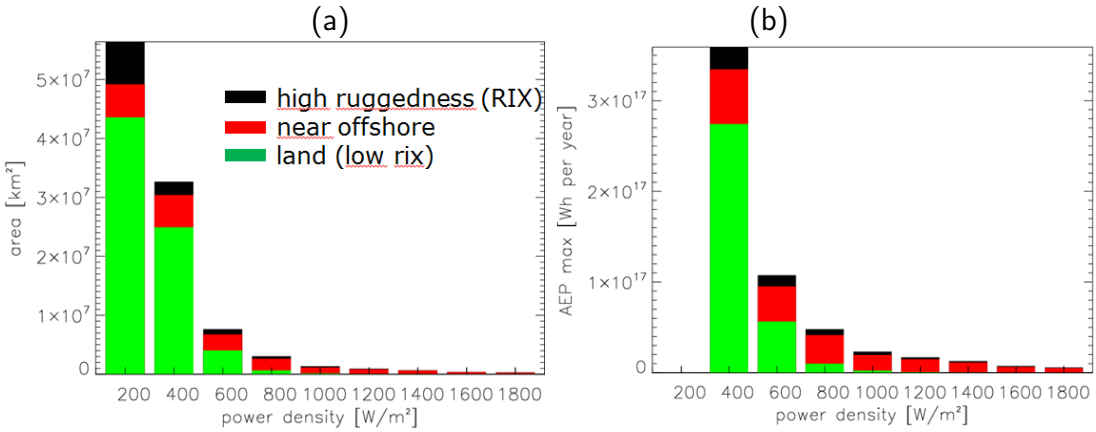

Figure 10.2 – (a) Graph showing an estimate of the area (y-axis) within a given wind power density interval (x-axis) at 100 m above surface. (b) Graph showing an estimate of the annual energy production, AEP, (y-axis) within a given wind power density interval (x-axis) at 100 m above surface, based on installed capacity assumptions stated in the main text.

Figure 10.2a shows the land and coastal water area with a given power density range at 100 m. The areas are broken down into high ruggedness (i.e. complex terrain), near offshore (coastal waters) and land with low ruggedness (i.e. simple terrain). We can see that high ruggedness land occupies about 10% of the area. Highest power densities are mainly on the coastal waters, but there is a very large area of low ruggedness land with high wind power density.

Next we can calculate the annual energy production and plot this against intervals of power density, shown in Fig. 10.2b. The 200 W/m^2 interval has zero production because we assume that building wind farms in these areas is not financially viable. We can now sum up the annual energy production for the globe in different ways. We can sum up all areas or we can sum up area excluding the high ruggedness land, or all areas that are low ruggedness land; giving:

- all areas (land and coastal waters) 581 PWh
- low ruggedness land and coastal waters 528 PWh
- low ruggedness land only 344 PWh

First we can see that the production is very large, several times larger than the global primary energy production. However, new assumptions can be introduced to reduce the production to more realistic values. For example, by saying that only 1% of low ruggedness land resource will be used gives us around 3 PWh per year.

Collaboration underway during the project with DTU Management Engineering has developed a method to more carefully determine how the faction of land on which wind energy is exploited influences the area aggregated technical potential. This was presented at IRENA's International Energy Workshop in Abu Dhabi June 2015, Karlsson (2015).

Development of this and other applications of the Global Wind Atlas will be exciting areas for projects in the coming years. The potential impact of the Global Wind Atlas is a significant acceleration towards a higher level of wind energy production globally in the future.

Bibliography

Badger, J., H. Frank, A. N. Hahmann, and G. Giebel, 2014a: Wind-Climate Estimation Based on Mesoscale and Microscale Modeling: Statistical-Dynamical Downscaling for Wind Energy Applications. *J. Appl. Meteorol. Climatol.*, **53**, 1901–1919.
URL http://journals.ametsoc.org/doi/abs/10.1175/JAMC-D-13-0147.1

Badger, J., P. J. Volker, A. N. Hahmann, J. C. Hansen, and B. O. Hansen, 2014b: Wind resource mapping in vietnam. Tech. rep.

Badger, M., C. B. Hasager, A. N. Hahmann, P. Volker, A. di Bella, and F. Bingöl, 2015: Esa resgrow: Trial cases for sar lifting. aegean sea. Tech. rep., DTU Wind Energy.

Bingöl, F., C. B. Hassager, M. Badger, and J. Badger, 2013: Rzgm2013-14.

Bowen, A. J. and N. G. Mortensen, 1996: Exploring the limits of wa s p the wind atlas analysis and application program. *1996 European Wind Energy Conference and Exhibition*.

Calaudi, R., F. Arena, M. Badger, and A. M. Sempreviva, 2013: Offshore wind mapping mediterranean area using sar. *Energy Procedia*, **40**, 38–47.

Chang, R., R. Zhu, M. Badger, C. B. Hasager, X. Xing, and Y. Jiang, 2015: Offshore wind resources assessment from multiple satellite data and wrf modeling over south china sea. *Remote Sensing*, **7**, 467–487.

Chang, R., R. Zhu, M. Badger, C. B. Hasager, R. Zhou, D. Ye, and X. Zhang, 2014: Applicability of synthetic aperture radar wind retrievals on offshore wind resources assessment in hangzhou bay, china. *Energies*, **7**, 3339–3354.

Dagestad, K.-F., J. Horstmann, A. Mouche, W. Perrie, H. Shen, B. Zhang, X. Li, F. Monaldo, et al., 2012: Wind retrieval from synthetic aperture radar-an overview. *4th SAR Oceanography Workshop (SEASAR 2012)*.

Dee, D. P., S. M. Uppala, A. J. Simmons, P. Berrisford, P. Poli, S. Kobayashi, U. Andrae, M. A. Balmaseda, et al., 2011: The ERA-Interim reanalysis: configuration and performance of the data assimilation system. *Q. J. R. Meteorol. Soc.*, **137**, 553–597.
URL http://doi.wiley.com/10.1002/qj.828

Doubrawa, P., R. J. Barthelmie, S. C. Pryor, C. B. Hasager, M. Badger, and I. Karagali, 2015: Satellite winds as a tool for offshore wind resource assessment: The great lakes wind atlas. *Remote Sensing of Environment*, **168**, 349–359.

Dunkerley, F., J. Moreno, T. Mikkelsen, and I. Griffiths, 2001: Lincom wind flow model: Application to complex terrain with thermal stratification. *Physics and Chemistry of the Earth Part B - Hydrology Oceans and Atmosphere*, **26**, 839–842.

Frank, H., O. Rathmann, N. Mortensen, and L. Landberg, 2001: The numerical wind atlas - the kamm/wasp method. Tech. rep.

Gryning, S.-E., J. Badger, A. Hahmann, and E. Batchvarova, 2014: *Current Status and Challenges in Wind Energy Assessment*. Springer Science+Business Media B.V., 275–293.

Hahmann, A. N., J. Badger, C. L. Vincent, M. C. Kelly, P. J. H. Volker, and J. Refslund, 2014: Mesoscale modeling for the wind atlas for South Africa (WASA) Project. Tech. rep., DTU Wind Energy.
URL `http://orbit.dtu.dk/services/downloadRegister/107110172/DTU_Wind_Energy_E_0050.pdf`

Hahmann, A. N., D. Rostkier-Edelstein, T. T. Warner, F. Vandenberghe, Y. Liu, R. Babarsky, and S. P. Swerdlin, 2010: A Reanalysis System for the Generation of Mesoscale Climatographies. *J. Appl. Meteor. Clim.*, **49**, 954–972.

Hasager, C., M. Badger, N. Nawri, B. Rugaard Furevik, G. Petersen, H. BjÃ¶rnsson, and N.-E. Clausen, 2015a: Mapping offshore winds around iceland using satellite synthetic aperture radar and mesoscale model simulations. *I E E E Journal of Selected Topics in Applied Earth Observations and Remote Sensing*.

Hasager, C. B., A. Mouche, M. Badger, F. Bingöl, I. Karagali, T. Driesenaar, A. Stoffelen, A. Peña, et al., 2015b: Offshore wind climatology based on synergetic use of envisat asar, ascat and quikscat. *Remote Sensing of Environment*, **156**, 247–263.

Hersbach, H., 2010: Comparison of c-band scatterometer cmod5. n equivalent neutral winds with ecmwf. *Journal of Atmospheric and Oceanic Technology*, **27**, 721–736.

Karlsson, K., 2015: Microscale spatial variability of wind on estimation of technical and economic wind potential. *IRENA International Energy Workshop*.

Kelly, M. C., I. Troen, and H. E. Jørgensen, 2014: Weibull-k Revisited: "Tall" Profiles and Height Variation of Wind Statistics. *Boundary-Layer Meteorol.*, **152**, 107–124.

Monaldo, F., V. Kerbaol, et al., 2004: The sar measurement of ocean surface winds: an overview for the 2nd workshop on coastal and marine applications of sar. *Proc. of the 2nd workshop on SAR coastal and marine applications*.

Munoz-Najar, A., 2015: Measurement based wind atlas for illinois. Master's thesis, Technical University of Denmark.

Nygaard, I., K. Rasmussen, J. Badger, T. T. Nielsen, L. B. Hansen, S. Stisen, S. Larsen, A. Mariko, et al., 2010: Using modeling, satellite images and existing global datasets for rapid preliminary assessments of renewable energy resources: The case of mali. *Renewable and Sustainable Energy Reviews*, **14**, 2359–2371.

Quilfen, Y., B. Chapron, T. Elfouhaily, K. Katsaros, and J. Tournadre, 1998: Observation of tropical cyclones by high-resolution scatterometry. *Journal of Geophysical Research (JGR)-Oceans*, **103**, 7767–7786.

Rienecker, M. M., M. J. Suarez, R. Gelaro, R. Todling, J. Bacmeister, E. Liu, M. G. Bosilovich, S. D. Schubert, et al., 2011: MERRA: NASA's modern-era retrospective analysis for research and applications. *J. Clim.*, **24**, 3624–3648.

Rife, D. L., J. O. Pinto, A. J. Monaghan, C. a. Davis, and J. R. Hannan, 2010: Global Distribution and Characteristics of Diurnally Varying Low-Level Jets. *J. Clim.*, **23**, 5041–5064.
URL `http://journals.ametsoc.org/doi/abs/10.1175/2010JCLI3514.1`

Saha, S., S. Moorthi, H.-L. Pan, X. Wu, J. Wang, S. Nadiga, P. Tripp, R. Kistler, et al., 2010: The NCEP Climate Forecast System Reanalysis. *Bull. Am. Meteorol. Soc.*, **91**, 1015–1057.
URL `http://journals.ametsoc.org/doi/abs/10.1175/2010BAMS3001.1`

Stoffelen, A. and D. Anderson, 1997: Scatterometer data interpretation: Estimation and validation. *Journal of geophysical research*, **102**, 5767–5780.

Troen, I., 1990: A high resolution spectral model for flow in complex terrain. *Ninth Symposium on Turbulence and Diffusion, Roskilde*.

Troen, I. and E. Petersen, 1989a: European wind atlas. risø national laboratory, roskilde, denmark, 656 pp. published for the commission of the european communities. directorate general for science. *Research and Development, Brussels, Belgium*.

Troen, I. and E. L. Petersen, 1989b: *European Wind Atlas*. Published for the Commission of the European Communities, Directorate-General for Science, Research, and Development, Brussels, Belgium by Risø National Laboratory.

Tuller, S. E. and A. C. Brett, 1984: The characteristics of wind velocity that favor the fitting of a Weibull distribution in wind-speed analysis. *J. Appl. Meteor. Clim.*, **23**, 124–134.

Valenzuela, G. R., 1978: Theories for the interaction of electromagnetic and oceanic waves?a review. *Boundary-Layer Meteorology*, **13**, 61–85.

Wood, N., 1995: The onset of separation in neutral, turbulent flow over hills. *Boundary-Layer Meteorology*, **76**, 137–164.